Charge-Recombinative Triplet Sensitization of Alkenes for DeMayo-type [2+2] Cycloaddition

Yunjeong Lee,[1,‡] Byung Hak Jhun,[2,‡] Sihyun Woo,[3,‡] Seoyeon Kim,[1] Jaehan Bae,[1] Youngmin You,[2,*] and Eun Jin Cho[1,*]

[1]Department of Chemistry, Chung-Ang University, 84 Heukseok-ro, Dongjak-gu, Seoul 06974, Republic of Korea, E-mail: ejcho@cau.ac.kr (E. J. Cho)
[2]Department of Chemical and Biomolecular Engineering, Yonsei University, 50 Yonsei-ro, Seodaemun-gu, Seoul 03722, Republic of Korea, E-mail: odds2@yonsei.ac.kr (Y. You)
[3]Division of Chemical Engineering and Materials Science, Ewha Womans University, 52 Ewhayeodae-gil, Seodaemun-gu, Seoul 03760, Republic of Korea
‡These authors contributed equally.

Supplementary Information

General Methods

1,4-Dioxane was purchased from Sigma-Aldrich in sure-seal bottles. All commercially available reagents were purchased from Sigma-Aldrich, Alfa Aesar, Combi blocks or TCI companies and used without further purification. Flash column chromatography was performed using ZEOCHEM ZEOprep silica gel 60 (60-200 mesh). The synthesized compounds were characterized by ^{1}H NMR, ^{13}C NMR, ^{19}F NMR, and FT-IR spectroscopy. NMR spectra were recorded on a Varian 600 MHz instrument (600 MHz for ^{1}H NMR, 151 MHz for ^{13}C NMR, and 564 MHz for ^{19}F NMR). Copies of ^{1}H, ^{13}C, and ^{19}F spectra can be found at the end of the Supporting Information. ^{1}H NMR experiments are reported in units, parts per million (ppm), and were measured relative to residual chloroform (7.26 ppm) in the deuterated solvent. ^{13}C NMR spectra are reported in ppm relative to deuterochloroform (77.23 ppm), and all were obtained with ^{1}H decoupling. Coupling constants were reported in Hz. FT-IR spectra were recorded on a Nicolet 6700 Thermo Scientific FT-IR spectrometer. Reactions were monitored by thin layer chromatography and gas chromatography (GC). Mass spectral data of all unknown compounds were obtained from the Korea Basic Science Institute (Daegu) on a Jeol JMS 700 high-resolution mass spectrometer. Melting points of unknown compounds were recorded on a Stuart SMP30 apparatus. Single crystal X-ray diffraction data were collected in Bruker-AXS SMART BREEZE X-ray diffractometers. The structures were solved with direct methods using the SHELXL programs.

Experimental Details

Steady-State UV−Vis Absorption Measurements

UV−Vis absorption spectra were collected on an Agilent, Cary 300 spectrophotometer at 298 K. Sample solutions were prepared prior to measurements at a concentration of 10 μM in 1,4-dioxane, unless otherwise stated. The prepared solution was transferred into a quartz cell (Hellma, beam path length = 1.0 cm) for the measurements.

Steady-State Photoluminescence Measurements

Photoluminescence spectra were collected on a Photon Technology International, Quanta Master 400 scanning spectrofluorimeter at 298 K. The solutions used for the steady-state UV−Vis absorption studies were also used for the photoluminescence measurements. The excitation wavelengths were 341 nm for **A**, 374 nm for **B**, 378 nm for **C**, 379 nm for **D**, 380 nm for **E**, 375 nm for **F**, 380 nm for **G**, 419 nm for **H**, and 307 nm for **1**. All the solutions were deaerated by bubbling Ar prior to the measurements. A quartz cell (Hellma, beam path length = 1.0 cm) was used for deaerated solution samples.

Determination of Photochemical Quantum Yields

The quantum yield for the reaction was determined by conducting standard ferrioxalate actinometry. A 6 mM $K_3[Fe(C_2O_4)_3]$ solution as chemical actinometer prepared and 1 mL of solution was transferred to the same glassware used in the photoreaction (glass tube having diameter of 1.5 cm), and the solution was photoirradiated with a beam of photoreaction at 450 nm for 20 s. The same volume of 1 wt % 1,10-phenanthroline in sodium acetate buffer solution was added and stored in the dark for 1 h. The absorbance changes at 510 nm was measured by UV−Vis spectrophotometer (Agilent, Cary 300); inserting the value to the following equation returned light intensities 3.15×10^9 einstein s^{-1} at 450 nm:

$$\text{light intensity } (I_0, \text{ einstein s}^{-1}) = (\Delta\text{Abs}(510\text{ nm}) \times V) / (\Phi \times 11050\ \text{M}^{-1}\ \text{cm}^{-1} \times \Delta t)$$

where, ΔAbs(510 nm), V, Φ, and Δt are the absorbance change at 510 nm, volume (L), quantum yield (0.85) of the ferrioxalate actinometer at 450 nm, and photoirradiation time (s), respectively. Finally, the reaction yield for the reaction condition utilizing 2.5 mol% photocatalyst was quantified and inserted into following equation to afford PCQY:

$$\text{PCQY} = \frac{[\text{product}] \times V}{I_0 \times \Delta t}$$

where, [product] is the molar concentration of the products calculated from ^{1}H NMR, Δt (s) is the photoirradiated time, V is the volume of the solution (L), and I_0 is the light intensity obtained by actinometry described above.

Determination of Relative Photoluminescence Quantum Yield

The photoluminescence quantum yield (Φ_{PL}) was determined for 10 μM sample solutions dissolved in Ar-saturated 1,4-dioxane. The Φ was calculated using the equation $\Phi_{PL} = \Phi_{ref} \times (I/I_{ref}) \times (A_{ref}/A) \times (n/n_{ref})^2$, where A, I, and n are the absorbance at the excitation wavelength, the integrated photoluminescence intensity, and the refractive index of the solvent, respectively. 9,10-Diphenylanthracene (Φ_{ref} = 1.00, toluene; λ_{ex} = 366 nm)[S1] was used as the reference material. Photoluminescence spectra were collected at 298 K in the emission range 350–850 nm, and were integrated using the OriginLab, OriginPro 2023b software.

Photoluminescence Lifetime Measurements

Photoluminescence decay traces were collected by employing time-correlated single-photon-counting (TCSPC) technique using a PicoQuant, FluoTime 200 instrument through a motorized monochromator at the peak emission wavelength of each sample. A pulsed light-emitting diode that produced 345 nm pulses (PicoQuant, PLS 340) was driven by a PDL800-D driver (PicoQuant). Photoluminescence decay traces were acquired with 25 ps of a pulse duration. Transient photon signals were collected at the following wavelengths: 489 nm for **A**, 484 nm for **B**, 491 nm for **C**, 539 nm for **D**, 479 nm for **E**, 478 nm for **F**, 486 nm for **G**, and 462 nm for **H**. Photoluminescence decay profiles were fitted to a mono-exponential decay model embedded on an OriginLab, OriginPro 2023b software.

Electrochemical Characterization

Cyclic and differential pulse voltammograms of the Ar-saturated anhydrous *N,N*-dimethylformamide (DMF) solutions (3.0 mL) containing sample (2.0 mM for organoPCs and 10 mM for **1**) and 0.10 M tetrabutylammonium hexafluorophosphate ($TBAPF_6$) were collected using a CH instruments, CHI630B potentiostat at 298 K. A standard three-electrode-assembly cell consisting of a platinum working electrode, a platinum counter electrode and an $Ag/AgNO_3$

pseudo reference electrode was used. The potentials were reported against saturated calomel electrode. The ferrocene/ferrocenium redox couple was employed as an external standard. Scan rates for cyclic and differential pulse voltammetries were 0.1 V s^{-1} and 4 mV s^{-1}, respectively. A blank sample containing 0.10 M $TBAPF_6$ only was also examined in the same range in order to assess the validity of the reduction potential. The excited-state oxidation (E_{ox}*) and reduction (E_{red}*) potentials of catalysts were calculated from the ground-state redox potentials and the singlet-state energy which was determined by optical bandgap from the onset of UV–Vis absorption spectra.

Spectroelectrochemical Measurements

UV–Vis–NIR absorption spectra were obtained on an Agilent, Cary 5000 spectrophotometer using the amperometric *I–t* curve method. A baseline was established with a 0.10 M $TBAPF_6$ solution (DMF) placed in a spectroelectrochemical cell (beam path length = 0.5 mm) equipped with a Pt mesh working electrode, a Pt wire counter electrode, and an $Ag/AgNO_3$ pseudo-reference electrode. An Ar-saturated DMF (500 μL) containing 2.0 mM **A** and 0.10 M $TBAPF_6$ was then transferred to the spectroelectrochemical cell and applied under a cathodic potential of −2.0 V vs $Ag/AgNO_3$.

Experimental Procedure

Synthetic procedure for the preparation of 2-(2-(prop-1-yn-1-yl)phenyl)-1H-benzo[f]isoindole-1,3(2H)-dione (S2)

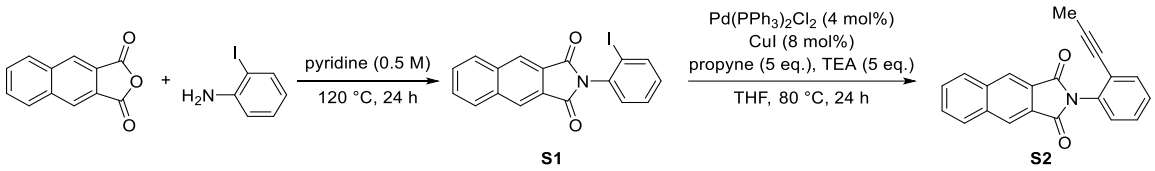

Step 1: An oven-dried round-bottom flask equipped with a magnetic stir bar was charged with a 2,3-naphthalic anhydride (1.0 eq.), 2-iodoaniline (1.0 eq.), and pyridine (0.5 M). Then, the mixture was stirred at 120 °C for 24 h. After the reaction had completed, the reaction was quenched with NH_4Cl and extracted with DCM. The organic layer was washed with NH_4Cl and brine, dried over $MgSO_4$ and the mixture was concentrated in vacuo to give a crude residue. Hexanes were added to the crude, and then it was filtered with cold hexanes to give the product, **S1** (white solid, 80%).

Step 2: A pressure vessel equipped with a magnetic stir bar was charged **S1** (1.0 eq.), $Pd(PPh_3)_2Cl_2$ (4 mol%), CuI (8 mol%), TEA (5.0 eq.), and THF (1.0 M) under argon. Then, argon was bubbled through the reaction mixture for 10 min, this was followed by the addition of propyne (1.0 M in DMF, 5.0 eq.). Then, the mixture was stirred at 80 °C for 24 h. After the reaction had completed, the mixture was concentrated in vacuo to give a crude residue that was purified by silica gel column chromatography to give the product, **S2** (white solid, 78%).

Synthesis of indole-fused polycyclic organophotocatalysts (A)

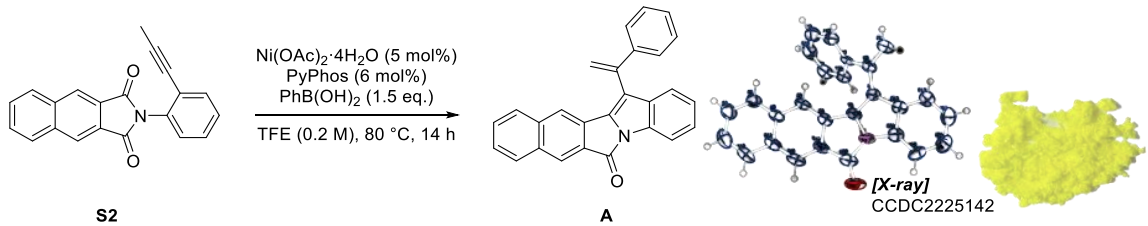

An oven-dried 100 mL round-bottom flask equipped with a magnetic stir bar was charged with **S2** (1.0 eq.), Pyphos(6 mol%), $Ni(OAc)_2 \cdot 4H_2O$ (5 mol%), and phenyl boronic acid (1.5 eq.), and TFE (0.2 M) in a glove box. Then, the mixture was stirred at 80 ℃ for 14 h. Upon completion of the reaction, the reaction mixture was cooled to room temperature and filtered.

The filter cake was washed with cold methanol with three times, then purified by silica gel column chromatography to give the product, **A** (yellow solid, 80%).

Synthetic procedure for the preparation of phthalimide derivatives (S4)[S2,S3]

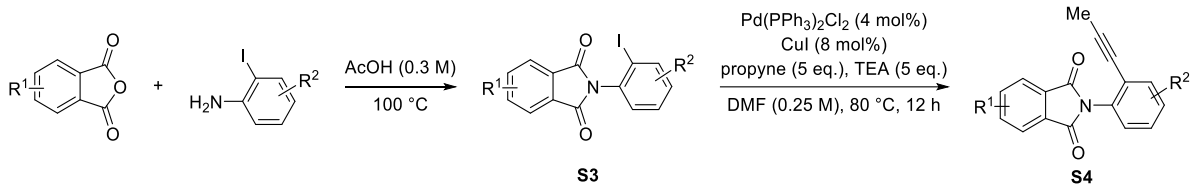

Step 1: 2-iodoaniline derivative (1.0 eq.) and phthalic anhydride derivative (1.0 eq.) were dissolved in AcOH (0.3 M). The above solution was vigorously stirred under reflux for 1 hour before pouring to a flask with ice water (0.02 M), and white precipitation rapidly dissolved out. The solvent was removed through filtration, then the residue was washed with water and petroleum ether to give the product, **S3**.

Step 2: A round-bottom flask equipped with a magnetic stir bar was charged **S3** (1.0 eq.), $Pd(PPh_3)_2Cl_2$ (4 mol%), CuI (8 mol%), TEA (5.0 eq.), and DMF (0.25 M) under argon. Then, argon was bubbled through the reaction mixture for 10 min, this was followed by the addition of propyne (1.0 M in DMF, 5.0 eq.). Then, the mixture was stirred at 80 °C for 12 h. After 12 h, saturated aqueous NH_4Cl was added to the reaction mixture, and the mixture was diluted with EtOAc and washed with brine. The organic layer was dried over anhydrous $MgSO_4$, filtered, and concentrated in vacuo. The crude product was purified by flash column chromatography using hexanes/EtOAc as the eluent to afford the corresponding coupled product **S4**.

Synthesis of indole-fused polycyclic organophotocatalysts (B-H)[S2]

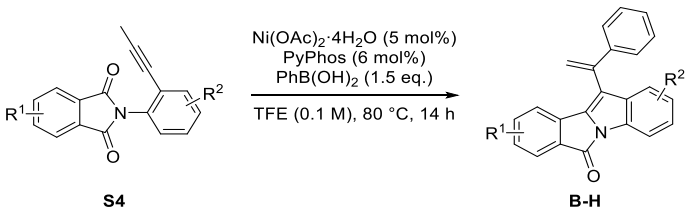

An oven-dried 100 mL reaction tube with rubber septum, equipped with a magnetic stirrer bar, was charged with **S4** (1.0 eq.), Pyphos (6 mol%), $Ni(OAc)_2 \cdot 4H_2O$ (5 mol%), phenyl boronic acid (1.5 eq.) and TFE (0.1 M) in a glove box. Then, the mixture was stirred at 80 °C for 14 h. Upon completion of the reaction, the reaction mixture was cooled to room temperature and

filtered. The filter cake was washed with cold methanol with three times, then purified by silica gel column chromatography to give the indole-fused polycyclic organophotocatalyst.

Procedure for the synthesis of methyl 2-(quinolin-2-yl)acetate (1)[S4]

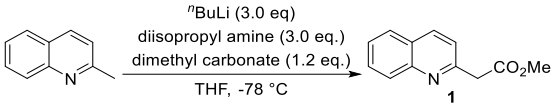

Following the reported procedure, an oven-dried 100 mL round-bottom flask equipped with a magnetic stir bar was charged with to a diisopropyl amine (2.0 eq.) and dry THF (1.0 M) under argon atmosphere at 0 ºC. Then, ^{n}BuLi (2.0 M in hexanes, 2.0 eq.) was added to the solution and the solution was stirred at this temperature for 15 min. A solution of 2-methylquinoline (1.0 eq.) in dry THF (0.5 M) was added dropwise to the LDA solution at -78 ºC. The reaction mixture was stirred at this temperature for 2 h. After this time, dimethyl carbonate (1.2 eq.) was added to the reaction mixture quickly. After stirring at -78 ºC for 15 min, the reaction mixture was quenched by water and warmed to room temperature. The mixture was diluted by water (50 mL) and extracted with EtOAc (100 mL). The organic layer was dried over $MgSO_4$, filtered, concentrated under reduced pressure, and purified by flash column chromatography to give the product, **1**. The analytical data of the synthesized compound (**1**) matched with reported literature data.

General procedure for [2+2] cycloaddition reaction[S5]

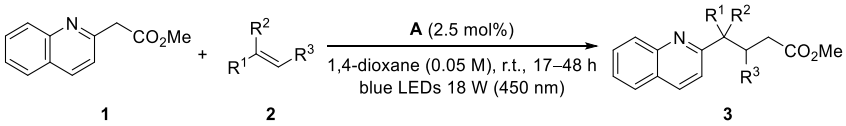

An oven-dried reusable test tube equipped with a magnetic stir bar was charged with a **1** (1.0 eq.) then was brought into a glove box. An alkene derivative **2** (5.0 eq.), indole-fused polycyclic organophotocatalyst (2.5 mol%) and 1,4-dioxane (0.05 M) were added to the reaction mixture in the glove box and the tube was sealed with a silicon septum screw cap. The tube placed under the light from blue LEDs (18 W, 450 nm) at room temperature. The reaction progress was monitored by thin layer chromatography or gas chromatography (GC). Upon completion of the reaction, the mixture was concentrated in vacuo to give a crude residue that was purified by silica gel column chromatography to give the corresponding [2+2] cycloaddition product, **3**.

Photoluminescence titration experiments. Photoluminescence spectra were recorded for a 1,4-dioxane solution containing 1.0 mM catalysts with added **1** (0–500 mM). A gradual decrease in the photoluminescence emission was ascribed to excited-state interactions between an organoPC and **1**. The photoluminescence quenching of organoPCs were also supported by the photoluminescence decay experiments for 1.0 mM organoPC in deaerated 1,4-dioxane with increased concentrations of substrate. The quenching rate was evaluated as $1/\tau - 1/\tau_0$, where τ and τ_0 are the photoluminescence lifetime of an organoPC in the presence and absence of **1**, respectively. The $1/\tau - 1/\tau_0$ values were fit to the pseudo-first-order plot $1/\tau - 1/\tau_0 = k_Q \times [\mathbf{1}]$, where k_Q and [**1**] are the quenching rate constant and the molar concentration of **1**, respectively.

Quantum chemical calculations. Quantum chemical calculations based on the density functional theory (DFT) were performed using the Amsterdam Density Functional (ADF) package, a component of the Amsterdam Modeling Suites software (AMS2023.101 release). The ground state geometries of all compounds have been optimized at B3LYP-D3(BJ)/TZP level, with the conductor-like screening model (COSMO) parameterized for 1,4-dioxane. Subsequently, single-point energy calculations were performed for 15 states of singlet and triplet excited states at the w-B97X-D/TZP level, employing Tamm-Dancoff Approximation (TDA) and the COSMO parameterized for 1,4-dioxane. To account for relativistic effects, the zeroth-order regular approximation (ZORA) was employed, thus returning the spin-orbit coupling matrix element (SOCME) between the singlet states and triplet states. The intersystem crossing rate constants between the lowest singlet excited state (S_1) and the lowest triplet excited state (T_1) for benzenoid and quinoid form of substrate were calculated according to the following equations:

$$k_{ISC} = \frac{2\pi}{\hbar}|V_{SOC}^2|\frac{1}{\sqrt{4\pi k_B T}}exp\left[-\frac{(\Delta E_{ST}+\lambda)^2}{4\lambda k_B T}\right]$$

where the V_{SOC} is SOCME, k_B is the Boltzmann constant, ΔE_{ST} is the adiabatic energy difference between S_1 energy level at the S_1 optimized geometry and T_1 energy level at the T_1 optimized geometry, λ is the reorganization energy. To evaluate parameters consisting this equation, the S_1 and T_1 state geometries were optimized at the level of w-B97X-D/TZP with TDA using the COSMO parameterized for 1,4-dioxane. Note that reorganization energy is calculated as the energy gap between T_1 energy level at the optimized S_1 geometries and T_1 energy level at the optimized T_1 geometries for k_{ISC}. The temperature (T) is taken as 298.15 K

(All parameters are listed in the Table S3). The geometries of the radical anionic form of organoPCs were also optimized at the level of unrestricted B3LYP-D3(BJ)/TZP with the COSMO parameterized for 1,4-dioxane, followed by single point calculations at the level of unrestricted w-B97X-D/TZP with TDA using the COSMO parameterized for 1,4-dioxane. The calculated oscillator strengths for first doublet excited state is used to estimate the molar absorbance of radical anion of catalysts to perform second-order kinetics analyses.

Laser flash photolysis. An Ar-saturated 1,4-dioxane solution in a quartz cell (path length = 1.0 cm) was excited by a Nd:YAG laser (EKSPLA, NT342) at a wavelength of 355 nm with 20 mJ pulse^{-1}. No positive transient signal was observed for dopant-only solutions under the measurement conditions. Time courses of the transient absorption were measured using Hamamatsu, photomultiplier tube R2949/InGaAs photodiode as detectors. The output from the detectors was recorded with a Tektronix, TDS3032 digitized oscilloscope. All experiments were performed at 298 K. The decays of the positive ΔAbs signals of **PC**$^{\bullet-}$ were analyzed through a second-order kinetics model. Briefly, the molar absorbance (ε) of **PC**$^{\bullet-}$ determined from the spectroelectrochemical measurement was divided by ΔAbs values at 1400 nm. The ε/ΔAbs data were plotted as a function of delay time, and fit to a linear line. The slope (in M^{-1} s^{-1}) of the linear line corresponded to the k_{CR} value. The values were plotted as a function of $-\Delta G_{CR}$, and correlated with parabolic curves calculated from the Jortner equation for adiabatic outer-sphere electron transfer:

$$k_{CR} = \frac{2\pi}{\hbar}\frac{J^2}{\sqrt{4\pi\lambda_{out}k_BT}}\cdot\left(\sum_{n=0}^{\infty}\frac{1}{n!}\left(\frac{\lambda_{in}}{\hbar\omega}\right)^n\cdot exp\left(-\frac{\lambda_{in}}{\hbar\omega}\right)\cdot exp\left(-\frac{(\Delta G_{CR}+\lambda_{in}+n\hbar\omega)^2}{4\pi\lambda_{out}k_BT}\right)\right)$$

In this equation, J^2 is taken as 5.0×10^{-5} eV, $\hbar\omega$ is approximated 0.21 eV which is typical for C=C stretching in aromatic hydrocarbons, k_B is the Boltzmann constant, and T is 298 K. λ_{out} is estimated from the equation:

$$\lambda_{\text{out}} = \frac{e^2}{4\pi\varepsilon_0}\cdot\left(\frac{1}{d_{\mathbf{PC}}}+\frac{1}{d_{\mathbf{1}}}-\frac{1}{d_{\text{vdW}}}\right)\cdot\left(\frac{1}{n^2}-\frac{1}{\varepsilon}\right)$$

In this equation, e is elementary charge, ε_0 is the vacuum permittivity, $d_{\mathbf{PC}}$ is the mean diameter of an optimized geometry of **PC**, $d_{\mathbf{1}}$ is the mean diameter of **1**, d_{vdW} is the longest diameter of the optimized geometry of a van der Waals contact pair of **PC** and **1**, n is the refractive index of 1,4-dioxane, and ε is the dielectric constant of 1,4-dioxane.

Table S1. Reaction yields and photochemical quantum yields determined at 17 h of reaction[a]

photocatalyst	reaction yield after 17 h (%)	quantum yield (%)
A	94	49
B	14	7
C	14	7
D	7	4
E	45	23
F	28	15
G	17	9
H	93	48

[a]Reaction scale: **1** (0.1 mmol), **2a** (0.5 mmol), photocatalyst (2.5 μmol) in 1,4-dioxane under Ar (0.05 M reaction concentration irradiated under 450 nm).

Table S2. Calculated k_{ISC} values of **1**[a]

1	$\lvert V_{SOC}\rvert^2$ (eV^2)[b]	λ (eV)[c]	ΔE_{ST} (eV)[d]	k_{ISC} (s^{-1})
benzenoid form	4.01×10^{-7}	0.71	0.43	1.43×10^{2}
quinoid form	5.13×10^{-13}	0.09	0.06	2.74×10^{3}

[a]Calculated from the equation $k_{ISC} = \frac{2\pi}{\hbar}\left|V_{SOC}^2\right|\frac{1}{\sqrt{4\pi k_B T}} exp\left[-\frac{(\Delta E_{ST}+\lambda)^2}{4\lambda k_B T}\right]$. [b]The spin-orbit coupling matrix elements squared, evaluated at the optimized S_1 geometries and expressed in units of eV. [c]Reorganization energy calculated as the difference between the T_1 energy at the optimized S_1 geometry and the T_1 energy at the optimized T_1 geometry. [d]Adiabatic energy differences between the S_1 energy at the optimized S_1 geometry and the T_1 energy at the optimized T_1 geometry.

Table S3. Cartesian coordinate for the optimized ground state geometry of the benzenoid form of **1**

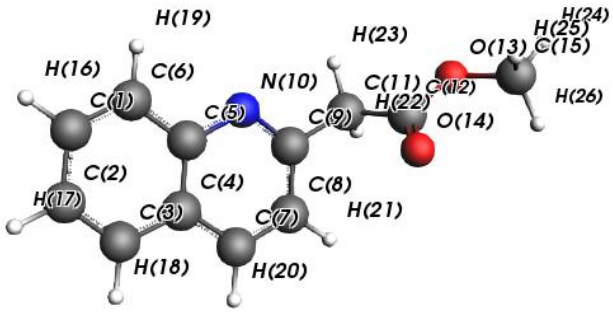

label	atom	coordinates (Å)		
		x	*y*	*z*
1	C	-8.4919	-3.6962	0.3611
2	C	-9.5806	-3.1663	-0.3676
3	C	-9.6262	-1.8276	-0.6675
4	C	-8.5846	-0.965	-0.252
5	C	-7.4867	-1.4994	0.4824
6	C	-7.4675	-2.8827	0.7783
7	C	-8.5692	0.4225	-0.5276
8	C	-7.5226	1.1826	-0.0893
9	C	-6.4708	0.5635	0.6346
10	N	-6.4501	-0.7216	0.9119
11	C	-5.309	1.3851	1.1245
12	C	-4.3916	1.8534	0.0118
13	O	-3.2788	2.415	0.5231
14	O	-4.6113	1.7597	-1.1743
15	C	-2.3304	2.9152	-0.4488
16	H	-8.4689	-4.7544	0.5905
17	H	-10.3796	-3.8227	-0.6887
18	H	-10.458	-1.4144	-1.2259
19	H	-6.6264	-3.2728	1.3371
20	H	-9.3869	0.866	-1.0836
21	H	-7.4788	2.2446	-0.2907
22	H	-5.6584	2.2803	1.647
23	H	-4.7231	0.8052	1.836
24	H	-1.5108	3.3248	0.133
25	H	-1.9834	2.1036	-1.085
26	H	-2.7922	3.6874	-1.061

Table S4. Cartesian coordinate for the optimized S_1 state geometry of the benzenoid form of **1**

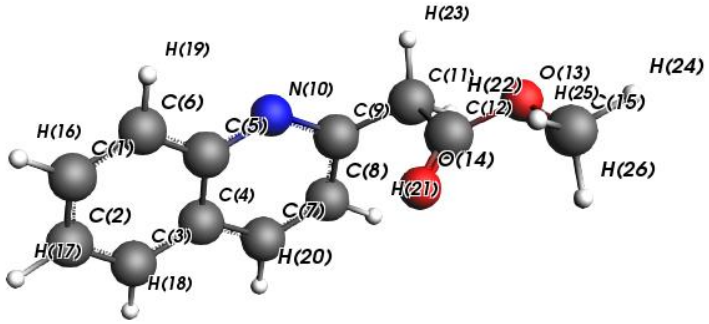

label	atom	coordinates (Å)		
		x	*y*	*z*
1	C	-8.04124	-3.59464	-0.00467
2	C	-9.15982	-3.13764	-0.69107
3	C	-9.42852	-1.77644	-0.754
4	C	-8.59852	-0.83425	-0.15013
5	C	-7.44956	-1.33375	0.566058
6	C	-7.18511	-2.70468	0.629132
7	C	-8.80201	0.587306	-0.17373
8	C	-7.87918	1.44628	0.368879
9	C	-6.74072	0.957065	1.025965
10	N	-6.76679	-0.37549	1.191707
11	C	-5.49847	1.736889	1.270558
12	C	-4.50581	1.610225	0.127354
13	O	-3.39723	2.314822	0.386442
14	O	-4.68006	0.978626	-0.88423
15	C	-2.40414	2.287587	-0.65459
16	H	-7.83002	-4.65636	0.043807
17	H	-9.82668	-3.8415	-1.17404
18	H	-10.3112	-1.41406	-1.27138
19	H	-6.30584	-3.04394	1.161014
20	H	-9.65702	0.974263	-0.71463
21	H	-7.95349	2.522028	0.240341
22	H	-5.742	2.79564	1.380043
23	H	-4.99488	1.425633	2.188959
24	H	-1.58278	2.900213	-0.293
25	H	-2.07716	1.263098	-0.83079
26	H	-2.81947	2.698681	-1.57468

Table S5. Cartesian coordinate for the optimized T_1 state geometry of the benzenoid form of **1**

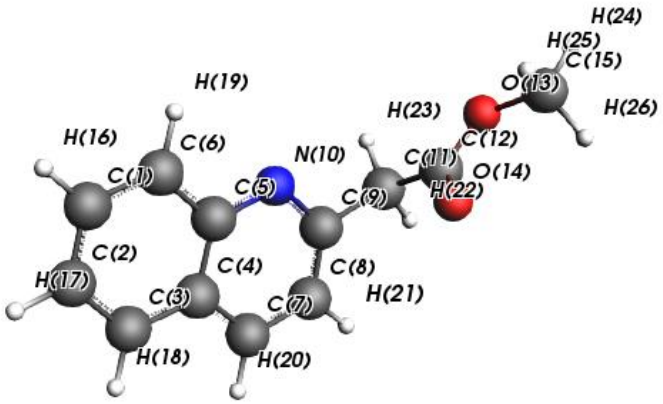

	atom	coordinates (Å)		
		x	*y*	*z*
1	C	-8.0633	-3.6519	0.0673
2	C	-9.28	-3.2663	-0.398
3	C	-9.6068	-1.8643	-0.5185
4	C	-8.6724	-0.8717	-0.1577
5	C	-7.3875	-1.2746	0.3357
6	C	-7.095	-2.6638	0.4444
7	C	-8.9301	0.4981	-0.2511
8	C	-7.9189	1.4126	0.1391
9	C	-6.7246	0.9378	0.5949
10	N	-6.4454	-0.4041	0.704
11	C	-5.603	1.841	1.0007
12	C	-4.4625	1.8045	0.0081
13	O	-3.3141	2.1961	0.5763
14	O	-4.561	1.5009	-1.1553
15	C	-2.186	2.2491	-0.3132
16	H	-7.8139	-4.7019	0.1577
17	H	-10.0191	-4.0046	-0.6848
18	H	-10.5785	-1.5649	-0.8889
19	H	-6.1201	-2.9454	0.8173
20	H	-9.8863	0.8455	-0.6207
21	H	-8.0863	2.4808	0.0726
22	H	-5.939	2.8795	1.056
23	H	-5.2197	1.5587	1.9826
24	H	-1.3471	2.5772	0.2949
25	H	-1.997	1.2616	-0.7338
26	H	-2.3801	2.9556	-1.1204

Table S6. Cartesian coordinate for the optimized ground state geometry of the quinoid form of **1**

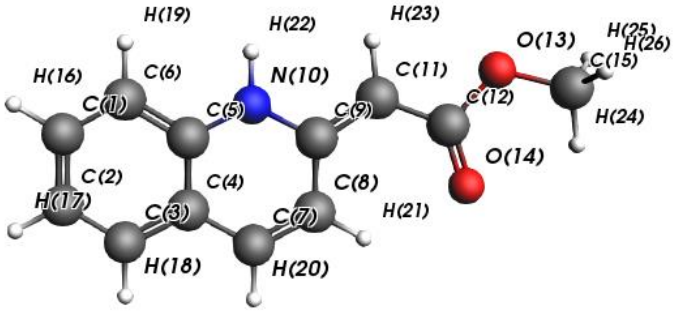

label	atom	coordinates (Å)		
		x	*y*	*z*
1	C	-4.2052	0.6557	-0.4842
2	C	-4.3687	-0.6258	0.0563
3	C	-3.2567	-1.3522	0.4432
4	C	-1.9667	-0.8216	0.3009
5	C	-1.818	0.4707	-0.2457
6	C	-2.9437	1.2051	-0.6364
7	C	-0.7717	-1.5213	0.6817
8	C	0.4539	-0.975	0.5274
9	C	0.6191	0.3461	-0.032
10	N	-0.5492	0.9871	-0.3842
11	C	1.8185	0.989	-0.2325
12	C	3.1116	0.4488	0.0878
13	O	4.0907	1.3553	-0.2456
14	O	3.3759	-0.6434	0.58
15	C	5.4556	0.9777	0.0079
16	H	-5.0732	1.2272	-0.788
17	H	-5.3604	-1.0437	0.1698
18	H	-3.3676	-2.3448	0.8628
19	H	-2.8199	2.1969	-1.0548
20	H	-0.87	-2.5148	1.1031
21	H	1.354	-1.4956	0.8111
22	H	-0.4668	1.9132	-0.7779
23	H	1.8098	1.9819	-0.6637
24	H	5.5002	-0.0175	0.4405
25	H	5.9928	1.0027	-0.9395
26	H	5.8853	1.7074	0.6933

Table S7. Cartesian coordinate for the optimized S_1 state geometry of the quinoid form of **1**

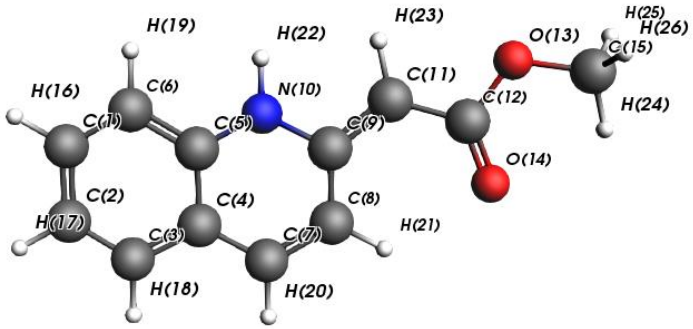

label	atom	coordinates (Å)		
		x	*y*	*z*
1	C	-4.1666	0.714	-0.504
2	C	-4.3623	-0.5719	0.0401
3	C	-3.2983	-1.3416	0.4417
4	C	-1.9648	-0.8696	0.3222
5	C	-1.7925	0.4445	-0.2366
6	C	-2.8868	1.2144	-0.6394
7	C	-0.8304	-1.5921	0.7083
8	C	0.4593	-1.0451	0.555
9	C	0.6164	0.2212	0.0156
10	N	-0.522	0.9217	-0.3634
11	C	1.806	0.9317	-0.2159
12	C	3.1344	0.4472	0.0888
13	O	4.061	1.3773	-0.2563
14	O	3.4099	-0.6347	0.5826
15	C	5.4414	1.0648	-0.0264
16	H	-5.0176	1.3067	-0.8151
17	H	-5.3706	-0.9569	0.1422
18	H	-3.4591	-2.329	0.8589
19	H	-2.7117	2.2011	-1.0556
20	H	-0.9553	-2.5818	1.1289
21	H	1.3476	-1.5827	0.8453
22	H	-0.3968	1.8433	-0.7548
23	H	1.7402	1.9215	-0.6545
24	H	5.5496	0.0562	0.3676
25	H	5.9636	1.1575	-0.9784
26	H	5.8348	1.7913	0.6846

Table S8. Cartesian coordinate for the optimized T_1 state geometry of the quinoid form of **1**

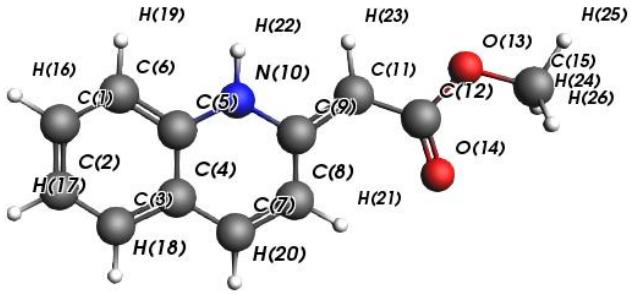

label	atom	coordinates (Å)		
		x	*y*	*z*
1	C	-4.1948	0.6536	-0.5349
2	C	-4.3684	-0.5919	0.0822
3	C	-3.2774	-1.3091	0.5193
4	C	-1.9628	-0.8201	0.3616
5	C	-1.8111	0.4492	-0.2694
6	C	-2.9221	1.1675	-0.7076
7	C	-0.8131	-1.5202	0.7948
8	C	0.4665	-0.9518	0.5976
9	C	0.6116	0.2778	-0.015
10	N	-0.5427	0.9521	-0.4389
11	C	1.8298	0.9575	-0.2726
12	C	3.1481	0.4783	0.0652
13	O	4.0941	1.37	-0.3179
14	O	3.4249	-0.5743	0.6178
15	C	5.4405	0.9788	-0.0247
16	H	-5.0542	1.2166	-0.877
17	H	-5.3666	-0.9918	0.2166
18	H	-3.4112	-2.2732	0.9971
19	H	-2.7731	2.131	-1.1837
20	H	-0.9201	-2.483	1.2741
21	H	1.366	-1.4565	0.9171
22	H	-0.4394	1.8492	-0.8827
23	H	1.7876	1.9217	-0.7644
24	H	5.6846	0.0506	-0.5426
25	H	6.0666	1.7936	-0.3794
26	H	5.5665	0.8338	1.0488

Table S9. Cartesian coordinate for the optimized ground state geometry of **A**

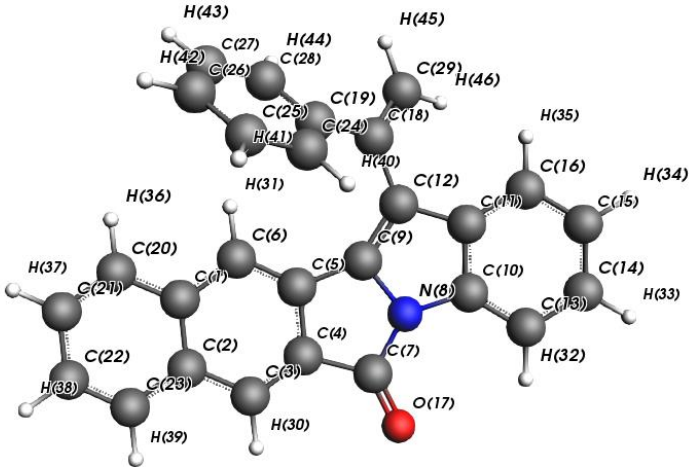

label	atom	coordinates (Å)		
		x	*y*	*z*
1	C	-2.7187	-1.1796	0.3749
2	C	-2.5675	-2.5642	0.7133
3	C	-1.2757	-3.1527	0.665
4	C	-0.2127	-2.3808	0.3032
5	C	-0.3539	-0.9965	-0.0366
6	C	-1.5891	-0.4071	-0.0062
7	C	1.217	-2.7731	0.1848
8	N	1.8545	-1.595	-0.2157
9	C	0.978	-0.5062	-0.361
10	C	3.151	-1.2058	-0.5226
11	C	3.084	0.1659	-0.8757
12	C	1.6889	0.5944	-0.7744
13	C	4.3376	-1.923	-0.4948
14	C	5.4998	-1.2346	-0.8291
15	C	5.4659	0.1252	-1.165
16	C	4.2696	0.8336	-1.1892
17	O	1.7584	-3.8454	0.376
18	C	1.1663	1.9342	-1.07
19	C	0.0818	2.4616	-0.2017
20	C	-4.01	-0.6035	0.4345
21	C	-5.0997	-1.3537	0.8047
22	C	-4.95	-2.7179	1.134
23	C	-3.7102	-3.3081	1.0886
24	C	0.1092	2.2468	1.1802
25	C	-0.9133	2.7207	1.9923
26	C	-1.9875	3.4106	1.4363
27	C	-2.0252	3.6317	0.0622
28	C	-0.9985	3.1621	-0.7494
29	C	1.6538	2.6638	-2.0842

30	H	-1.142	-4.198	0.9155
31	H	-1.7279	0.6338	-0.2569
32	H	4.3496	-2.9679	-0.2196
33	H	6.4475	-1.7579	-0.8206
34	H	6.3903	0.6341	-1.4071
35	H	4.2622	1.8859	-1.4379
36	H	-4.1233	0.4447	0.1849
37	H	-6.0813	-0.8984	0.8461
38	H	-5.8172	-3.2979	1.4237
39	H	-3.5905	-4.3546	1.3422
40	H	0.9328	1.6969	1.6163
41	H	-0.8755	2.5454	3.0602
42	H	-2.791	3.7682	2.068
43	H	-2.8611	4.1591	-0.3805
44	H	-1.0485	3.3077	-1.8208
45	H	1.2974	3.6681	-2.2705
46	H	2.4092	2.2723	-2.7508

Table S10. Cartesian coordinate for the optimized ground state geometry of **B**

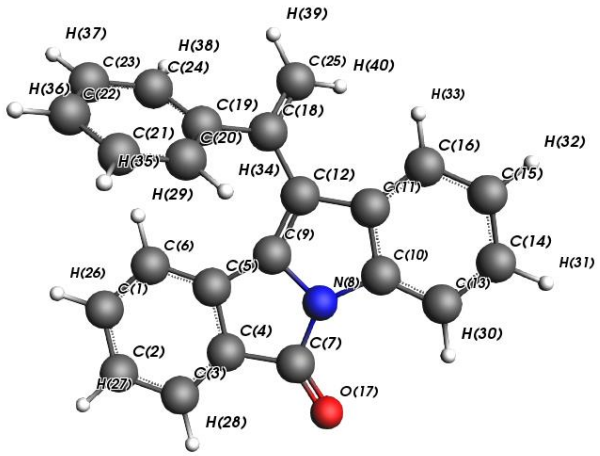

label	atom	coordinates (Å)		
		x	*y*	*z*
1	C	-4.0651	-2.137	0.4086
2	C	-3.8125	-3.4481	0.0038
3	C	-2.5011	-3.8905	-0.1757
4	C	-1.4752	-2.9958	0.0627
5	C	-1.7221	-1.6693	0.477
6	C	-3.0295	-1.2326	0.6492
7	C	-0.0078	-3.2117	-0.0637
8	N	0.5428	-1.9763	0.2924

9	C	-0.426	-1.0184	0.6281
10	C	1.813	-1.4214	0.3882
11	C	1.6311	-0.0743	0.7913
12	C	0.194	0.1671	0.9338
13	C	3.0619	-1.9848	0.1799
14	C	4.1678	-1.1651	0.3909
15	C	4.0182	0.1635	0.8071
16	C	2.7587	0.7172	1.0127
17	O	0.6155	-4.2012	-0.3967
18	C	-0.44	1.4342	1.3193
19	C	-1.6146	1.375	2.2268
20	C	-1.649	0.4621	3.2863
21	C	-2.7451	0.4039	4.1378
22	C	-3.8324	1.2507	3.9393
23	C	-3.8111	2.1612	2.8861
24	C	-2.7112	2.2234	2.0382
25	C	0.0336	2.6078	0.8758
26	H	-5.0892	-1.8109	0.5407
27	H	-4.6391	-4.1238	-0.1736
28	H	-2.284	-4.9023	-0.4929
29	H	-3.2481	-0.2236	0.9642
30	H	3.1641	-3.0156	-0.1279
31	H	5.1614	-1.5665	0.2374
32	H	4.8997	0.7692	0.9744
33	H	2.6582	1.741	1.346
34	H	-0.8117	-0.2059	3.44
35	H	-2.7528	-0.3069	4.9548
36	H	-4.6917	1.1974	4.5961
37	H	-4.6571	2.8158	2.717
38	H	-2.7121	2.9134	1.2042
39	H	-0.4059	3.5436	1.1941
40	H	0.8607	2.6572	0.1817

Table S11. Cartesian coordinate for the optimized ground state geometry of **C**

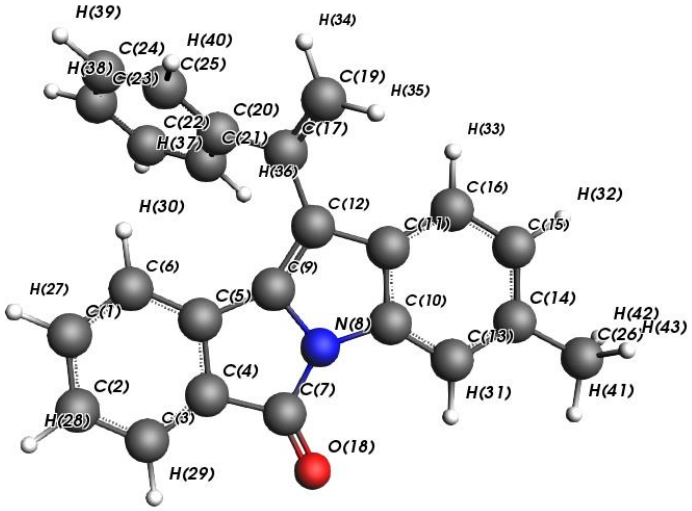

label	atom	coordinates (Å)		
		x	*y*	*z*
1	C	-3.8542	-1.4853	0.6434
2	C	-3.7324	-2.8538	0.3986
3	C	-2.4817	-3.4141	0.1362
4	C	-1.3832	-2.5754	0.1246
5	C	-1.498	-1.1892	0.3671
6	C	-2.7454	-0.6375	0.6322
7	C	0.0443	-2.9207	-0.1154
8	N	0.7068	-1.695	-0.0047
9	C	-0.1566	-0.6252	0.2791
10	C	2.0177	-1.2414	-0.0813
11	C	1.9731	0.1509	0.1681
12	C	0.5783	0.5287	0.4007
13	C	3.191	-1.9252	-0.3605
14	C	4.3793	-1.1958	-0.4019
15	C	4.3475	0.1924	-0.1745
16	C	3.1683	0.87	0.1053
17	C	0.0842	1.8757	0.7125
18	O	0.5657	-3.9936	-0.3527
19	C	0.7778	2.7001	1.5113
20	C	-1.2028	2.3018	0.1042
21	C	-1.5153	1.9541	-1.2143
22	C	-2.7191	2.3463	-1.7858
23	C	-3.6384	3.0852	-1.0454
24	C	-3.3396	3.4353	0.2688
25	C	-2.1321	3.0475	0.8382
26	C	5.6884	-1.8799	-0.6967
27	H	-4.8327	-1.0681	0.8464
28	H	-4.6133	-3.4825	0.4142

29	H	-2.3648	-4.4736	-0.0525
30	H	-2.8645	0.4186	0.8211
31	H	3.1771	-2.9907	-0.544
32	H	5.2758	0.7494	-0.2234
33	H	3.1795	1.9401	0.2617
34	H	0.4336	3.7064	1.7091
35	H	1.6942	2.3845	1.9899
36	H	-0.8104	1.3701	-1.7913
37	H	-2.9428	2.0705	-2.8088
38	H	-4.582	3.3808	-1.4868
39	H	-4.0533	4.0001	0.8559
40	H	-1.918	3.2963	1.8697
41	H	5.5484	-2.9477	-0.8617
42	H	6.1587	-1.4566	-1.5874
43	H	6.3906	-1.7532	0.1309

Table S12. Cartesian coordinate for the optimized ground state geometry of **D**

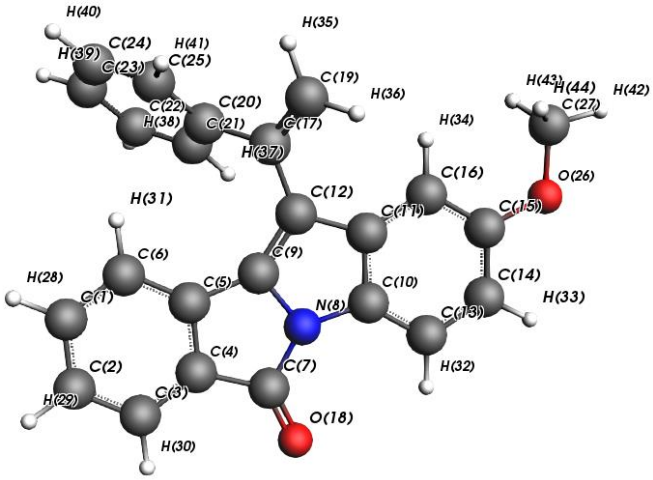

label	atom	coordinates (Å)		
		x	*y*	*z*
1	C	-3.8911	-1.9854	0.7081
2	C	-3.7673	-3.3431	0.3435
3	C	-2.5207	-3.8706	-0.0335
4	C	-1.4258	-3.0108	-0.044
5	C	-1.5439	-1.6661	0.2984
6	C	-2.7726	-1.1332	0.693
7	C	-0.0131	-3.2502	-0.3537
8	N	0.647	-2.0748	-0.1906
9	C	-0.1899	-1.1023	0.1657
10	C	1.8852	-1.5773	-0.2702
11	C	1.8454	-0.2304	0.0444

12	C	0.5021	0.1066	0.3211
13	C	3.0634	-2.2353	-0.6052
14	C	4.247	-1.4812	-0.6254
15	C	4.2378	-0.1003	-0.322
16	C	3.0152	0.5377	0.0152
17	C	-0.0518	1.4424	0.7038
18	O	0.5054	-4.3062	-0.6794
19	C	0.6665	2.2109	1.5473
20	C	-1.3663	1.9245	0.1468
21	C	-1.8891	1.3505	-1.0344
22	C	-3.1004	1.7904	-1.5746
23	C	-3.8142	2.8134	-0.9533
24	C	-3.3155	3.4025	0.2074
25	C	-2.1031	2.9696	0.7531
26	O	5.4184	0.5694	-0.3707
27	C	5.5962	1.9117	-0.1072
28	H	-4.856	-1.5967	1.0068
29	H	-4.6377	-3.9858	0.3634
30	H	-2.4147	-4.9136	-0.3014
31	H	-2.8792	-0.1019	0.9886
32	H	3.0718	-3.2905	-0.8442
33	H	5.1789	-1.9682	-0.8838
34	H	2.9859	1.5935	0.2345
35	H	0.3537	3.1984	1.8583
36	H	1.6032	1.8651	1.9685
37	H	-1.362	0.5644	-1.5562
38	H	-3.4845	1.3373	-2.4794
39	H	-4.7526	3.152	-1.3731
40	H	-3.8705	4.1978	0.6883
41	H	-1.7687	3.4539	1.6579
42	H	6.6694	2.1653	-0.2274
43	H	5.0056	2.5248	-0.8208
44	H	5.2927	2.1416	0.9364

Table S13. Cartesian coordinate for the optimized ground state geometry of **E**

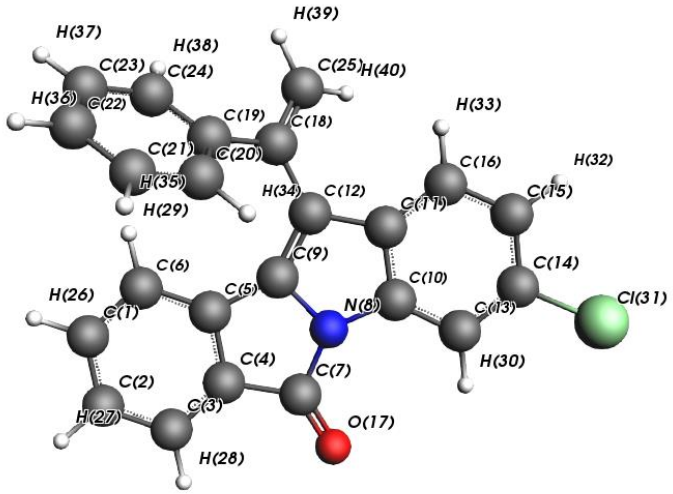

label	atom	coordinates (Å)		
		x	*y*	*z*
1	C	-4.0629	-2.1352	0.4077
2	C	-3.8105	-3.4465	0.0028
3	C	-2.4996	-3.8902	-0.1755
4	C	-1.4731	-2.9955	0.0618
5	C	-1.72	-1.668	0.4734
6	C	-3.0271	-1.231	0.6474
7	C	-0.0063	-3.2131	-0.0633
8	N	0.5447	-1.9748	0.2924
9	C	-0.4252	-1.0162	0.6251
10	C	1.8117	-1.4197	0.3878
11	C	1.6298	-0.0718	0.7892
12	C	0.1941	0.1694	0.9321
13	C	3.0572	-1.9903	0.1807
14	C	4.1508	-1.1612	0.3976
15	C	4.0205	0.1673	0.8105
16	C	2.7592	0.7156	1.0102
17	O	0.6198	-4.2003	-0.3939
18	C	-0.4395	1.4367	1.3194
19	C	-1.6131	1.3762	2.2284
20	C	-1.6475	0.4602	3.2852
21	C	-2.7425	0.4011	4.1381
22	C	-3.8298	1.2485	3.9422
23	C	-3.8099	2.16	2.8898
24	C	-2.7108	2.2237	2.041
25	C	0.0304	2.6092	0.8693
26	H	-5.0869	-1.809	0.5399
27	H	-4.6375	-4.1217	-0.175
28	H	-2.2833	-4.9024	-0.4921

29	H	-3.2447	-0.2218	0.9632
30	H	3.1688	-3.0195	-0.1245
31	Cl	5.7668	-1.816	0.156
32	H	4.9078	0.7615	0.9767
33	H	2.665	1.7398	1.3435
34	H	-0.8106	-0.2087	3.437
35	H	-2.7496	-0.3113	4.9536
36	H	-4.6883	1.1943	4.6
37	H	-4.6564	2.8145	2.7224
38	H	-2.7136	2.9136	1.207
39	H	-0.4114	3.5455	1.1826
40	H	0.8524	2.6571	0.1689

Table S14. Cartesian coordinate for the optimized ground state geometry of **F**

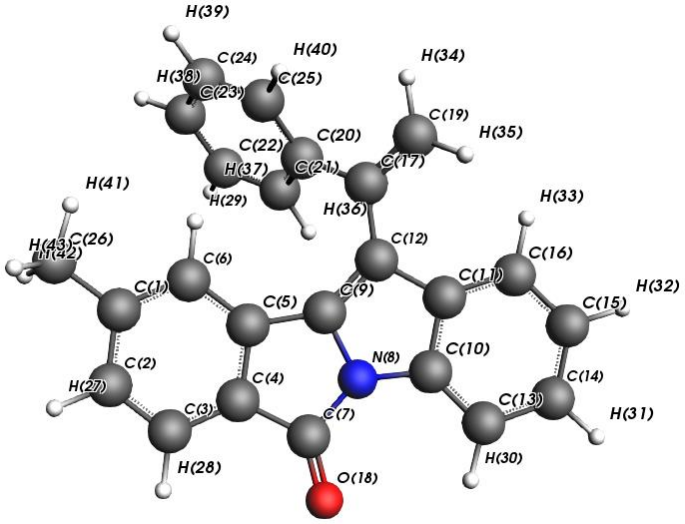

label	atom	coordinates (Å)		
		x	*y*	*z*
1	C	1.985	2.1704	-0.1951
2	C	1.6293	3.3189	-0.9432
3	C	0.3001	3.5325	-1.3446
4	C	-0.6485	2.5774	-0.9944
5	C	-0.3102	1.4358	-0.2746
6	C	1.0013	1.218	0.1495
7	C	-2.0941	2.5206	-1.2316
8	N	-2.5581	1.3785	-0.662
9	C	-1.5659	0.6849	-0.1069
10	C	-3.7073	0.7221	-0.475
11	C	-3.4452	-0.4434	0.2268
12	C	-2.0552	-0.4967	0.4676
13	C	-4.9892	1.0809	-0.8847

14	C	-6.0414	0.2061	-0.568
15	C	-5.7903	-0.9915	0.1353
16	C	-4.4844	-1.3292	0.5368
17	C	-1.2856	-1.563	1.1809
18	O	-2.7828	3.3443	-1.8124
19	C	-1.8401	-2.1243	2.2741
20	C	0.0625	-2.0127	0.6801
21	C	0.4382	-1.7691	-0.6607
22	C	1.6794	-2.1862	-1.1485
23	C	2.5702	-2.8585	-0.314
24	C	2.2194	-3.1198	1.0096
25	C	0.9785	-2.7076	1.5049
26	C	3.4106	1.9784	0.2293
27	H	2.3832	4.0509	-1.2053
28	H	0.0224	4.4158	-1.9046
29	H	1.2628	0.3495	0.7326
30	H	-5.172	1.9978	-1.4292
31	H	-7.0514	0.4498	-0.8707
32	H	-6.6104	-1.6595	0.3644
33	H	-4.3109	-2.2575	1.0606
34	H	-1.3654	-2.9171	2.8361
35	H	-2.8005	-1.7951	2.6533
36	H	-0.2271	-1.263	-1.3458
37	H	1.9491	-1.9889	-2.178
38	H	3.5313	-3.18	-0.6938
39	H	2.9119	-3.6433	1.6563
40	H	0.7626	-2.927	2.5394
41	H	3.5421	1.0385	0.8069
42	H	4.0633	1.9324	-0.6677
43	H	3.728	2.8301	0.8669

Table S15. Cartesian coordinate for the optimized ground state geometry of **G**

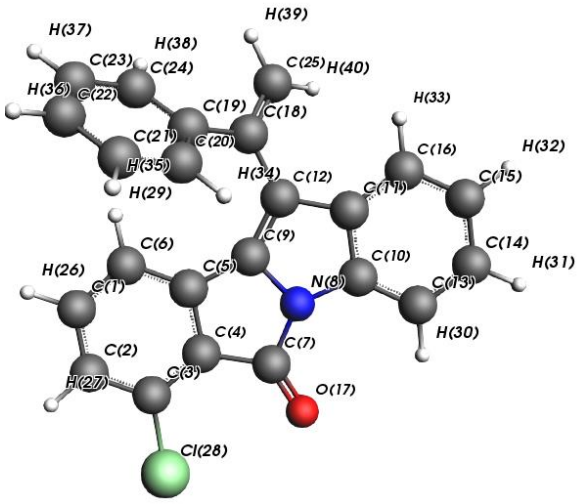

label	atom	coordinates (Å)		
		x	*y*	*z*
1	C	-4.0567	-2.1222	0.3898
2	C	-3.8211	-3.4345	-0.0077
3	C	-2.5115	-3.8845	-0.1772
4	C	-1.4571	-3.0177	0.0552
5	C	-1.7115	-1.6851	0.4629
6	C	-3.0115	-1.2307	0.6296
7	C	0.0177	-3.2253	-0.058
8	N	0.5527	-1.983	0.3001
9	C	-0.4204	-1.0302	0.6229
10	C	1.8199	-1.4225	0.4007
11	C	1.6287	-0.0747	0.7971
12	C	0.1905	0.1607	0.9302
13	C	3.0731	-1.9805	0.2024
14	C	4.1727	-1.154	0.418
15	C	4.0139	0.1758	0.8283
16	C	2.7508	0.724	1.0233
17	O	0.6617	-4.2017	-0.3803
18	C	-0.4487	1.4275	1.309
19	C	-1.6183	1.371	2.2231
20	C	-1.6449	0.4635	3.2874
21	C	-2.7383	0.4044	4.1424
22	C	-3.8294	1.2465	3.9438
23	C	-3.8147	2.1532	2.8872
24	C	-2.7181	2.2155	2.035
25	C	0.0177	2.5992	0.8529
26	H	-5.0791	-1.7896	0.5155
27	H	-4.6438	-4.112	-0.1883
28	Cl	-2.2472	-5.5386	-0.6807

29	H	-3.2154	-0.2179	0.9406
30	H	3.1829	-3.0118	-0.1005
31	H	5.1695	-1.5509	0.2732
32	H	4.8914	0.7862	0.9995
33	H	2.6422	1.7486	1.3517
34	H	-0.8039	-0.1998	3.4421
35	H	-2.7409	-0.3029	4.9623
36	H	-4.6859	1.1933	4.6042
37	H	-4.6632	2.8049	2.7191
38	H	-2.7239	2.9023	1.1983
39	H	-0.4274	3.5354	1.162
40	H	0.8443	2.6461	0.158

Table S16. Cartesian coordinate for the optimized ground state geometry of **H**

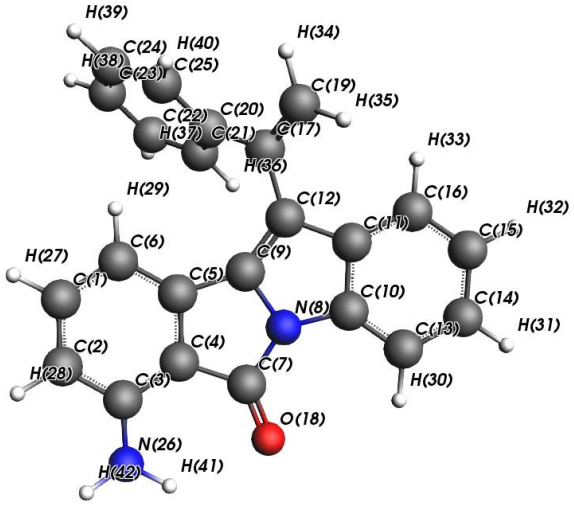

label	atom	coordinates (Å)		
		x	*y*	*z*
1	C	1.9241	2.1253	0.1506
2	C	1.5908	3.2929	-0.5643
3	C	0.2755	3.508	-1.0223
4	C	-0.679	2.5171	-0.7502
5	C	-0.341	1.3533	-0.0574
6	C	0.9551	1.145	0.4148
7	C	-2.12	2.4221	-1.043
8	N	-2.5683	1.2472	-0.5315
9	C	-1.5787	0.5624	0.0352
10	C	-3.7046	0.5532	-0.4116

11	C	-3.4353	-0.6291	0.2578
12	C	-2.0544	-0.6527	0.5486
13	C	-4.9805	0.8912	-0.8565
14	C	-6.018	-0.023	-0.6106
15	C	-5.7585	-1.238	0.0589
16	C	-4.459	-1.5539	0.4972
17	C	-1.2832	-1.7244	1.2515
18	O	-2.8203	3.2396	-1.6179
19	C	-1.8607	-2.3347	2.3059
20	C	0.0902	-2.1278	0.7802
21	C	0.5054	-1.8241	-0.5364
22	C	1.7697	-2.1996	-0.9981
23	C	2.645	-2.8889	-0.1611
24	C	2.2559	-3.2087	1.1387
25	C	0.9918	-2.8384	1.6077
26	N	-0.0522	4.6941	-1.7258
27	H	2.9374	1.9843	0.5037
28	H	2.3582	4.0334	-0.7516
29	H	1.2233	0.2648	0.9763
30	H	-5.1699	1.8219	-1.3747
31	H	-7.0229	0.2037	-0.9424
32	H	-6.5668	-1.9361	0.2334
33	H	-4.2777	-2.4953	0.9945
34	H	-1.3874	-3.1357	2.8573
35	H	-2.8407	-2.0395	2.6624
36	H	-0.1464	-1.3034	-1.2236
37	H	2.0693	-1.957	-2.0095
38	H	3.624	-3.1783	-0.5207
39	H	2.9365	-3.7452	1.7873
40	H	0.7463	-3.1031	2.6248
41	H	-1.0061	4.87	-2.0679
42	H	0.6686	5.4071	-1.9099

Table S17. Calculated spin densities in the optimized geometries of the ground state, the radical cation, and the triplet state of **1**

label[a]	atom	spin density		
		ground state	radical cation	triplet state
1	C	0.0938	-0.0049	0.0937
2	C	0.0049	0.1112	0.0049
3	C	0.0728	-0.0654	0.0728
4	C	0.0063	0.1173	0.0063
5	C	0.0445	0.0272	0.0444
6	C	0.0142	0.0334	0.0142
7	C	0.1723	-0.055	0.1724
8	C	0.1021	0.1539	0.102
9	C	0.0061	-0.1461	0.0062
10	N	0.1076	0.146	0.1077
11	C	0.3501	0.6652	0.35
12	C	-0.0053	-0.0499	-0.0054
13	O	0.02	0.0295	0.02
14	O	0.0618	0.0842	0.0619
15	C	-0.0018	-0.0025	-0.0018
16	H	-0.0062	-0.0001	-0.0062
17	H	-0.0005	-0.0064	-0.0005
18	H	-0.0046	0.0027	-0.0046
19	H	-0.0015	-0.0024	-0.0015
20	H	-0.0118	0.0023	-0.0118
21	H	-0.0063	-0.008	-0.0063
22	H	-0.0042	-0.0062	-0.0042
23	H	-0.0181	-0.0319	-0.0181
24	H	0.0018	0.0028	0.0018
25	H	0.0002	0.0003	0.0002
26	H	0.0018	0.0027	0.0018

[a]Refer to Table S3 for labels

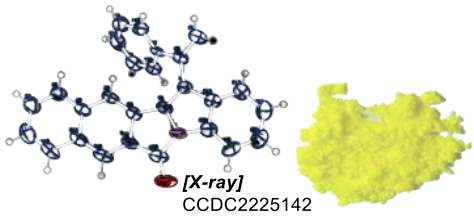

Figure S1. X-ray crystal structure of A. Oak Ridge Thermal Ellipsoid Plot (ORTEP) drawing at the 50% probability level and their image of yellow powder.

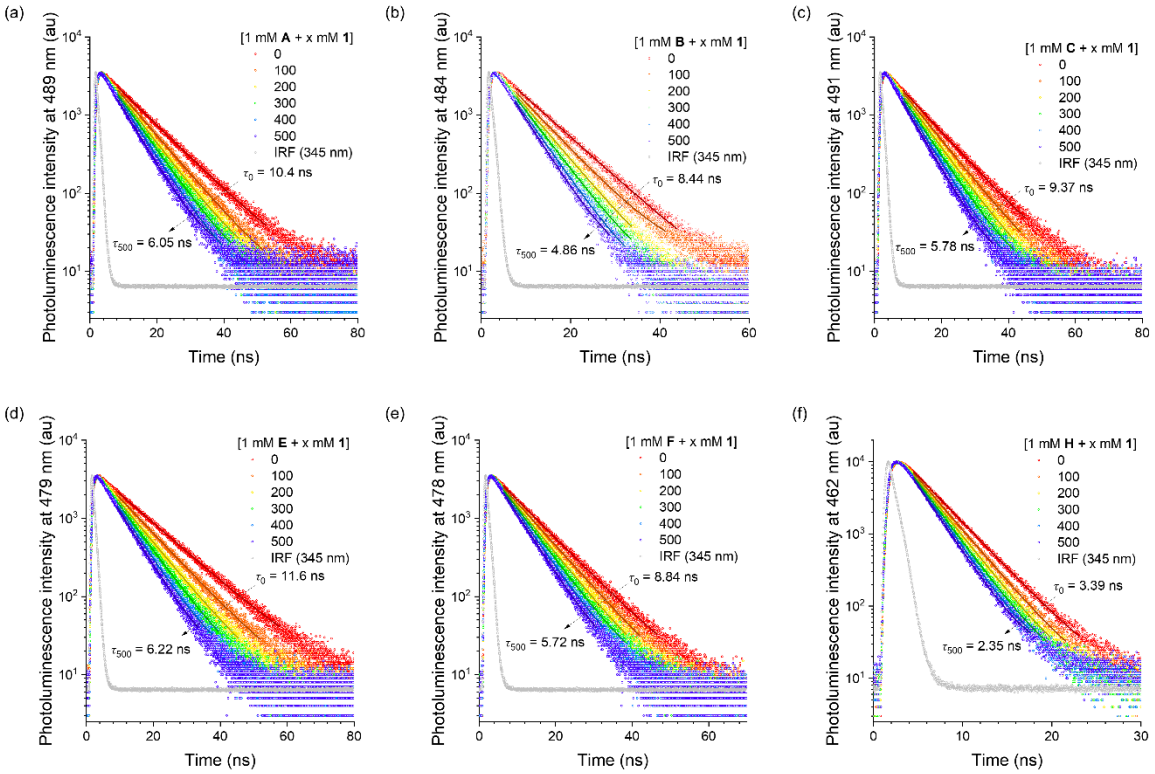

Figure S2. **Photoluminescence quenching.** Photoluminescence decay traces of 1.0 mM organoPCs monitored after picosecond pulsed laser photoexcitation (temporal resolution = 0.025 ns) at 345 nm with increased concentrations of **1** (0−500 mM) in 1,4-dioxane. Solid curves are nonlinear least-squares fits to a monoexponential decay model.

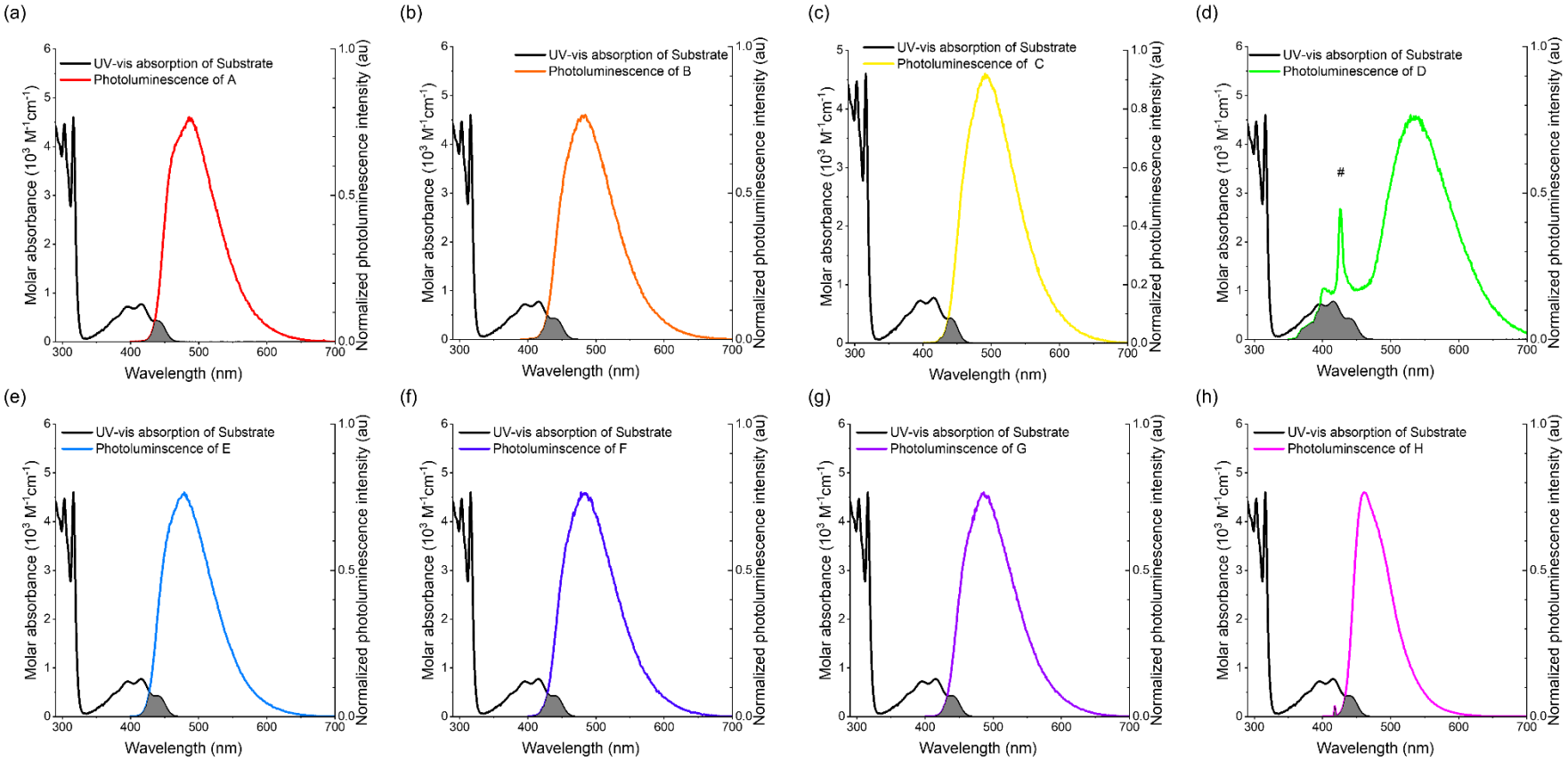

Figure S3. Spectral overlap. Overlaps between the UV–Vis absorption spectrum of **1** (black curves) and the photoluminescence spectra of organoPCs (colored curves). The spectral overlap integrals are indicated in grey, and their values (*J*) are listed in Table 2 in the main text. The peak marked with a hashtag (#) corresponds to the Raman scattering of the solvent (1,4-dioxane).

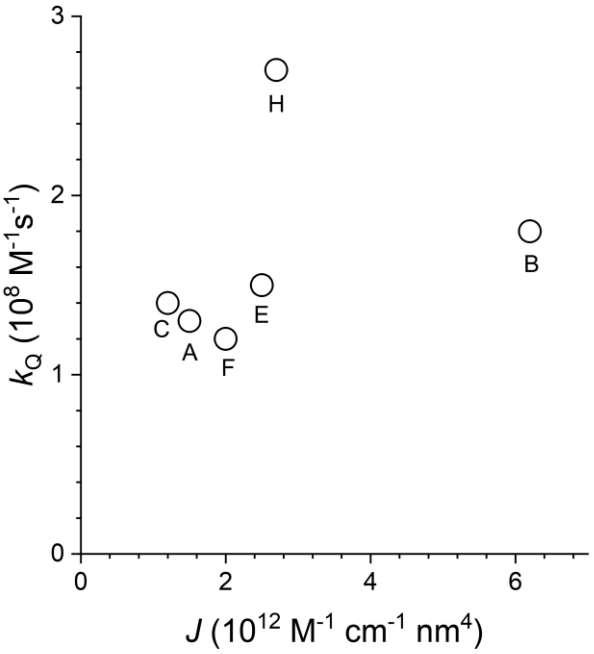

Figure S4. Correlation. Plot of the k_Q value as a function of J.

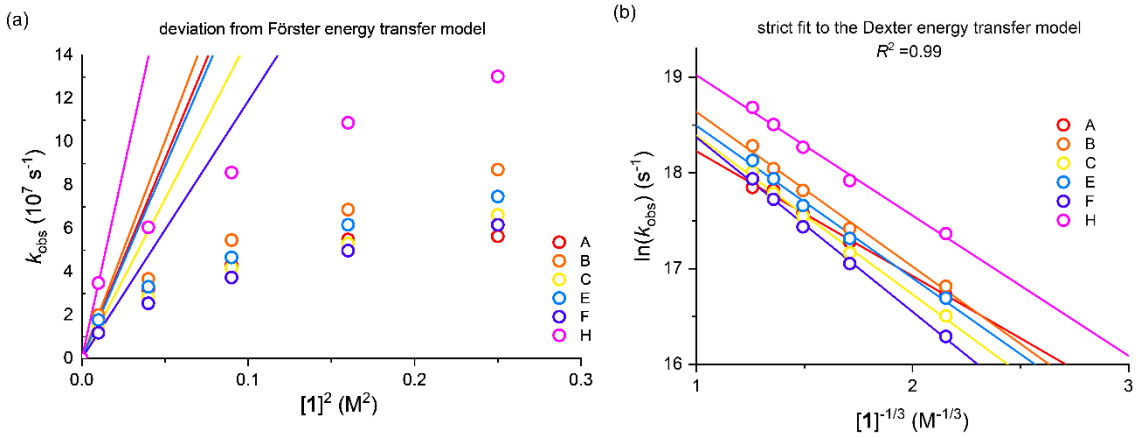

Figure S5. **Energy transfer.** Analyses of the photoluminescence (fluorescence quenching rate constant (k_{obs}) based on two energy transfer mechanisms of (a) the Förster formalism and (b) the Dexter formalism. The lines in (a) show visual guidance where the Förster energy transfer mechanism applies (i.e., $k_{obs} \propto [\mathbf{1}]^2$), whereas the lines in (b) show visual guidance where the Dexter energy transfer mechanism applies (i.e., ln (k_{obs}) $\propto [\mathbf{1}]^{-1/3}$).

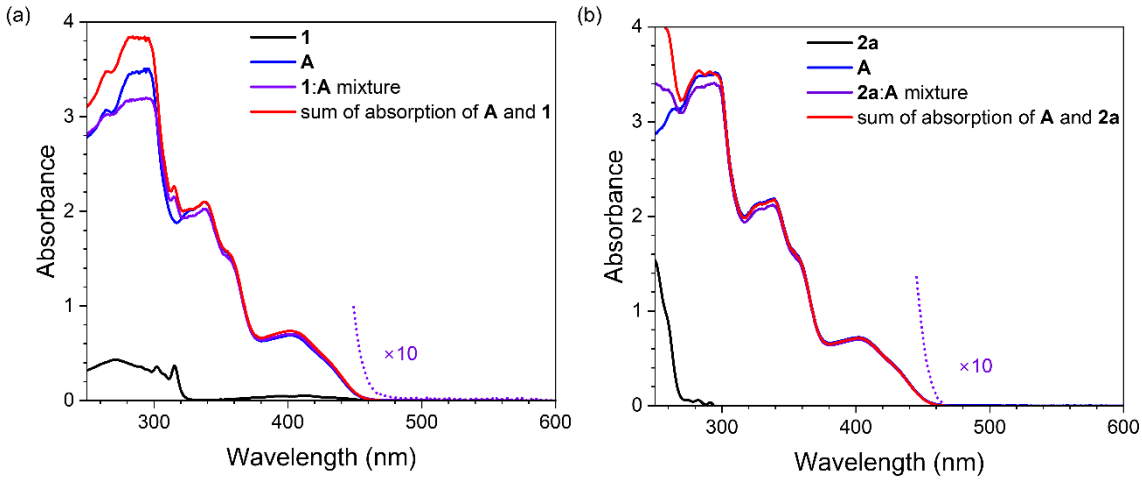

Figure S6. Comparisons of UV–Vis absorption spectra. UV–Vis absorption spectra for (a) **1**, **A**, and their equimolar mixture, and (b) **2a**, **A**, and their equimolar mixture recorded in 1,4-dioxane (1 mM). Mathematical sums of the spectra of individual species (i.e., **A** and **1** or **2a**) are included.

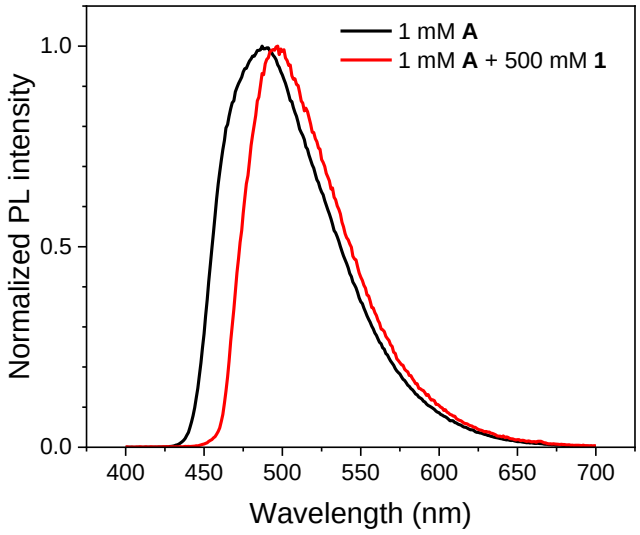

Figure S7. Photoluminescence spectra. Normalized photoluminescence spectra of 1.0 mM **A** recorded in the absence (black) and presence (red) of 500 mM **1** (λ_{ex} = 345 nm, 1,4-dioxane).

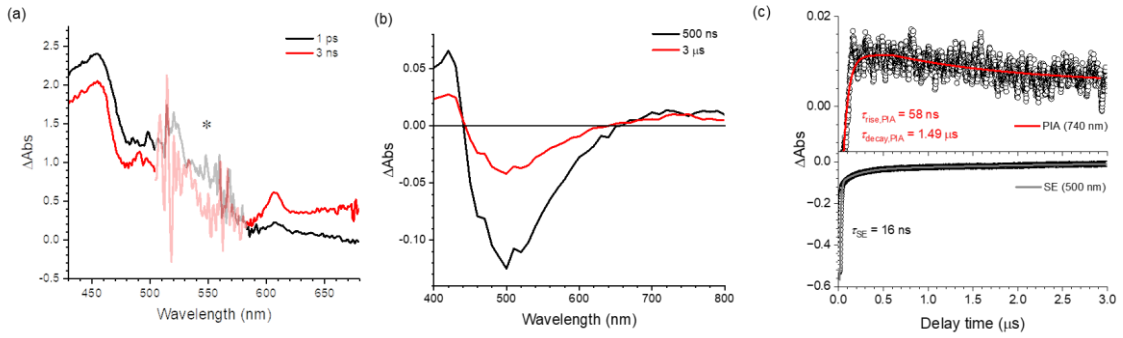

Figure S8. **Intersystem crossing.** (a) Femtosecond (λ_{ex} = 340 nm) transient UV–Vis absorption spectra of 1.0 mM **A** recorded at delay times of 1 ps (black) and 3 ns (red). The region marked with an asterisk (*) contain instrumental drifts due to the excitation beam. (b) Nanosecond (λ_{ex} = 355 nm) transient UV–Vis–NIR absorption spectra of 100 μM **A** recorded at delay times of 500 ns (black) and 3 μs (red). (c) Traces of the transient absorption signals monitored at wavelengths of 740 (top panel) and 500 nm (bottom panel). The thick curves are nonlinear least-squares fits.

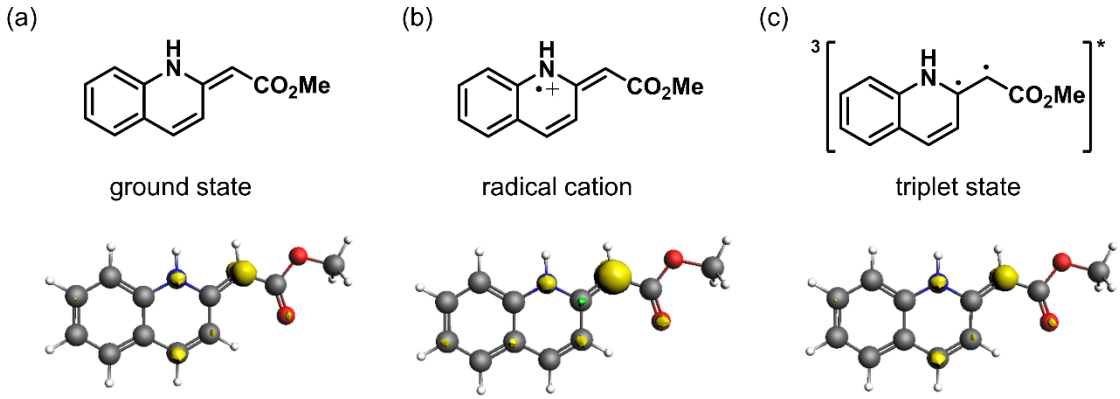

Figure 9. Spin densities. Spin density isosurface plots (isovalue = 0.01) in the optimized geometries for (a) the ground state, (b) the radical cation, and (c) the triplet state of **1** calculated at the level of uB3LYP-D3(BJ)/TZP with the solvation method based on the conductor-like screening model parameterized for 1,4-dioxane.

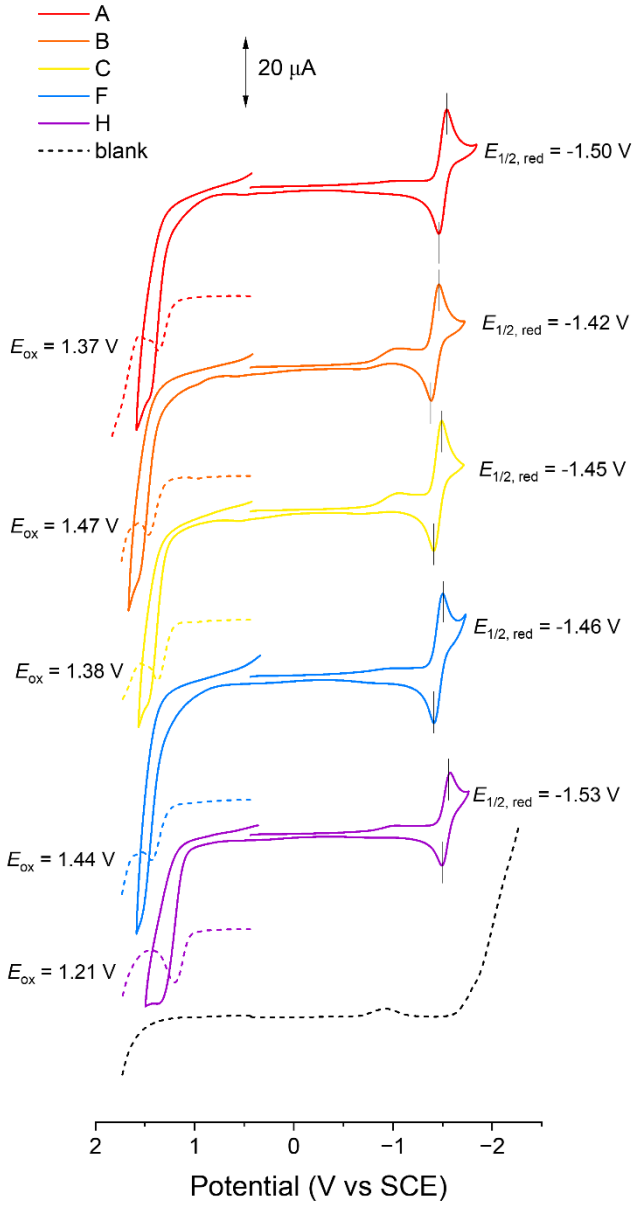

Figure S10. **Electrochemical potentials**. Cyclic (CV) and differential pulse (DPV) voltammograms of organoPCs. Conditions: Ar-saturated DMF containing 2.0 mM organoPC and 0.10 M $TBAPF_6$; a Pt disc and a Pt wire as the working and the counter electrodes, respectively; an $Ag/AgNO_3$ pseudo reference electrode; scan rate = 0.10 V s^{-1} for CV and 4 mV s^{-1} for DPV.

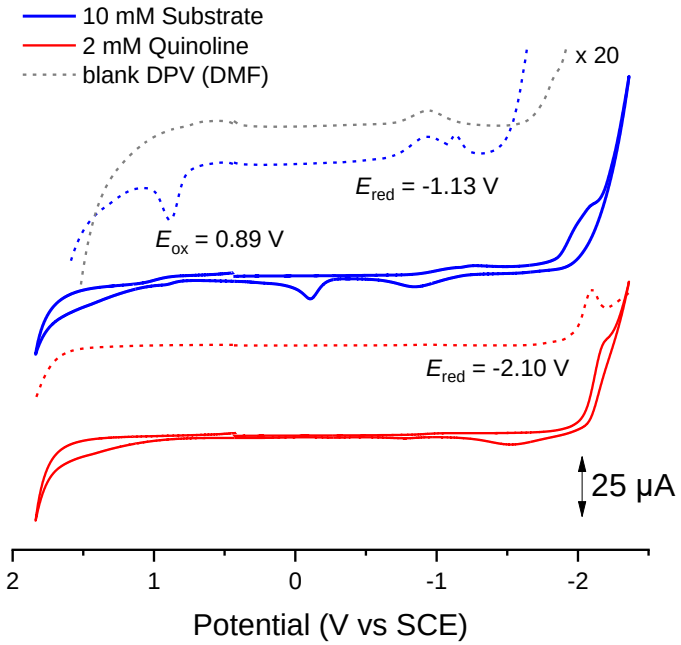

Figure S11. **Electrochemical potentials of substrate**. Cyclic (CV) and differential pulse (DPV) voltammograms of 2.0 mM quinoline (red) and 10 mM **1** (blue). Conditions: Ar-saturated DMF containing the sample and 0.10 M $TBAPF_6$; a Pt disc and a Pt wire as the working and the counter electrodes, respectively; an $Ag/AgNO_3$ pseudo reference electrode; scan rate = 0.10 V s^{-1} for CV and 4 mV s^{-1} for DPV.

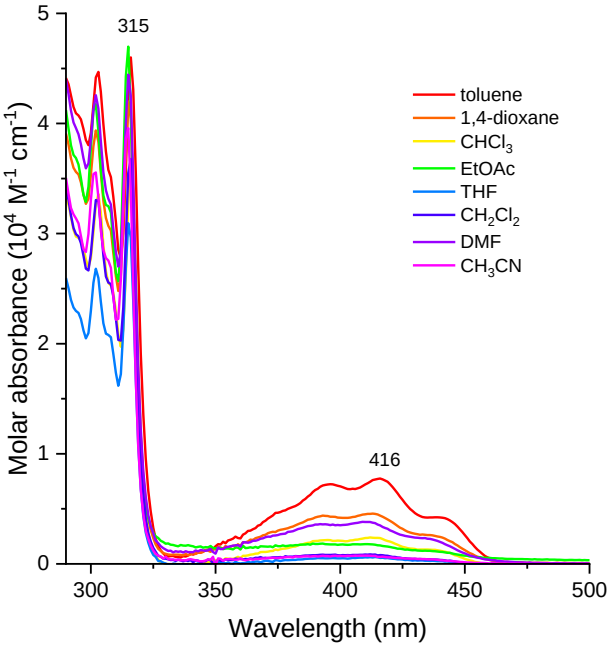

Figure S12. **Absorption of substrate.** UV–Vis absorption spectra of 100 µM **1** recorded in a variety of solutions. The numbers are the peak wavelengths of the benzenoid (315 nm) and the quinoid (416 nm) forms of **1**.

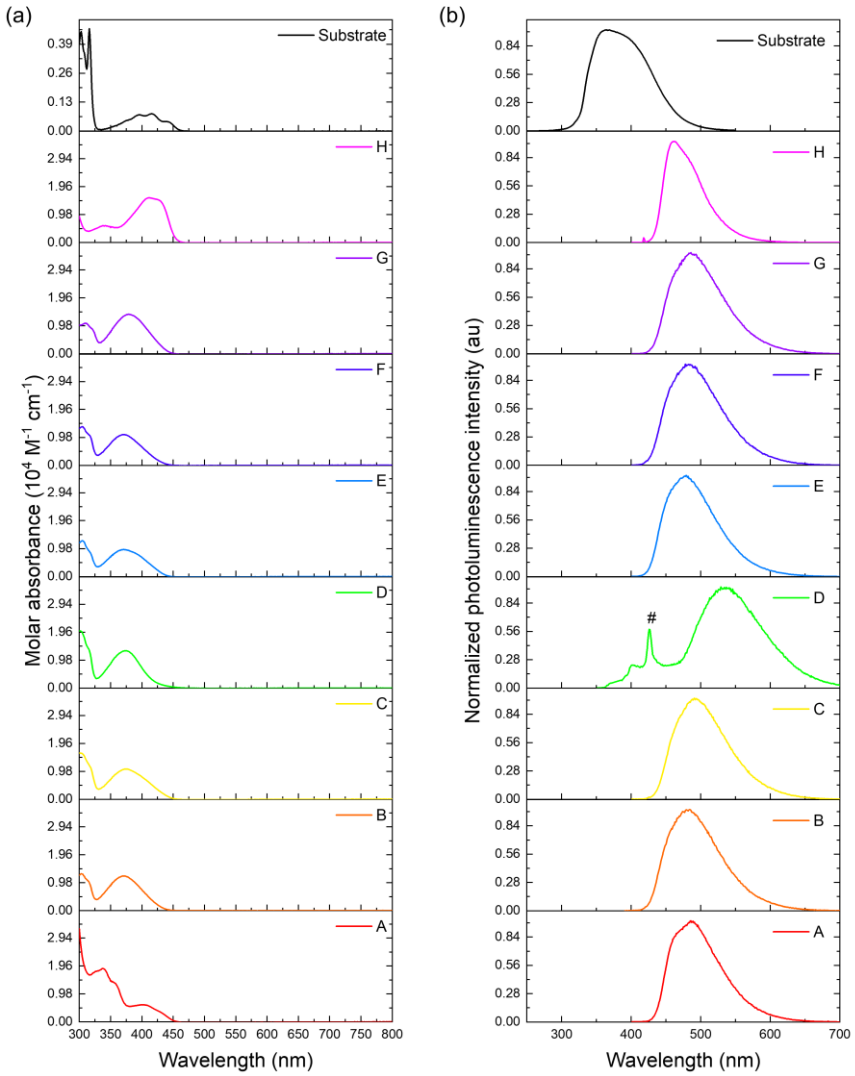

Figure S13. **Steady-state electronic spectra**. (a) UV–Vis absorption and (b) photoluminescence spectra of 10 μM organoPCs recorded in 1,4-dioxane. λ_{ex} (nm) = 341 (**A**), 374 (**B**), 378 (**C**), 379 (**D**), 380 (**E**), 375 (**F**), 380 (**G**), 419 (**H**), and 307 (**1**). The peak marked with a hashtag (#) corresponds to the Raman scattering of the solvent (1,4-dioxane).

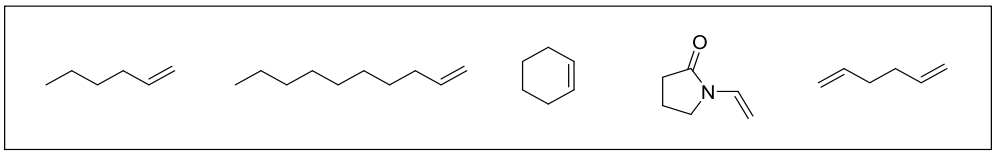

Figure S14. **Unsuccessful alkene substrates.**

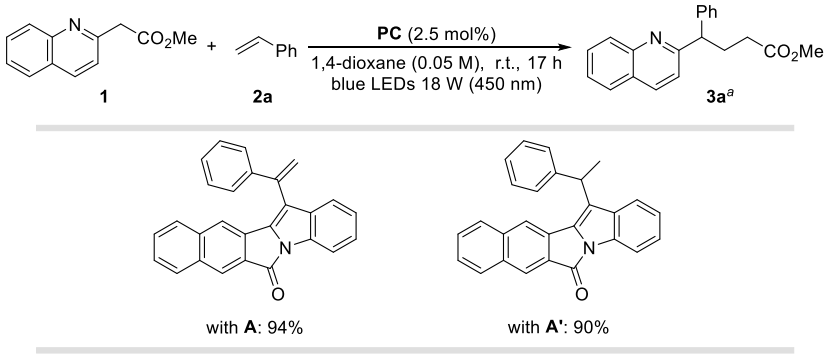

[a]The yields were determined by ^{1}H NMR spectroscopy using bromoform as an internal standard.

Figure S15. The effect of alkenyl moiety of photocatalyst on photocatalytic reactivity: the alkenyl substituent did not affect the photocatalytic reactivity.

Analytic Data for Synthesized Compounds

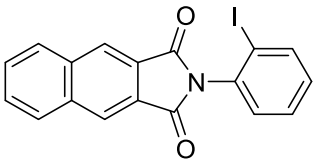

2-(2-iodophenyl)-1H-benzo[f]isoindole-1,3(2H)-dione, **S1**: white solid; melting point 216~218 ℃; **^{1}H NMR (600 MHz, $CDCl_3$)** δ 8.50 (s, 2H), 8.12 (dd, *J* = 6.1, 3.3 Hz, 2H), 8.01 (dd, *J* = 8.0, 1.3 Hz, 1H), 7.75 (dd, *J* = 6.1, 3.3 Hz, 2H), 7.53 (ddd, *J* = 7.8, 7.6, 1.3 Hz, 1H), 7.37 (dd, *J* = 7.8, 1.6 Hz, 1H), 7.22 (ddd, *J* = 8.0, 7.6, 1.6 Hz, 1H); **^{13}C NMR (151 MHz, $CDCl_3$)** δ 166.55, 140.12, 135.93, 135.68, 131.23, 130.63, 130.37, 129.68, 129.61, 127.80, 125.87, 99.04; **HRMS** (ESI) *m/z*: $[M]^+$ calc. for $C_{18}H_{10}INO_2$, 398.9756; found, 398.9758; **IR (neat)**: ν_{max} = 3059, 2353, 1717, 1372 cm^{-1}; ***R*$_f$** 0.32 (Hex/EtOAc, 4/1).

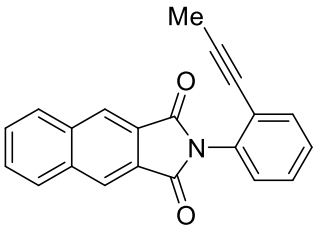

2-(2-(prop-1-yn-1-yl)phenyl)-1H-benzo[f]isoindole-1,3(2H)-dione, **S2**: white solid; melting point 212~214 ℃; **^{1}H NMR (600 MHz, $CDCl_3$)** δ 8.48 (s, 2H), 8.11 (dd, *J* = 6.2, 3.3 Hz, 2H), 7.74 (dd, *J* = 6.2, 3.3 Hz, 2H), 7.59 (dd, *J* = 7.5, 1.6 Hz, 1H), 7.44 (ddd, *J* = 7.7, 7.4, 1.6 Hz, 1H), 7.41 (ddd, *J* = 7.7, 7.5, 1.5 Hz, 1H), 7.34 (dd, *J* = 7.4, 1.5 Hz, 1H), 1.83 (s, 3H); **^{13}C NMR (151 MHz, $CDCl_3$)** δ 167.00, 135.87, 133.68, 133.35, 130.56, 129.51, 129.29, 129.05, 128.64, 128.04, 125.48, 124.12, 91.68, 76.00, 4.63; **HRMS** (ESI) *m/z*: $[M]^+$ calc. for $C_{21}H_{13}NO_2$, 311.0946; found, 311.0944; **IR (neat)**: ν_{max} = 3028, 2251, 1718, 1372 cm^{-1}; ***R*$_f$** 0.32 (Hex/EtOAc, 4/1).

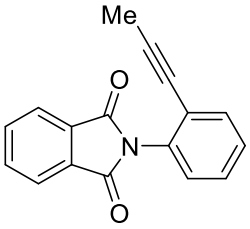

2-(2-(prop-1-yn-1-yl)phenyl)isoindoline-1,3-dione, **S4a**: colorless solid; melting point 134~136 ℃; **^{1}H NMR (600 MHz, $CDCl_3$)** δ 7.96 (dd, *J* = 5.4, 3.1 Hz, 2H), 7.78 (dd, *J* = 5.4, 3.1 Hz, 2H), 7.56 (dd, *J* = 7.5, 1.8 Hz, 1H), 7.41 (td, *J* = 7.5, 1.6 Hz, 1H), 7.38 (td, *J* = 7.5, 1.6 Hz, 1H), 7.28 (dd, *J* = 7.7, 1.5 Hz, 1H), 1.83 (s, 3H); **^{13}C NMR (151 MHz, $CDCl_3$)** δ 167.13, 134.39, 133.36, 133.20, 132.19, 129.15, 129.06, 128.53, 124.08, 123.85, 91.55, 75.92, 4.50; **IR (neat)**: ν_{max} = 2988, 2901, 2338, 1720, 1382, 1079, 718 cm^{-1}; **HRMS** (EI) *m/z*: calc. for $C_{17}H_{11}NO_2$ $[M]^+$ 261.0790, found 261.0789; ***R*$_f$** 0.31 (Hex/EtOAc, 4/1).

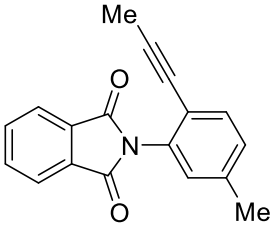

2-(5-methyl-2-(prop-1-yn-1-yl)phenyl)isoindoline-1,3-dione, **S4b**: colorless solid; melting point 156~158 ℃; **^{1}H NMR (600 MHz, $CDCl_3$)** δ 7.96 (dd, *J* = 5.4, 3.1 Hz, 2H), 7.78 (dd, *J* = 5.4, 3.1 Hz, 2H), 7.45 (d, *J* = 7.9 Hz, 1H), 7.20 (d, *J* = 7.9 Hz, 1H), 7.10 (s, 1H), 2.39 (s, 3H), 1.82 (s, 3H); **^{13}C NMR (151 MHz, $CDCl_3$)** δ 167.31, 139.00, 134.38, 133.19, 132.97, 132.27, 130.15, 129.65, 123.87, 121.07, 90.62, 75.88, 21.45, 4.53. **IR (neat)**: ν_{max} = 2987, 2323, 1721, 1372, 1082, 718 cm^{-1}; **HRMS** (EI) *m/z*: calc. for $C_{18}H_{13}NO_2$ $[M]^+$ 275.0946, found 275.0945; ***R*$_f$** 0.31 (Hex/EtOAc, 4/1).

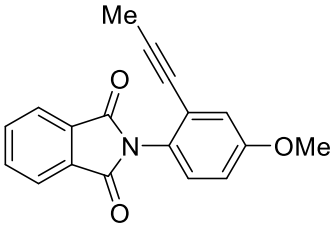

2-(4-methoxy-2-(prop-1-yn-1-yl)phenyl)isoindoline-1,3-dione, **S4c**: colorless solid; melting point 144~146 ℃; **^{1}H NMR (600 MHz, $CDCl_3$)** δ 7.95 (dd, *J* = 5.4, 3.1 Hz, 2H), 7.78 (dd, *J* = 5.4, 3.1 Hz, 2H), 7.18 (d, *J* = 8.7 Hz, 1H), 7.07 (d, *J* = 2.8 Hz, 1H), 6.94 (dd, *J* = 8.7, 2.8 Hz, 1H), 3.82 (s, 3H), 1.83 (s, 3H); **^{13}C NMR (151 MHz, $CDCl_3$)** δ 167.55, 159.90, 134.35, 132.27, 130.07, 126.05, 125.08, 123.85, 117.82, 115.03, 91.33, 75.91, 55.76, 4.54. **IR (neat)**: ν_{max} = 2972, 2358, 1723, 1504, 1385, 1082, 720 cm^{-1}; **HRMS** (EI) *m/z*: calc. for $C_{18}H_{13}NO_3$ $[M]^+$ 291.0895, found 291.0898; $\boldsymbol{R_f}$ 0.24 (Hex/EtOAc, 4/1).

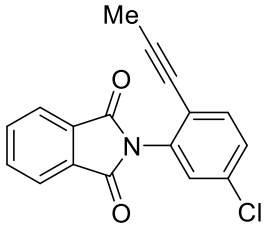

2-(5-chloro-2-(prop-1-yn-1-yl)phenyl)isoindoline-1,3-dione, **S4d**: yellow solid; melting point 168~170 ℃; **^{1}H NMR (600 MHz, $CDCl_3$)** δ 7.97 (dd, *J* = 5.4, 3.1 Hz, 2H), 7.80 (dd, *J* = 5.4, 3.1 Hz, 2H), 7.48 (d, *J* = 8.4 Hz, 1H), 7.37 (dd, *J* = 8.4, 2.1 Hz, 1H), 7.30 (d, *J* = 2.1 Hz, 1H), 1.83 (s, 3H); **^{13}C NMR (151 MHz, $CDCl_3$)** δ 166.75, 134.62, 134.38, 134.05, 133.91, 132.08, 129.54, 129.46, 124.06, 122.78, 92.73, 75.16, 4.59; **IR (neat)**: ν_{max} = 2988, 2355, 1723, 1489, 1369, 1077, 718 cm^{-1}; **HRMS** (EI) *m/z*: calc. for $C_{17}H_{10}ClNO_2$ $[M]^+$ 295.0400, found 295.0398; $\boldsymbol{R_f}$ 0.31 (Hex/EtOAc, 4/1).

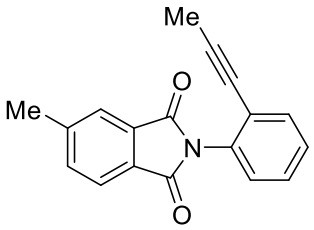

5-methyl-2-(2-(prop-1-yn-1-yl)phenyl)isoindoline-1,3-dione, **S4e**: colorless solid; melting point 148~150 ℃; **^{1}H NMR (600 MHz, $CDCl_3$)** δ 7.84 (d, *J* = 7.6 Hz, 1H), 7.76 (s, 1H), 7.57 (d, *J* = 7.6 Hz, 1H), 7.55 (dd, *J* = 7.6, 1.4 Hz, 1H), 7.40 (ddd, *J* = 7.6, 7.6, 1.9 Hz, 1H), 7.37 (ddd, *J* = 7.6, 7.6, 1.9 Hz, 1H), 7.27 (dd, *J* = 7.6, 1.4 Hz, 1H), 2.54 (s, 3H), 1.84 (s, 3H); **^{13}C NMR (151 MHz, $CDCl_3$)** δ 167.36, 167.26, 145.72, 134.98, 133.50, 133.22, 132.62, 129.65, 129.11, 129.10, 128.53, 124.39, 124.13, 123.81, 91.47, 75.98, 22.21, 4.55; **IR (neat)**: ν_{max} = 2917, 2355, 1718, 1493, 1374, 1104, 740 cm^{-1}; **HRMS** (EI) *m/z*: calc. for $C_{18}H_{13}NO_2$ $[M]^+$ 275.0946, found 275.0948 $\boldsymbol{R_f}$ 0.36 (Hex/EtOAc, 4/1).

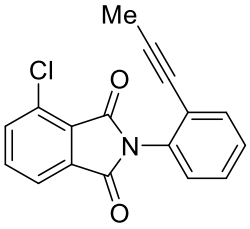

4-chloro-2-(2-(prop-1-yn-1-yl)phenyl)isoindoline-1,3-dione, **S4f**: yellow solid; melting point 190~192 ℃; **^{1}H NMR (600 MHz, $CDCl_3$)** δ 7.88 (dd, *J* = 5.2, 3.0 Hz, 1H), 7.73-7.68 (m, 2H), 7.56 (dd, *J* = 6.6, 2.4 Hz, 1H), 7.45-7.37 (m, 2H), 7.27 (dd, *J* = 7.3, 1.8 Hz, 1H), 1.86 (s, 3H); **^{13}C NMR (151 MHz, $CDCl_3$)** δ 165.62, 164.68, 136.18, 135.34, 134.26, 133.28, 132.96, 131.95, 129.34, 129.01, 128.57, 127.90, 124.06, 122.39, 91.79, 75.89, 4.60; **IR (neat)**: ν_{max} = 2917, 2241, 1719, 1374, 1114, 900, 737 cm^{-1}; **HRMS** (EI) *m/z*: calc. for $C_{17}H_{10}ClNO_2$ $[M]^+$ 295.0400, found 295.0401; $\boldsymbol{R_f}$ 0.32 (Hex/EtOAc, 4/1).

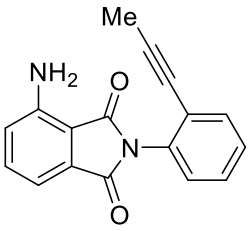

4-amino-2-(2-(prop-1-yn-1-yl)phenyl)isoindoline-1,3-dione, **S4g:** yellow solid; melting point 210~212 ℃; **^{1}H NMR (600 MHz, $CDCl_3$)** δ 7.55 (dd, *J* = 7.5, 1.8 Hz, 1H), 7.46 (dd, *J* = 8.2, 7.2 Hz, 1H), 7.40 (ddd, *J* = 7.6, 7.6, 1.8 Hz, 1H), 7.37 (ddd, *J* = 7.6, 7.6, 1.8 Hz, 1H), 7.27 (dd, *J* = 7.6, 1.4 Hz, 1H), 7.24 (d, *J* = 7.2 Hz, 1H), 6.89 (d, *J* = 8.2 Hz, 1H), 5.33 (s, 2H), 1.88 (s, 3H); **^{13}C NMR (151 MHz, $CDCl_3$)** δ 169.13, 167.43, 145.91, 135.55, 133.50, 133.24, 132.90, 129.21, 129.01, 128.53, 124.21, 121.36, 113.21, 111.46, 91.48, 76.09, 4.65. **IR (neat)**: ν_{max} = 3369, 2987, 2355, 1700, 1493, 1371, 738 cm^{-1}; **HRMS** (EI) *m/z*: calc. for $C_{17}H_{12}N_2O_2$ $[M]^+$ 276.0899, found 276.0896; ***R*$_f$** 0.54 (Hex/EtOAc, 1/1).

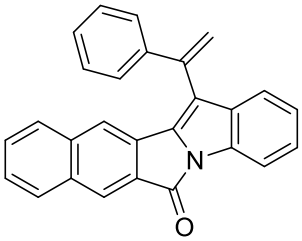

13-(1-phenylvinyl)-6H-benzo[5,6]isoindolo[2,1-a]indol-6-one, **A**: yellow solid; melting point 203~206 ℃; **^{1}H NMR (600 MHz, $CDCl_3$)** δ 8.24 (s, 1H), 8.06 (d, *J* = 7.9 Hz, 1H), 7.85 (d, *J* = 7.7 Hz, 1H), 7.62 – 7.55 (m, 2H), 7.51 – 7.43 (m, 3H), 7.43 – 7.38 (m, 3H), 7.38 (d, *J* = 7.9 Hz, 1H), 7.34 (dd, *J* = 7.9, 7.3 Hz, 1H), 7.17 (dd, *J* = 7.9, 7.3 Hz, 1H), 6.94 (s, 1H), 6.01 (d, *J* = 1.3 Hz, 1H), 5.84 (d, *J* = 1.3 Hz, 1H); **^{13}C NMR (151 MHz, $CDCl_3$)** δ 162.73, 140.94, 140.49, 136.26, 135.82, 134.78, 133.45, 132.83, 131.84, 130.17, 129.20, 129.16, 129.03, 128.92, 128.59, 127.91, 127.35, 126.49, 126.41, 124.39, 122.43, 121.99, 118.92, 117.79, 113.90; **UV-vis (1,4-dioxane)**: λ_{max} (ε) = 403 nm (6540); **HRMS** (ESI) *m/z*: $[M]^+$ calc. for $C_{27}H_{17}NO$, 371.1310; found, 371.1312; **IR (neat)**: ν_{max} = 3054, 1731, 1636, 1606 cm^{-1}; ***R*$_f$** 0.59 (Hex/EtOAc, 4/1).

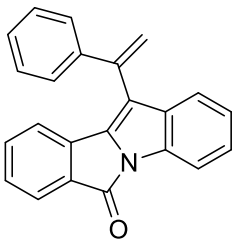

11-(1-phenylvinyl)-6*H*-isoindolo[2,1-*a*]indol-6-one, **B**: yellow solid; melting point 163~165 ℃; **^{1}H NMR (600 MHz, $CDCl_3$)** δ 7.97 (d, *J* = 8.0 Hz, 1H), 7.75 (d, *J* = 6.4 Hz, 1H), 7.54 (dd, *J* = 6.4, 2.8 Hz, 2H), 7.41-7.34 (m, 3H), 7.31 (t, *J* = 7.6 Hz, 1H), 7.28-7.23 (m, 3H), 7.10 (t, *J* = 7.6 Hz, 1H), 6.82 (d, *J* = 6.8 Hz, 1H), 5.96 (d, *J* = 1.1 Hz, 1H), 5.76 (d, *J* = 1.1 Hz, 1H); **^{13}C NMR (151 MHz, $CDCl_3$)** δ 162.72, 140.59, 140.20, 135.85, 134.68, 134.52, 133.96, 133.77, 133.66, 128.92, 128.66, 128.61, 127.58, 126.80, 125.27, 124.02, 122.62, 122.15, 120.20, 117.83, 113.51; **IR (neat)**: ν_{max} = 2927, 1719, 1443, 1361, 916, 744, 701 cm^{-1}; **HRMS** (EI) *m/z*: calc. for $C_{23}H_{15}NO$ $[M]^+$ 321.1154, found 321.1155; ***R*$_f$** 0.62 (Hex/EtOAc, 4/1).

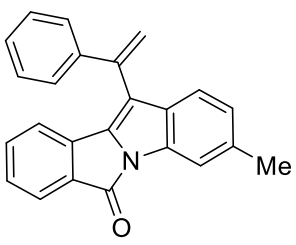

3-methyl-11-(1-phenylvinyl)-6*H*-isoindolo[2,1-*a*]indol-6-one, **C**: yellow solid; melting point 175~177 ℃; **^{1}H NMR (600 MHz, $CDCl_3$)** δ 7.79 (s, 1H), 7.74 (dd, *J* = 6.5, 2.2 Hz, 1H), 7.52 (dd, *J* = 6.5, 3.0 Hz, 2H), 7.39-7.34 (m, 3H), 7.27-7.21 (m, 2H), 7.11 (d, *J* = 8.0 Hz, 1H), 6.92 (d, *J* = 8.7 Hz, 1H), 6.78 (dd, *J* = 6.2, 1.7 Hz, 1H), 5.93 (d, *J* = 1.1 Hz, 1H), 5.74 (d, *J* = 1.1

Hz, 1H), 2.45 (s, 3H); **^{13}C NMR (151 MHz, $CDCl_3$)** δ 162.81, 140.73, 140.28, 137.41, 135.28, 134.83, 134.14, 133.91, 133.59, 132.24, 128.91, 128.58, 128.42, 127.62, 125.34, 125.25, 122.45, 121.80, 120.39, 117.70, 113.94, 21.90; **IR (neat)**: ν_{max} = 2970, 1739, 1437, 1366, 1229, 890, 528 cm^{-1}; **HRMS** (EI) *m/z*: calc. for $C_{24}H_{17}NO$ $[M]^+$ 335.1310, found 335.1307; $\boldsymbol{R_f}$ 0.63 (Hex/EtOAc, 4/1).

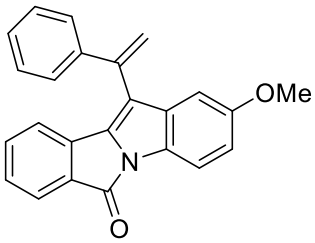

2-methoxy-11-(1-phenylvinyl)-6*H*-isoindolo[2,1-*a*]indol-6-one, **D**: yellow solid; melting point 189~191 ℃; **^{1}H NMR (600 MHz, $CDCl_3$)** δ 7.83 (d, *J* = 8.7 Hz, 1H), 7.71 (dd, *J* = 5.5, 3.0 Hz, 1H), 7.53 (dd, *J* = 6.5, 3.0 Hz, 2H), 7.39-7.35 (m, 3H), 7.26-7.20 (m, 2H), 6.89 (dd, *J* = 8.7, 2.4 Hz, 1H), 6.78 (dd, *J* = 5.5, 2.6 Hz, 1H), 6.72 (d, *J* = 2.4 Hz, 1H), 5.95 (s, 1H), 5.74 (s, 1H), 3.72 (s, 3H); **^{13}C NMR (151 MHz, $CDCl_3$)** δ 162.43, 156.92, 140.62, 140.11, 136.71, 135.54, 134.66, 134.04, 133.50, 128.92, 128.62, 128.62, 128.40, 127.59, 125.15, 122.45, 120.02, 117.68, 114.40, 114.02, 105.97, 55.82; **IR (neat)**: ν_{max} = 2970, 1739, 1367, 1217, 918, 702, 541 cm^{-1}; **HRMS** (EI) *m/z*: calc. for $C_{24}H_{17}NO_2$ $[M]^+$ 351.1259, found 351.1260; $\boldsymbol{R_f}$ 0.54 (Hex/EtOAc, 4/1).

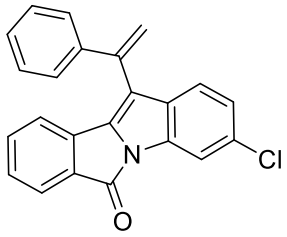

3-chloro-11-(1-phenylvinyl)-6*H*-isoindolo[2,1-*a*]indol-6-one, **E**: yellow solid; melting point 182~184 ℃; **^{1}H NMR (600 MHz, $CDCl_3$)** δ 7.96 (d, *J* = 1.6 Hz, 1H), 7.75 (dd, *J* = 6.2, 2.0 Hz, 1H), 7.50 (dd, *J* = 6.5, 3.0 Hz, 2H), 7.39-7.35 (m, 3H), 7.32-7.27 (m, 2H), 7.11 (d, *J* = 8.4 Hz, 1H), 7.05 (dd, *J* = 8.4, 1.8 Hz, 1H), 6.85 (dd, *J* = 6.2, 1.8 Hz, 1H), 5.95 (s, 1H), 5.72 (s, 1H); **^{13}C NMR (151 MHz, $CDCl_3$)** δ 162.57, 140.31, 139.94, 136.21, 134.60, 134.04, 133.98, 133.61, 133.01, 132.84, 129.01, 128.96, 128.79, 127.58, 125.56, 124.50, 122.89, 122.76, 119.82, 118.03, 113.82; **IR (neat)**: ν_{max} = 2970, 1739, 1440, 1366, 1229, 1217, 900, 528 cm^{-1}; **HRMS** (EI) *m/z*: calc. for $C_{23}H_{14}ClNO$ $[M]^+$ 355.0764, found 355.0760; $\boldsymbol{R_f}$ 0.63 (Hex/EtOAc, 4/1).

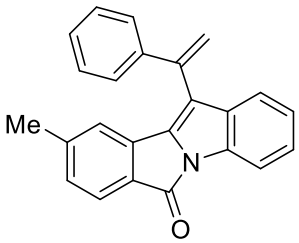

9-methyl-11-(1-phenylvinyl)-6*H*-isoindolo[2,1-*a*]indol-6-one, **F**: yellow solid; melting point 168~170 ℃; **^{1}H NMR (600 MHz, $CDCl_3$)** δ 7.95 (d, *J* = 7.8 Hz, 1H), 7.61 (d, *J* = 7.8 Hz, 1H), 7.54 (dd, *J* = 4.2, 2.8 Hz, 2H), 7.40-7.37 (m, 3H), 7.31-7.28 (m, 1H), 7.27 (d, *J* = 8.2 Hz, 1H), 7.10 (t, *J* = 8.2 Hz, 1H), 7.05 (t, *J* = 8.2 Hz, 1H), 6.52 (s, 1H), 5.95 (d, *J* = 1.1 Hz, 1H), 5.77 (d, *J* = 1.1 Hz, 1H) 2.20 (s, 3H); **^{13}C NMR (151 MHz, $CDCl_3$)** δ 162.84, 144.56, 140.75, 140.43, 135.91, 134.92, 134.35, 133.80, 131.35, 129.39, 128.90, 128.49, 127.74, 126.66, 125.09, 123.84, 123.48, 122.07, 119.86, 117.76, 113.41, 22.09; **IR (neat)**: ν_{max} = 3057, 1731, 1451, 1128, 777, 690 cm^{-1}; **HRMS** (EI) *m/z*: calc. for $C_{24}H_{17}NO$ $[M]^+$ 335.1316, found 335.1308; $\boldsymbol{R_f}$ 0.63 (Hex/EtOAc, 4/1).

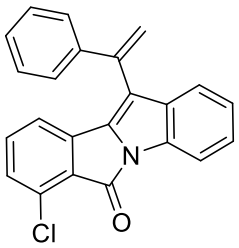

7-chloro-11-(1-phenylvinyl)-6*H*-isoindolo[2,1-*a*]indol-6-one, **G**: yellow solid; melting point 181~183 ℃; **^{1}H NMR (600 MHz, $CDCl_3$)** δ 7.96 (d, *J* = 8.0 Hz, 1H), 7.50 (dd, *J* = 6.6, 3.0 Hz, 2H), 7.39-7.34 (m, 3H), 7.31 (dt, *J* = 7.7, 0.8 Hz, 1H), 7.26 (d, *J* = 7.7 Hz, 1H), 7.17-7.13 (m, 2H), 7.11 (dt, *J* = 7.7, 0.8 Hz, 1H), 6.70 (dd, *J* = 5.2, 3.3 Hz, 1H), 5.97 (d, *J* = 0.9 Hz, 1H), 5.74 (d, *J* = 0.9 Hz, 1H); **^{13}C NMR (151 MHz, $CDCl_3$)** δ 160.23, 140.32, 140.02, 136.78, 134.44, 134.36, 133.80, 133.72, 133.09, 130.29, 129.36, 128.97, 128.70, 127.51, 127.20, 124.27, 122.24, 121.05, 120.88, 118.21, 113.63; **IR (neat)**: ν_{max} = 3060, 2970, 1739, 1380, 1217, 912, 737, 704 cm^{-1}; **HRMS** (EI) *m/z*: calc. for $C_{23}H_{14}ClNO$ $[M]^+$ 355.0764, found 355.0766; ***R*$_f$** 0.61 (Hex/EtOAc, 4/1).

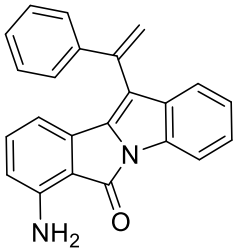

10-amino-11-(1-phenylvinyl)-6*H*-isoindolo[2,1-*a*]indol-6-one, **H**: yellow solid; melting point 193~195 ℃; **^{1}H NMR (600 MHz, $CDCl_3$)** δ 7.92 (d, *J* = 8.1 Hz, 1H), 7.51 (dd, *J* = 6.4, 3.2 Hz, 2H), 7.38-7.34 (m, 3H), 7.29 (t, *J* = 7.6 Hz, 1H), 7.22 (d, *J* = 7.8 Hz, 1H), 7.08 (t, *J* = 7.6 Hz, 1H), 7.00 (t, *J* = 7.8 Hz, 1H), 6.43 (d, *J* = 8.1 Hz, 1H), 6.22 (d, *J* = 7.4 Hz, 1H), 5.93 (d, *J* = 1.1 Hz, 1H), 5.73 (d, *J* = 1.1 Hz, 1H), 5.23 (s, 2H); **^{13}C NMR (151 MHz, $CDCl_3$)** δ 164.78, 147.32, 140.78, 140.24, 136.02, 135.23, 134.96, 134.32, 133.43, 128.82, 128.47, 127.57, 126.36, 123.49, 122.03, 119.54, 117.64, 116.08, 114.16, 113.07, 112.26; **IR (neat)**: ν_{max} = 3451, 3016, 2970, 1739, 1366, 1229, 528 cm^{-1}; **HRMS** (EI) *m/z*: calc. for $C_{23}H_{16}N_2O$ $[M]^+$ 336.1263, found 336.1264; ***R*$_f$** 0.39 (Hex/EtOAc, 4/1).

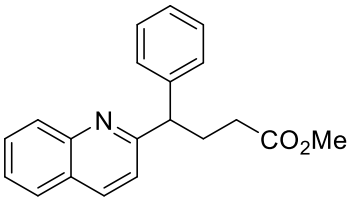

methyl 4-phenyl-4-(quinolin-2-yl)butanoate, **3a**: yellowish oil; **^{1}H NMR (600 MHz, $CDCl_3$)** δ 8.15 (d, *J* = 8.5 Hz, 1H), 7.98 (d, *J* = 8.5 Hz, 1H), 7.73 (d, *J* = 8.0 Hz, 1H), 7.70 (dd, *J* = 8.5, 7.0 Hz, 1H), 7.48 (dd, *J* = 8.0, 7.0 Hz, 1H), 7.40 (d, *J* = 7.7 Hz, 2H), 7.30 (dd, *J* = 7.7, 7.7 Hz, 2H), 7.23 (d, *J* = 8.5 Hz, 1H), 7.21 (t, *J* = 7.7 Hz, 1H), 4.32 (t, *J* = 7.8 Hz, 1H), 3.64 (s, 3H), 2.83 – 2.75 (m, 1H), 2.61 – 2.52 (m, 1H), 2.47 – 2.35 (m, 2H); **^{13}C NMR (151 MHz, $CDCl_3$)** δ 174.05, 163.05, 147.88, 142.94, 136.39, 129.52, 129.40, 128.74, 128.34, 127.56, 127.00, 126.85, 126.11, 121.47, 53.43, 51.59, 32.54, 29.86; **IR (neat)**: ν_{max} = 3026, 2948, 1731, 1597, 1427, 1238, 1151 cm^{-1}; ***R*$_f$** 0.40 (Hex/EtOAc, 4/1).

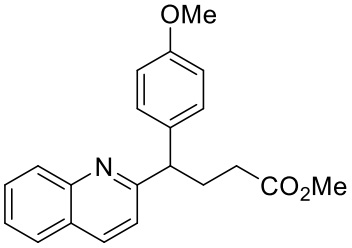

methyl 4-(4-methoxyphenyl)-4-(quinolin-2-yl)butanoate, **3b**: yellow oil; **^{1}H NMR (600 MHz, $CDCl_3$)** δ 8.13 (d, *J* = 8.5 Hz, 1H), 7.96 (d, *J* = 8.6 Hz, 1H), 7.71 (d, *J* = 8.2 Hz, 1H), 7.68 (dd, *J* = 8.6, 6.9 Hz, 1H), 7.46 (dd, *J* = 8.2, 6.9 Hz, 1H), 7.31 (d, *J* = 8.7 Hz, 2H), 7.21 (d, *J* = 8.5 Hz, 1H), 6.84 (d, *J* = 8.7 Hz, 2H), 4.26 (t, *J* = 7.7 Hz, 1H), 3.73 (s, 3H), 3.63 (s, 3H), 2.79 – 2.67 (m, 1H), 2.57 – 2.48 (m, 1H), 2.45 – 2.34 (m, 2H); **^{13}C NMR (151 MHz, $CDCl_3$)** δ 174.02, 163.38, 158.46, 147.81, 136.30, 134.97, 129.42, 129.31, 129.22, 127.51, 126.92, 126.00, 121.35, 114.08, 55.25, 52.54, 51.50, 32.49, 29.94; **IR (neat)**: ν_{max} = 2950, 2836, 1731, 1600, 1508, 1436, 1245, 1176, 1034 cm^{-1}; ***R*$_f$** 0.30 (Hex/EtOAc, 4/1).

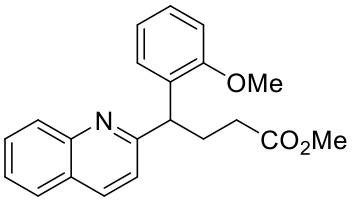

methyl 4-(2-methoxyphenyl)-4-(quinolin-2-yl)butanoate, **3c**: yellow oil; **^{1}H NMR (600 MHz, $CDCl_3$)** δ 8.13 (d, *J* = 8.5 Hz, 1H), 7.96 (d, *J* = 8.4 Hz, 1H), 7.73 (d, *J* = 8.1 Hz, 1H), 7.68 (dd, *J* = 8.4, 6.9 Hz, 1H), 7.47 (dd, *J* = 8.1, 6.9 Hz, 1H), 7.29 (d, *J* = 7.6 Hz, 1H), 7.22 (d, *J* = 8.5 Hz, 1H), 7.19 (ddd, *J* = 8.2, 7.4 Hz, 1H), 6.90 (dd, *J* = 7.6, 7.4 Hz, 1H), 6.88 (d, *J* = 8.2 Hz, 1H), 4.82 (t, *J* = 7.5 Hz, 1H), 3.82 (s, 3H), 3.63 (s, 3H), 2.83 – 2.72 (m, 1H), 2.52 – 2.44 (m, 1H), 2.45 – 2.39 (m, 2H); **^{13}C NMR (151 MHz, $CDCl_3$)** δ 174.34, 163.45, 157.17, 147.93, 136.00, 131.49, 129.58, 129.18, 128.88, 127.78, 127.53, 127.00, 125.91, 122.04, 120.93, 110.73, 55.62, 51.55, 45.06, 32.70, 29.14; **IR (neat)**: ν_{max} = 2948, 2837, 1731, 1598, 1436, 1239, 1150, 1027 cm^{-1}; **HRMS** (EI) *m/z*: calc. for $C_{21}H_{21}NO_3$ $[M]^+$ 335.1521, found 335.1523; ***R*$_f$** 0.36 (Hex/EtOAc, 4/1).

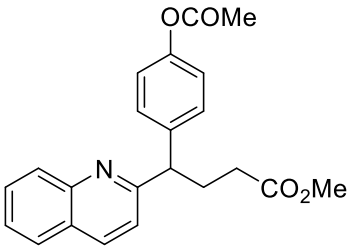

methyl 4-(4-acetoxyphenyl)-4-(quinolin-2-yl)butanoate **3d**: yellow oil; **^{1}H NMR (600 MHz, $CDCl_3$)** δ 8.10 (d, *J* = 8.4 Hz, 1H), 8.00 (d, *J* = 8.5 Hz, 1H), 7.74 (d, *J* = 8.1 Hz, 1H), 7.69 (dd, *J* = 8.4, 6.9 Hz, 1H), 7.49 (dd, *J* = 8.1, 6.9 Hz, 1H), 7.38 (d, *J* = 8.5 Hz, 2H), 7.21 (d, *J* = 8.5 Hz, 1H), 7.01 (d, *J* = 8.5 Hz, 2H), 4.29 (t, *J* = 7.7 Hz, 1H), 3.63 (s, 3H), 2.78 – 2.69 (m, 1H), 2.57 – 2.46 (m, 1H), 2.42 – 2.32 (m, 2H), 2.26 (s, 3H); **^{13}C NMR (151 MHz, $CDCl_3$)** δ 174.06, 169.61, 162.75, 149.59, 147.95, 140.53, 136.58, 129.55, 129.53, 129.33, 127.65, 127.10, 126.25, 121.78, 121.54, 52.85, 51.69, 32.53, 30.05, 21.30; **IR (neat)**: ν_{max} = 2950, 1754, 1731, 1502, 1194, 1166 cm^{-1}; **HRMS** (EI) *m/z*: calc. for $C_{22}H_{21}NO_4$ $[M]^+$ 363.1471, found 363.1473; ***R*$_f$** 0.17 (Hex/EtOAc, 4/1).

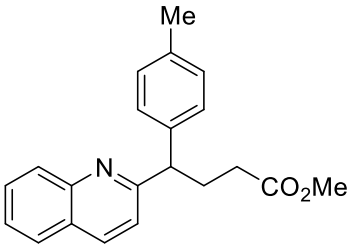

methyl 4-(quinolin-2-yl)-4-(p-tolyl)butanoate, **3e**: yellowish oil; **^{1}H NMR (600 MHz, $CDCl_3$)** δ 8.16 (d, *J* = 8.4 Hz, 1H), 7.98 (d, *J* = 8.5 Hz, 1H), 7.73 (d, *J* = 8.1 Hz, 1H), 7.70 (dd, *J* = 8.5, 6.9 Hz, 1H), 7.48 (dd, *J* = 8.1, 6.9 Hz, 1H), 7.31 (d, *J* = 8.0 Hz, 2H), 7.24 (d, *J* = 8.4 Hz, 1H), 7.13 (d, *J* = 8.0 Hz, 2H), 4.30 (t, *J* = 7.7 Hz, 1H), 3.65 (s, 3H), 2.83 – 2.75 (m, 1H), 2.63 – 2.51 (m, 1H), 2.45 – 2.40 (m, 2H), 2.32 (s, 3H); **^{13}C NMR (151 MHz, $CDCl_3$)** δ 174.03, 163.27, 147.83, 139.89, 136.31, 136.31, 129.46, 129.40, 129.31, 128.16, 127.51, 126.94, 126.01, 121.38, 53.00, 51.51, 32.52, 29.81, 21.07; **IR (neat)**: ν_{max} = 3019, 2949, 1735, 1600, 1503, 1435, 1239, 1153 cm^{-1}; ***R*$_f$** 0.44 (Hex/EtOAc, 4/1).

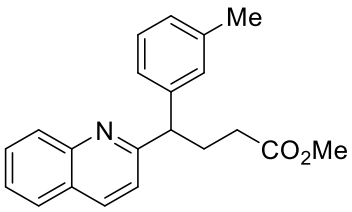

methyl 4-(quinolin-2-yl)-4-(m-tolyl)butanoate, **3f**: yellow oil; **^{1}H NMR (600 MHz, $CDCl_3$)** δ 8.11 (d, *J* = 8.4 Hz, 1H), 7.99 (d, *J* = 8.5 Hz, 1H), 7.74 (d, *J* = 8.1 Hz, 1H), 7.69 (dd, *J* = 8.5, 6.9 Hz, 1H), 7.49 (dd, *J* = 8.1, 6.9 Hz, 1H), 7.23 (d, *J* = 8.4 Hz, 1H), 7.19 – 7.14 (m, 3H), 7.03 – 6.99 (m, 1H), 4.25 (t, *J* = 7.7 Hz, 1H), 3.63 (s, 3H), 2.76 – 2.69 (m, 1H), 2.55 – 2.47 (m, 1H), 2.42 – 2.33 (m, 2H), 2.30 (s, 3H); **^{13}C NMR (151 MHz, $CDCl_3$)** δ 174.24, 163.30, 147.95, 142.93, 138.42, 136.48, 129.63, 129.46, 129.19, 128.70, 127.71, 127.65, 127.11, 126.18, 125.40, 121.53, 53.50, 51.70, 32.68, 29.87, 21.67; **IR (neat)**: ν_{max} = 3018, 2949, 1736, 1600, 1503, 1435, 1200, 1171 cm^{-1}; **HRMS** (EI) *m/z*: calc. for $C_{21}H_{21}NO_2$ $[M]^+$ 319.1572, found 319.1568; ***R*$_f$** 0.43 (Hex/EtOAc, 4/1).

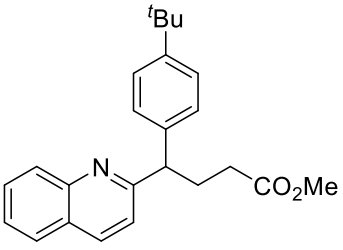

methyl 4-(4-(tert-butyl)phenyl)-4-(quinolin-2-yl)butanoate, **3g**: yellow oil; **^{1}H NMR (600 MHz, $CDCl_3$)** δ 8.13 (d, *J* = 8.5 Hz, 1H), 7.99 (d, *J* = 8.5 Hz, 1H), 7.73 (d, *J* = 8.1 Hz, 1H), 7.69 (dd, *J* = 8.5, 6.9 Hz, 1H), 7.48 (dd, *J* = 8.1, 6.9 Hz, 1H), 7.32 (s, 4H), 7.26 (d, *J* = 8.5 Hz, 1H), 4.28 (t, *J* = 7.8 Hz, 1H), 3.63 (s, 3H), 2.79 – 2.71 (m, 1H), 2.59 – 2.51 (m, 1H), 2.43 – 2.36 (m, 2H), 1.29 (s, 9H); **^{13}C NMR (151 MHz, $CDCl_3$)** δ 174.16, 163.39, 149.61, 147.93, 139.81, 136.40, 129.55, 129.40, 127.94, 127.59, 127.05, 126.09, 125.65, 121.48, 53.10, 51.62, 34.53, 32.68, 31.51, 29.95; **IR (neat)**: ν_{max} = 3055, 2960, 1736, 1600, 1503, 1434, 1238, 1156 cm^{-1}; **HRMS** (EI) *m/z*: calc. for $C_{24}H_{27}NO_2$ $[M]^+$ 361.2042, found 361.2044; ***R*$_f$** 0.45 (Hex/EtOAc, 4/1).

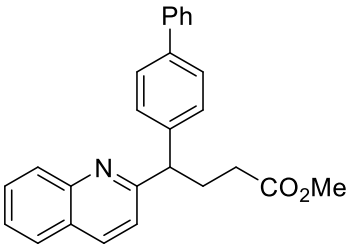

methyl 4-([1,1'-biphenyl]-4-yl)-4-(quinolin-2-yl)butanoate, **3h**: yellowish oil; **^{1}H NMR (600 MHz, $CDCl_3$)** δ 8.14 (d, *J* = 7.4 Hz, 1H), 8.03 (d, *J* = 8.4 Hz, 1H), 7.76 (d, *J* = 8.0 Hz, 1H), 7.71 (dd, *J* = 8.0, 7.3 Hz, 1H), 7.55 (d, *J* = 8.2 Hz, 2H), 7.53 (d, *J* = 8.1 Hz, 2H), 7.50 (t, *J* = 7.2 Hz, 1H), 7.45 (d, *J* = 8.1 Hz, 2H), 7.41 (dd, *J* = 8.2, 7.2 Hz, 2H), 7.32 (dd, *J* = 7.4, 7.3 Hz, 1H), 7.28 (d, *J* = 8.4 Hz, 1H), 4.35 (t, *J* = 8.0 Hz, 1H), 3.64 (s, 3H), 2.82 – 2.73 (m, 1H), 2.62 – 2.53 (m, 1H), 2.47 – 2.36 (m, 2H); **^{13}C NMR (151 MHz, $CDCl_3$)** δ 174.14, 163.05, 142.05, 140.99, 139.83, 136.63, 136.61, 129.58, 129.54, 128.90, 128.80, 127.66, 127.53, 127.35, 127.18, 127.12, 126.25, 121.52, 53.16, 51.70, 32.63, 29.97; **IR (neat)**: ν_{max} = 3028, 2924, 2853, 1733, 1202 cm^{-1}; **HRMS** (EI) *m/z*: calc. for $C_{26}H_{23}NO_2$ $[M]^+$ 381.1729, found 381.1727; $\boldsymbol{R_f}$ 0.40 (Hex/EtOAc, 4/1).

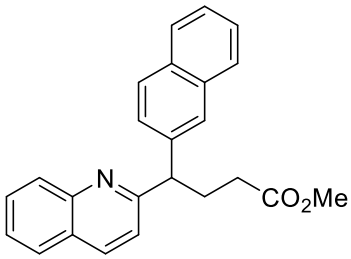

methyl 4-(naphthalen-2-yl)-4-(quinolin-2-yl)butanoate, **3i**: yellowish oil; **^{1}H NMR (600 MHz, $CDCl_3$)** δ 8.16 (d, *J* = 7.9 Hz, 1H), 7.99 (d, *J* = 8.4 Hz, 1H), 7.84 (s, 1H), 7.81 (d, *J* = 8.0 Hz, 1H), 7.78 (d, *J* = 8.2 Hz, 1H), 7.76 (d, *J* = 8.2 Hz, 1H), 7.74 (d, *J* = 8.2 Hz, 1H), 7.72 (dd, *J* = 8.5, 6.4 Hz, 1H), 7.51 (dd, *J* = 7.9, 6.4 Hz, 1H), 7.50 (d, *J* = 8.5 Hz, 1H), 7.46 (dd, *J* = 8.2, 6.9 Hz, 1H), 7.43 (dd, *J* = 8.0, 6.9 Hz, 1H), 7.27 (d, *J* = 8.4 Hz, 1H), 4.48 (t, *J* = 7.5 Hz, 1H), 3.64 (s, 3H), 2.88 – 2.80 (m, 1H), 2.70 – 2.62 (m, 1H), 2.49 – 2.38 (m, 2H); **^{13}C NMR (151 MHz, $CDCl_3$)** 174.16, 163.03, 140.42, 136.60, 133.73, 132.62, 129.59, 129.56, 128.55, 127.97, 127.79, 127.66, 127.10, 126.85, 126.84, 126.76, 126.28, 126.26, 125.85, 121.61, 53.50, 51.69, 32.61, 29.71; **IR (neat)**: ν_{max} = 3054, 2949, 1731, 1598, 1503, 1198, 1167 cm^{-1}; **HRMS** (EI) *m/z*: calc. for $C_{24}H_{21}NO_2$ $[M]^+$ 355.1572, found 355.1570; $\boldsymbol{R_f}$ 0.41 (Hex/EtOAc, 4/1).

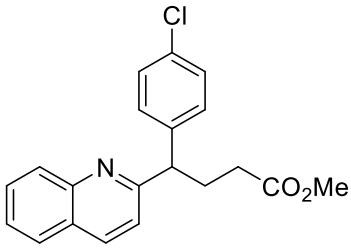

methyl 4-(4-chlorophenyl)-4-(quinolin-2-yl)butanoate, **3j**: yellowish oil; **^{1}H NMR (600 MHz, $CDCl_3$)** δ 8.10 (d, *J* = 8.5 Hz, 1H), 8.02 (d, *J* = 8.5 Hz, 1H), 7.75 (d, *J* = 8.1 Hz, 1H), 7.70 (dd, *J* = 8.5, 6.9 Hz, 1H), 7.50 (dd, *J* = 8.1, 6.9 Hz, 1H), 7.32 (d, *J* = 8.5 Hz, 2H), 7.25 (d, *J* = 8.5 Hz, 2H), 7.20 (d, *J* = 8.5 Hz, 1H), 4.27 (t, *J* = 7.8 Hz, 1H), 3.63 (s, 3H), 2.75 – 2.68 (m, 1H), 2.54 – 2.44 (m, 1H), 2.41 – 2.31 (m, 2H); **^{13}C NMR (151 MHz, $CDCl_3$)** δ 174.02, 162.52, 147.95, 141.53, 136.74, 132.77, 129.76, 129.66, 129.55, 128.94, 127.68, 127.12, 126.38, 121.41, 52.76, 51.75, 32.46, 29.97; **IR (neat)**: ν_{max} = 3044, 2950, 1735, 1600, 1503, 1489, 1231, 1153, 826 cm^{-1}; **HRMS** (EI) *m/z*: calc. for $C_{20}H_{18}ClNO_2$ $[M]^+$ 339.1026, found 339.1028; $\boldsymbol{R_f}$ 0.36 (Hex/EtOAc, 4/1).

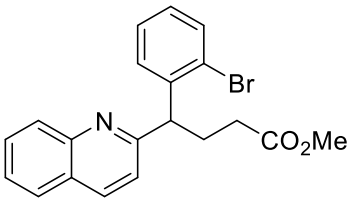

methyl 4-(2-bromophenyl)-4-(quinolin-2-yl)butanoate, **3k**: yellow solid; melting point 96~101 °C; **^{1}H NMR (600 MHz, $CDCl_3$)** δ 8.14 (d, *J* = 8.4 Hz, 1H), 7.98 (d, *J* = 8.4 Hz, 1H), 7.74 (d, *J* = 8.1 Hz, 1H), 7.70 (dd, *J* = 8.4, 6.9 Hz, 1H), 7.58 (d, *J* = 8.0 Hz, 1H), 7.49 (dd, *J* = 8.1, 6.9 Hz, 2H), 7.41 (d, *J* = 7.9 Hz, 1H), 7.24 (d, *J* = 8.4 Hz, 1H), 7.20 (dd, *J* = 7.9, 7.3 Hz, 1H), 7.04 (dd, *J* = 8.0, 7.3 Hz, 1H), 4.91 (t, *J* = 7.5 Hz, 1H), 3.65 (s, 3H), 2.89 – 2.80 (m, 1H), 2.54 – 2.45 (m, 2H), 2.45 – 2.36 (m, 1H); **^{13}C NMR (151 MHz, $CDCl_3$)** δ 174.03, 161.85, 148.03, 142.45, 136.33, 132.99, 129.93, 129.68, 129.40, 128.30, 127.96, 127.62, 127.11, 126.22, 125.13, 122.36, 51.68, 50.94, 32.43, 29.74; **IR (neat)**: ν_{max} = 3058, 2949, 1735, 1600, 1436, 1237, 1153, 753 cm^{-1}; **HRMS** (EI) *m/z*: calc. for $C_{20}H_{18}BrNO_2$ $[M]^+$ 383.0521, found 383.0520 ,385.0503; $\boldsymbol{R_f}$ 0.48 (Hex/EtOAc, 4/1).

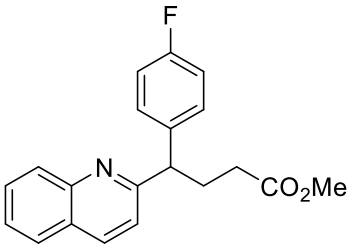

methyl 4-(4-fluorophenyl)-4-(quinolin-2-yl)butanoate, **3l**: yellow oil; **^{1}H NMR (600 MHz, $CDCl_3$)** δ 8.10 (d, *J* = 8.6 Hz, 1H), 8.01 (d, *J* = 8.6 Hz, 1H), 7.75 (d, *J* = 8.1 Hz, 1H), 7.70 (dd, *J* = 8.5, 6.9 Hz, 1H), 7.49 (dd, *J* = 8.1, 6.9 Hz, 1H), 7.34 (dd, *J* = 8.7, $^4J_{H-F}$ = 5.4 Hz, 2H), 7.20 (d, *J* = 8.5 Hz, 1H), 6.97 (dd, $^3J_{H-F}$ = 8.7, *J* = 8.7 Hz, 2H), 4.27 (t, *J* = 7.8 Hz, 1H), 3.63 (s, 3H), 2.76 – 2.69 (m, 1H), 2.52 – 2.45 (m, 1H), 2.39 – 2.33 (m, 2H); **^{13}C NMR (151 MHz, $CDCl_3$)** δ 174.06, 162.83, 161.90 (d, $^1J_{C-F}$ = 245.3 Hz), 147.98, 138.77, 138.75, 136.61, 129.83 (d, $^3J_{C-F}$ = 7.8 Hz), 129.58, 127.66, 127.09, 126.30, 121.42, 115.58 (d, $^2J_{C-F}$ = 21.1 Hz), 52.67, 51.72, 32.50, 30.14; **IR (neat)**: ν_{max} = 3043, 2950, 1732, 1504, 1220, 1158, 825 cm^{-1}; **HRMS** (EI) *m/z*: calc. for $C_{20}H_{18}FNO_2$ $[M]^+$ 323.1322, found 323.1323; $\boldsymbol{R_f}$ 0.35 (Hex/EtOAc, 4/1).

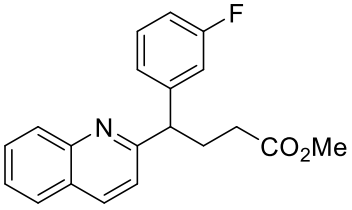

methyl 4-(3-fluorophenyl)-4-(quinolin-2-yl)butanoate, **3m**: yellow oil; **^{1}H NMR (600 MHz, $CDCl_3$)** δ 8.11 (d, *J* = 8.5 Hz, 1H), 8.03 (d, *J* = 8.5 Hz, 1H), 7.76 (d, *J* = 8.1 Hz, 1H), 7.71 (dd, *J* = 8.5, 6.9 Hz, 1H), 7.50 (dd, *J* = 8.1, 6.9 Hz, 1H), 7.24 (ddd, *J* = 8.2, 7.8, $^4J_{H-F}$ = 6.0 Hz, 1H), 7.22 (d, *J* = 8.5 Hz, 1H), 7.15 (d, *J* = 7.8 Hz, 1H), 7.11 (d, $^3J_{H-F}$ = 10.1 Hz, 1H), 6.89 (dd, $^3J_{H-F}$ = 8.6, *J* = 8.2 Hz, 1H), 4.30 (t, *J* = 7.8 Hz, 1H), 3.64 (s, 3H), 2.76 – 2.69 (m, 1H), 2.54 – 2.47 (m, 1H), 2.40 – 2.32 (m, 2H); **^{13}C NMR (151 MHz, $CDCl_3$)** δ 174.01, 163.20 (d, $^1J_{C-F}$ = 246.2 Hz), 162.36, 145.61 (d, $^3J_{C-F}$ = 6.7 Hz), 136.76, 130.21 (d, $^3J_{C-F}$ = 8.4 Hz), 129.67, 129.59, 127.68, 127.16, 126.41, 124.14 (d, $^4J_{C-F}$ = 2.9 Hz), 121.42, 115.26 (d, $^2J_{C-F}$ = 21.7 Hz), 113.87 (d, $^2J_{C-F}$ = 21.1 Hz), 113.80, 53.10, 51.76, 32.47, 29.94; **IR (neat)**: ν_{max} = 3059, 2926, 1735, 1589, 1487, 1241, 1140, 833 cm^{-1}; **HRMS** (EI) *m/z*: calc. for $C_{20}H_{18}FNO_2$ $[M]^+$ 323.1322, found 323.1319; $\boldsymbol{R_f}$ 0.38 (Hex/EtOAc, 4/1).

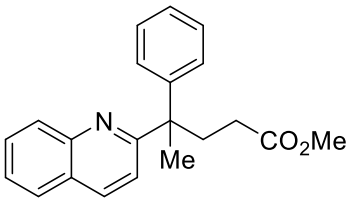

methyl 4-phenyl-4-(quinolin-2-yl)pentanoate, **3n**: yellowish solid; melting point 79~81 ℃; **^{1}H NMR (600 MHz, $CDCl_3$)** δ 8.16 (d, *J* = 8.4 Hz, 1H), 7.94 (d, *J* = 8.7 Hz, 1H), 7.75 (d, *J* = 8.0 Hz, 1H), 7.71 (dd, *J* = 8.4, 6.9 Hz, 1H), 7.51 (dd, *J* = 8.0, 6.9 Hz, 1H), 7.30 (dd, *J* = 8.7, 7.1 Hz, 2H), 7.26 (d, *J* = 8.7 Hz, 2H), 7.22 (t, *J* = 7.1 Hz, 1H), 7.05 (d, *J* = 8.7 Hz, 1H), 3.63 (s, 3H), 2.82 – 2.68 (m, 2H), 2.36 – 2.30 (m, 1H), 2.28 – 2.22 (m, 1H), 1.81 (s, 3H); **^{13}C NMR (151 MHz, $CDCl_3$)** δ 174.66, 166.91, 147.52, 147.14, 135.84, 129.83, 129.26, 128.45, 127.42, 126.66, 126.41, 126.26, 121.37, 51.64, 49.13, 35.81, 30.31, 26.11; **IR (neat)**: ν_{max} = 3058, 2972, 1735, 1600, 1500, 1436, 1195, 1123 cm^{-1}; $\boldsymbol{R_f}$ 0.51 (Hex/EtOAc, 4/1).

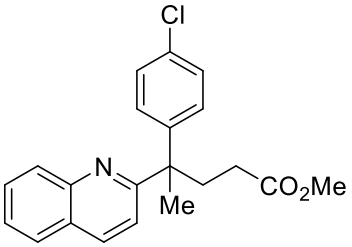

methyl 4-(4-chlorophenyl)-4-(quinolin-2-yl)pentanoate, **3o**: colorless oil; **^{1}H NMR (600 MHz, $CDCl_3$** δ 8.11 (d, *J* = 8.5 Hz, 1H), 7.96 (d, *J* = 8.7 Hz, 1H), 7.75 (d, *J* = 8.0 Hz, 1H), 7.71 (dd, *J* = 8.5, 6.9 Hz, 1H), 7.52 (dd, *J* = 8.0, 6.9 Hz, 1H), 7.25 (d, *J* = 8.7 Hz, 2H), 7.17 (d, *J* = 8.7 Hz, 2H), 7.02 (d, *J* = 8.7 Hz, 1H), 3.61 (s, 3H), 2.72 (ddd, *J* = 13.9, 11.1, 5.5 Hz, 1H), 2.65 (ddd, *J* = 13.9, 11.1, 5.3 Hz, 1H), 2.28 (ddd, *J* = 16.2, 11.1, 5.3 Hz, 1H), 2.20 (ddd, *J* = 16.2, 11.1, 5.5 Hz, 1H), 1.77 (s, 3H); **^{13}C NMR (151 MHz, $CDCl_3$)** δ 174.52, 166.26, 147.19, 146.20, 136.12, 132.35, 129.86, 129.45, 128.88, 128.60, 127.48, 126.71, 126.46, 121.06, 51.74, 48.86, 35.79, 30.25, 26.07; **IR (neat)**: ν_{max} = 3059, 2949, 1735, 1491, 1168, 1012, 758 cm^{-1}; **HRMS** (EI) *m/z*: calc. for $C_{21}H_{20}ClNO_2$ $[M]^+$ 353.1183, found 353.1186; $\boldsymbol{R_f}$ 0.51 (Hex/EtOAc, 4/1).

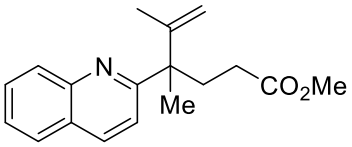

methyl 4,5-dimethyl-4-(quinolin-2-yl)hex-5-enoate, **3p**: colorless oil; **^{1}H NMR (600 MHz, $CDCl_3$)** δ 8.08 (d, *J* = 8.4 Hz, 1H), 8.02 (d, *J* = 8.7 Hz, 1H), 7.76 (d, *J* = 8.0 Hz, 1H), 7.67 (dd, *J* = 8.4, 7.0 Hz, 1H), 7.49 (dd, *J* = 8.0, 7.0 Hz, 1H), 7.37 (d, *J* = 8.7 Hz, 1H), 5.07 (s, 2H), 3.65 (s, 3H), 2.54 (ddd, *J* = 13.9, 11.6, 5.4 Hz, 1H), 2.42 (ddd, *J* = 13.9, 11.6, 4.8 Hz, 1H), 2.32 (ddd, *J* = 16.2, 11.6, 4.8 Hz, 1H), 2.21 (ddd, *J* = 16.2, 11.6, 5.4 Hz, 1H), 1.53 (s, 3H), 1.49 (s, 3H); **^{13}C NMR (151 MHz, $CDCl_3$)** δ 174.95, 165.73, 149.88, 147.51, 136.07, 129.83, 129.20, 127.44, 126.80, 126.18, 120.00, 112.58, 51.73, 50.34, 32.33, 30.14, 24.05, 20.51; **IR (neat)**: ν_{max} = 2972, 1736, 1600, 1171cm^{-1}; $\boldsymbol{R_f}$ 0.48 (Hex/EtOAc, 4/1).

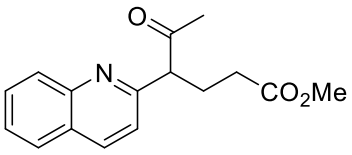

methyl 5-oxo-4-(quinolin-2-yl)hexanoate, **3q**: yellow oil; **^{1}H NMR (600 MHz, $CDCl_3$)** δ 8.14 (d, *J* = 8.5 Hz, 1H), 8.07 (d, *J* = 8.5 Hz, 1H), 7.80 (d, *J* = 8.1 Hz, 1H), 7.71 (dd, *J* = 8.5, 6.9 Hz, 1H), 7.53 (dd, *J* = 8.1, 6.9 Hz, 1H), 7.43 (d, *J* = 8.5 Hz, 1H), 4.04 (t, *J* = 7.4 Hz, 1H), 3.69 (s, 3H), 2.56 – 2.41 (m, 3H), 2.35 – 2.28 (m, 1H), 2.09 (s, 3H); **^{13}C NMR (151 MHz, $CDCl_3$)** δ 207.98,

173.25, 158.52, 148.00, 137.14, 129.83, 129.58, 127.73, 127.45, 126.71, 120.44, 53.70, 52.42, 41.25, 30.17, 26.11; **IR (neat)**: ν_{max} = 3060, 2952, 1735, 1714, 1260, 1159 cm^{-1}; **HRMS** (EI) *m/z*: calc. for $C_{16}H_{17}NO_3$ $[M]^+$ 271.1208, found 271.1207; $\boldsymbol{R_f}$ 0.24 (Hex/EtOAc, 1/1).

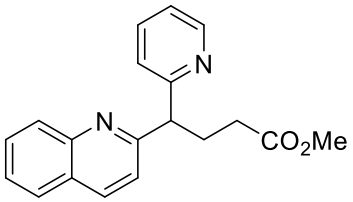

methyl 4-(pyridin-2-yl)-4-(quinolin-2-yl)butanoate, **3r**: yellow oil; **^{1}H NMR (600 MHz, $CDCl_3$)** δ 8.58 (ddd, *J* = 4.9, 1.7, 0.8 Hz, 1H), 8.09 (d, *J* = 8.4 Hz, 1H), 8.03 (d, *J* = 8.5 Hz, 1H), 7.75 (d, *J* = 8.0 Hz, 1H), 7.68 (dd, *J* = 8.4, 6.9 Hz, 1H), 7.56 (ddd, *J* = 7.9, 7.4, 1.7 Hz, 1H), 7.48 (dd, *J* = 8.0, 6.9 Hz, 1H), 7.47 (d, *J* = 8.5 Hz, 1H), 7.36 (ddd, *J* = 7.9, 1.1, 0.8 Hz, 1H), 7.11 (ddd, *J* = 7.4, 4.9, 1.1 Hz, 1H), 4.49 (t, *J* = 7.8 Hz, 1H), 3.62 (s, 3H), 2.73 – 2.68 (m, 2H), 2.42 – 2.31 (m, 2H); **^{13}C NMR (151 MHz, $CDCl_3$)** δ 173.96, 162.35, 161.89, 149.54, 147.99, 136.75, 136.63, 129.52, 129.51, 127.67, 127.28, 126.29, 123.71, 121.98, 121.34, 56.04, 51.73, 32.61, 29.46; **IR (neat)**: ν_{max} = 3058, 2950, 1734, 1588, 1433, 1217, 1151 cm^{-1}; **HRMS** (EI) *m/z*: calc. for $C_{19}H_{18}N_2O_2$ $[M]^+$ 306.1368, found 306.1367; $\boldsymbol{R_f}$ 0.16 (Hex/EtOAc, 1/1).

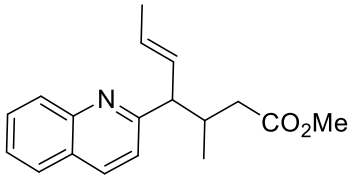

methyl 3-methyl-4-(quinolin-2-yl)hept-5-enoate (diastereoisomers, 1 : 0.36 : 0.13), **3s**: colorless oil; **^{1}H NMR (600 MHz, $CDCl_3$)** δ 8.08 (d, *J* = 8.4 Hz, 1H), 8.07 (d, *J* = 8.4 Hz, 1H), 8.07 (d, *J* = 8.4 Hz, 1H), 8.05 (dd, *J* = 7.9, 1.3 Hz, 3H), 7.76 (dd, *J* = 8.3, 0.9 Hz, 3H), 7.67 (ddd, *J* = 8.3, 6.9, 1.3 Hz, 3H), 7.48 (ddd, *J* = 7.9, 6.9, 0.9 Hz, 3H), 7.31 (d, *J* = 8.4 Hz, 1H), 7.30 (d, *J* = 8.4 Hz, 1H), 7.29 (d, *J* = 8.4 Hz, 1H), 5.82 – 5.73 (m, 2H), 5.77 (ddq, *J* = 15.0, 9.4, 1.6 Hz, 1H), 5.73 – 5.65 (m, 2H), 5.63 (dq, *J* = 15.0, 6.5 Hz, 1H), 3.90 – 3.85 (m, 1H), 3.67 (s, 3H), 3.55 (s, 3H), 3.55 (s, 3H), 3.43 (dd, *J* = 9.4, 8.7 Hz, 1H), 3.39 – 3.34 (m, 1H), 2.64 (ddqd, *J* = 9.3, 8.7, 6.7, 4.5 Hz, 1H), 2.67 – 2.59 (m, 2H), 2.30 – 2.24 (m, 2H), 2.24 (dd, *J* = 15.3, 4.5 Hz, 1H), 2.18 – 2.11 (m, 2H), 2.10 (dd, *J* = 15.3, 9.3 Hz, 1H), 1.70 (dd, *J* = 6.5, 1.6 Hz, 3H), 1.72 – 1.68 (m, 3H), 1.67 (dd, *J* = 6.2, 1.4 Hz, 3H), 1.04 (d, *J* = 6.7 Hz, 3H), 1.03 (d, *J* = 6.7 Hz, 3H), 0.81 (d, *J* = 6.7 Hz, 3H); **^{13}C NMR (151 MHz, $CDCl_3$)** δ 173.76, 173.74, 173.72, 163.78, 163.70, 163.68, 148.10, 136.56, 131.95, 131.32, 130.90, 129.48, 129.47, 129.44, 128.38, 127.66, 127.16, 127.14, 126.89, 126.08, 126.07, 126.06, 121.15, 121.13, 58.02, 51.64, 51.62, 51.51, 39.88, 39.76, 39.74, 35.38, 34.78, 34.75, 18.30, 17.81, 17.48, 13.65; **IR (neat)**: ν_{max} = 2952, 1735, 1619, 1165 cm^{-1}; **HRMS** (EI) *m/z*: calc. for $C_{18}H_{21}NO_2$ $[M]^+$ 283.1572, found 283.1570; $\boldsymbol{R_f}$ 0.40 (Hex/EtOAc, 4/1).

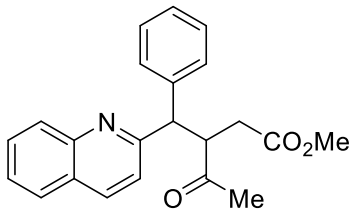

4-phenyl-4-(quinolin-2-yl)pentanoate methyl 4-oxo-3-(phenyl(quinolin-2-yl)methyl)pentanoate, **3t**: yellowish oil; **^{1}H NMR (600 MHz, $CDCl_3$)** δ 8.15 (d, *J* = 8.4 Hz, 1H), 8.00 (d, *J* = 8.4 Hz, 1H), 7.75 (d, *J* = 8.1 Hz, 1H), 7.72 (dd, *J* = 8.4, 6.9 Hz, 1H), 7.51 (dd, *J* = 8.1, 6.9 Hz, 1H), 7.41 (d, *J* = 8.0 Hz, 1H), 7.25 (dd, *J* = 8.0, 7.3 Hz, 1H), 7.21 (d, *J* = 8.4 Hz, 1H), 7.18 (t, *J* = 7.3 Hz, 1H), 4.41 (ddd, *J* = 11.0, 11.0, 3.3 Hz, 1H), 4.24 (d, *J* = 11.0 Hz, 1H), 3.58 (s, 3H), 2.85 (dd, *J* = 17.3, 11.0 Hz, 1H), 2.58 (dd, *J* = 17.3, 3.3 Hz, 1H), 1.82 (s, 3H); **IR (neat)**: ν_{max} = 3061, 2953, 2926, 1735, 1711 cm^{-1}; **^{13}C NMR (151 MHz, $CDCl_3$)** δ 213.26, 173.19, 160.56, 148.02, 140.46, 136.78, 129.69, 129.64, 129.04, 128.93, 127.70, 127.45, 127.10, 126.47, 122.64, 56.22, 51.82, 51.75, 36.23, 32.88; **IR (neat)**: ν_{max} = 3061, 2953, 2926, 1735, 1711 cm^{-1}; **HRMS** (EI) *m/z*: calc. for $C_{22}H_{21}NO_3$ $[M]^+$ 347.1521, found 347.1524; $\boldsymbol{R_f}$ 0.34 (Hex/EtOAc, 4/1).

References

S1. G. Heinrich, S. Schoof, H. Gusten, 9,10-Diphenylanthracene as a fluorescence quantum yield standard., *J. Photochem.,* 1974, **3**, 315–320.

S2. J. Bae, N. Iqbal, H. S. Hwang, E. J. Cho, Sustainable preparation of photoactive indole-fused tetracyclic molecules: a new class of organophotocatalysts, *Green Chem.,* 2022, **24**, 3985−3992.

S3. D. F. Chen, Z. Y. Han, Y. P. He, J. Yu, L. Z. Gong, Metal-Free Oxidation/C(sp)-H Functionalization of Unactivated Alkynes Using Pyridine-Oxide as the External Oxidant, *Angew. Chem., Int. Ed.,* 2012, **51**, 12307–12310.

S4. X. Jiang, P. Boehm, J. F. Hartwig, Stereodivergent Allylation of Azaaryl Acetamides and Acetates by Synergistic Iridium and Copper Catalysis, *J. Am. Chem. Soc.,* 2018, **140**, 1239–1242.

S5. N. Salaverri, R. Mas-Ballesté, L. Marzo, J. Alemán, Visible light mediated photocatalytic [2 + 2] cycloaddition/ring-opening rearomatization cascade of electron-deficient azaarenes and vinylarenes, *Commun. Chem.,* 2020, **3**, 132.

NMR Spectra (^{1}H NMR, ^{13}C NMR, and ^{19}F NMR)

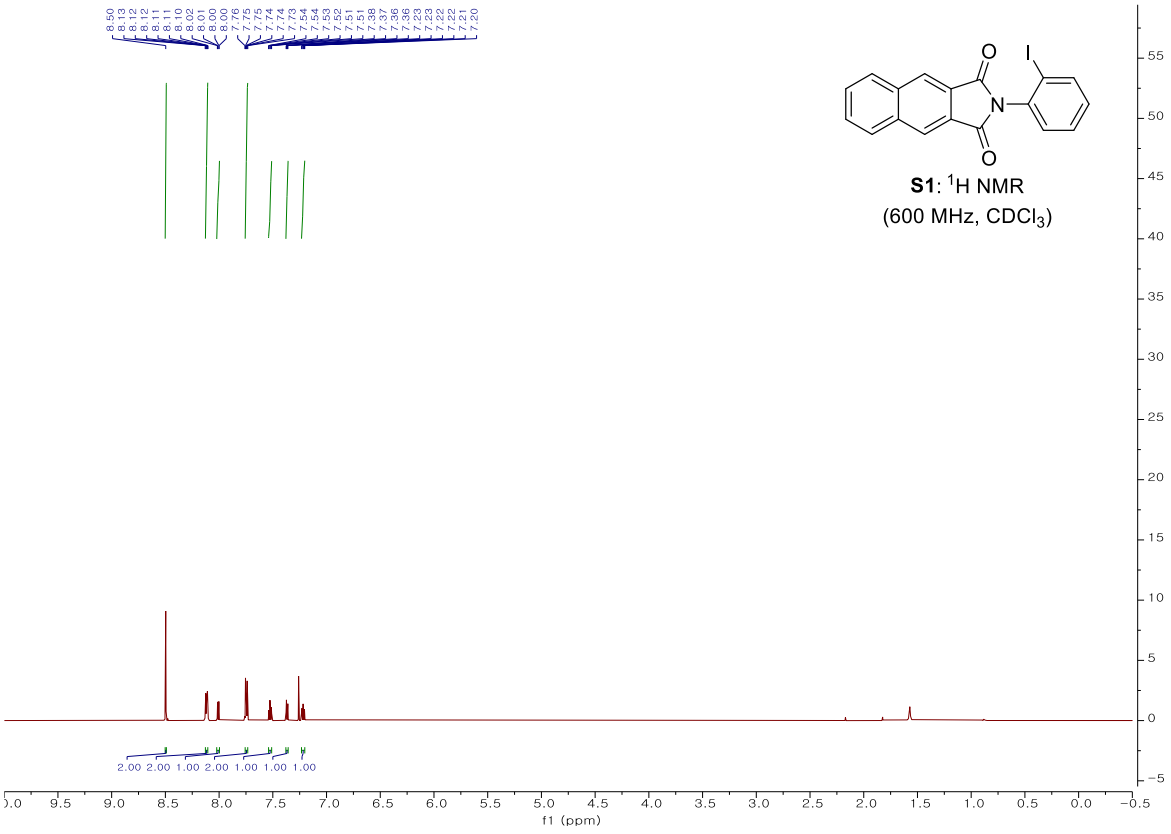

S1: ^{1}H NMR
(600 MHz, $CDCl_3$)

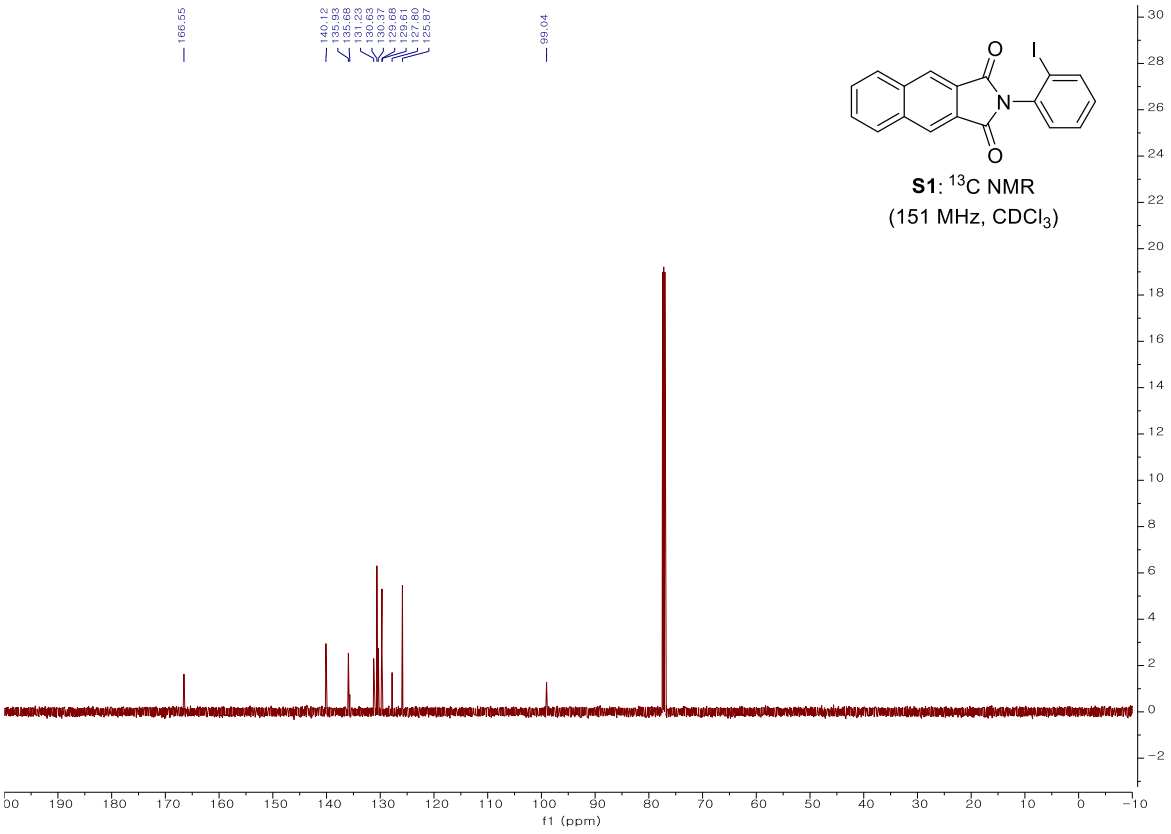

S1: ^{13}C NMR
(151 MHz, $CDCl_3$)

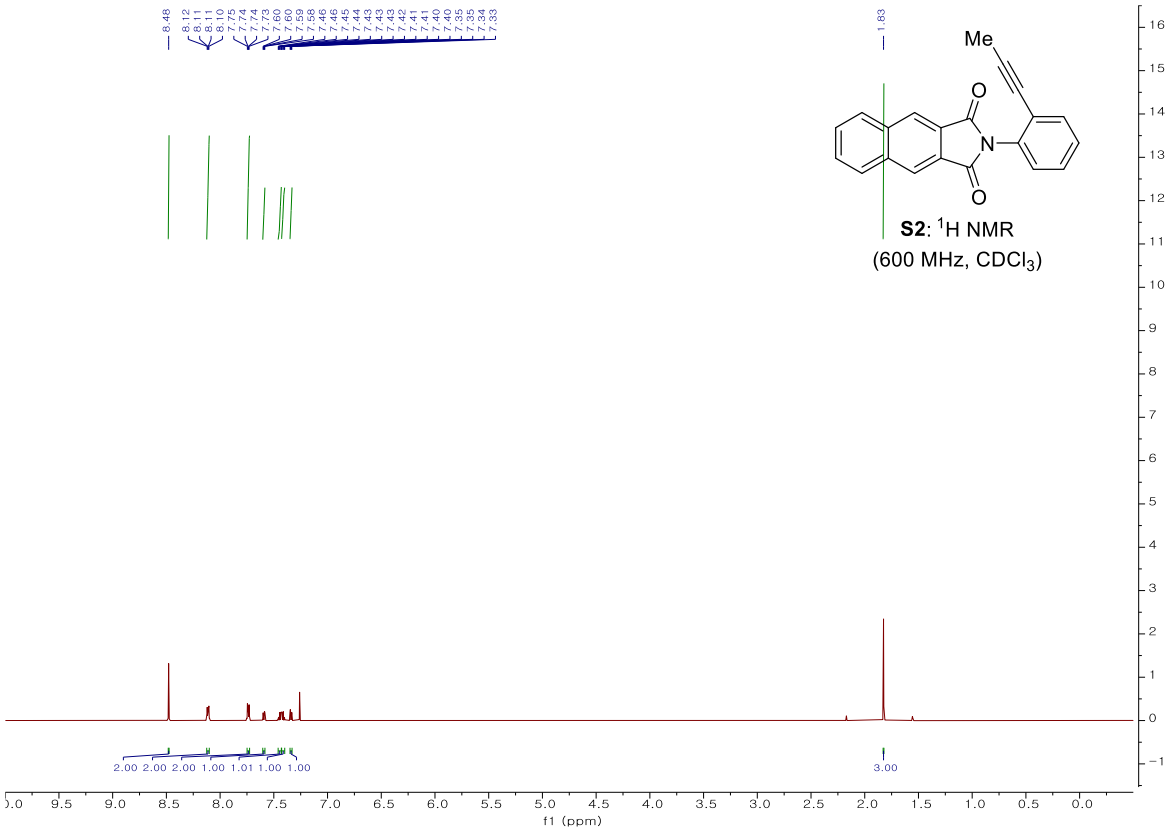

S2: ^{1}H NMR
(600 MHz, $CDCl_3$)

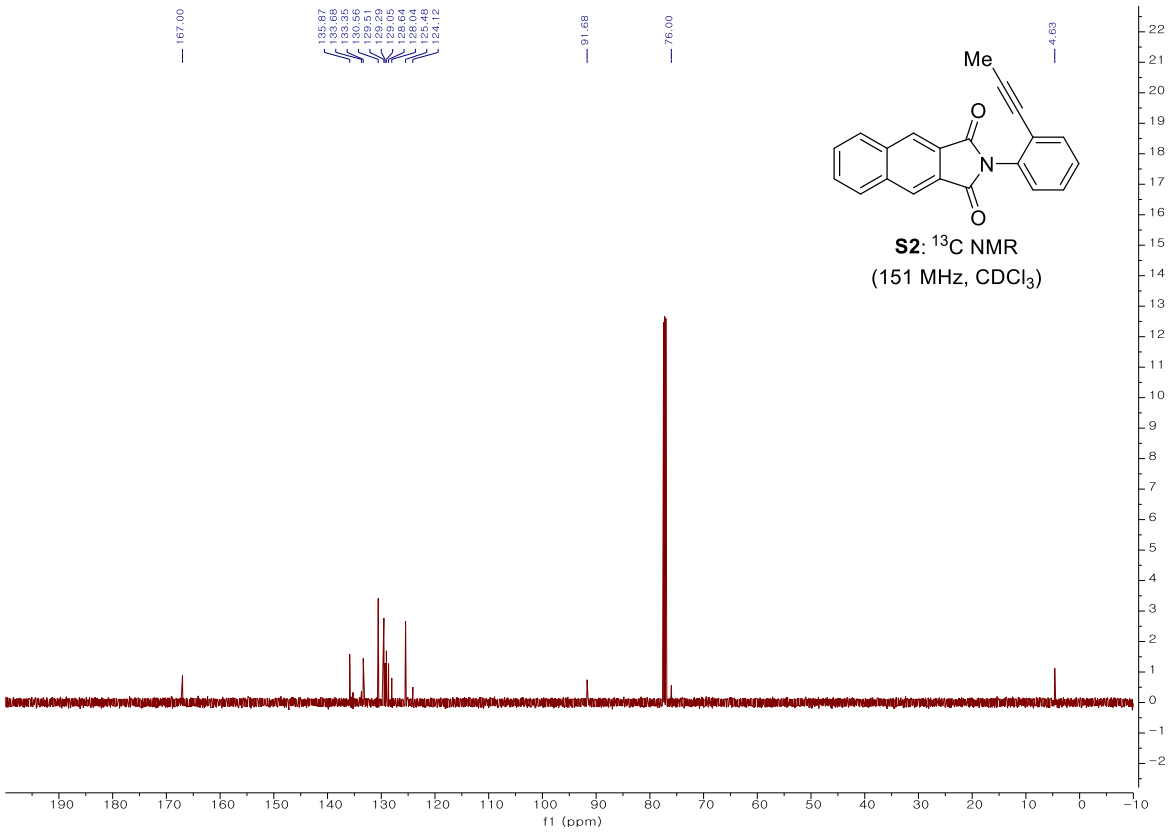

S2: ^{13}C NMR
(151 MHz, $CDCl_3$)

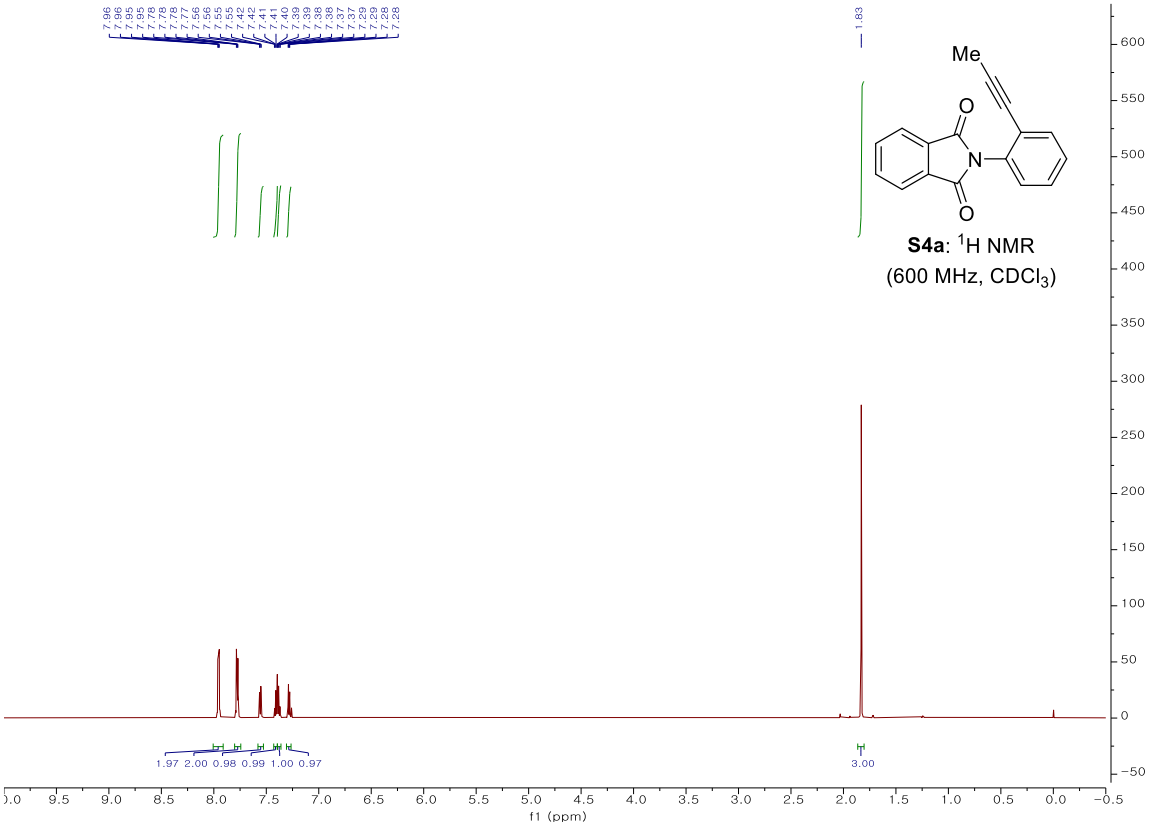

S4a: ^{1}H NMR
(600 MHz, $CDCl_3$)

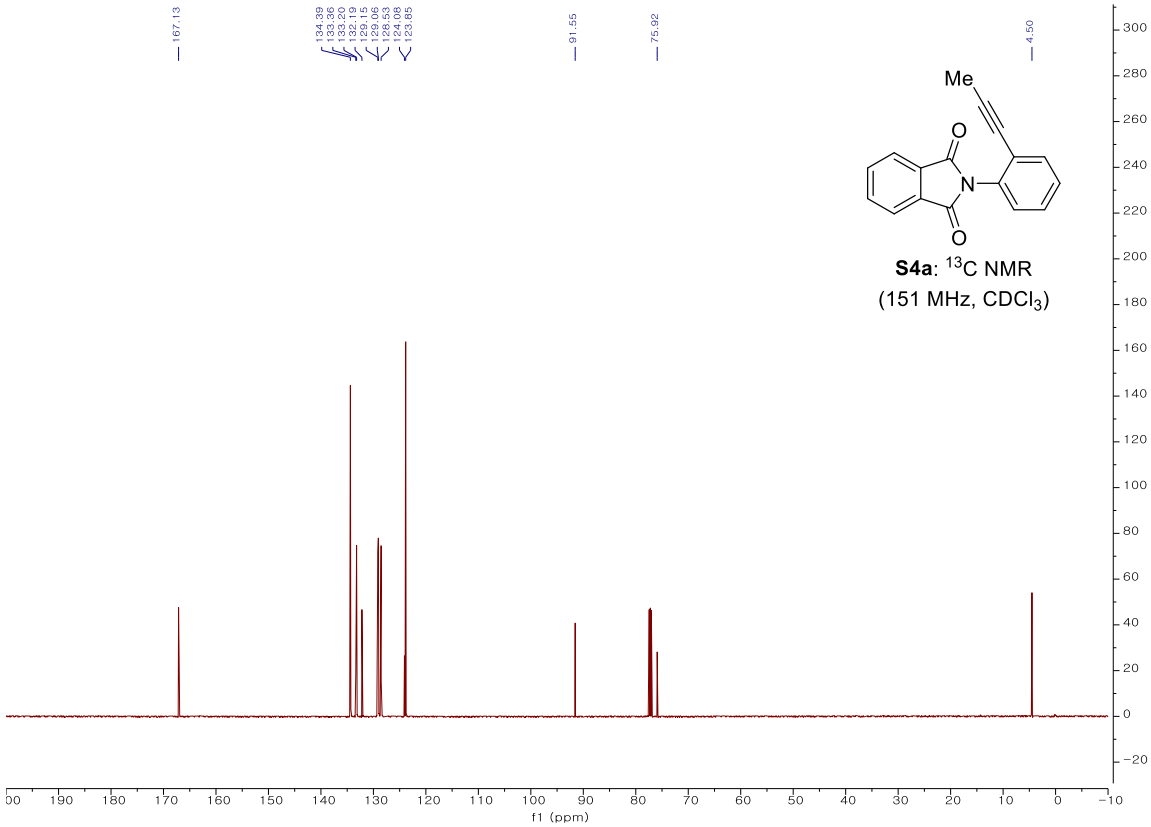

S4a: ^{13}C NMR
(151 MHz, $CDCl_3$)

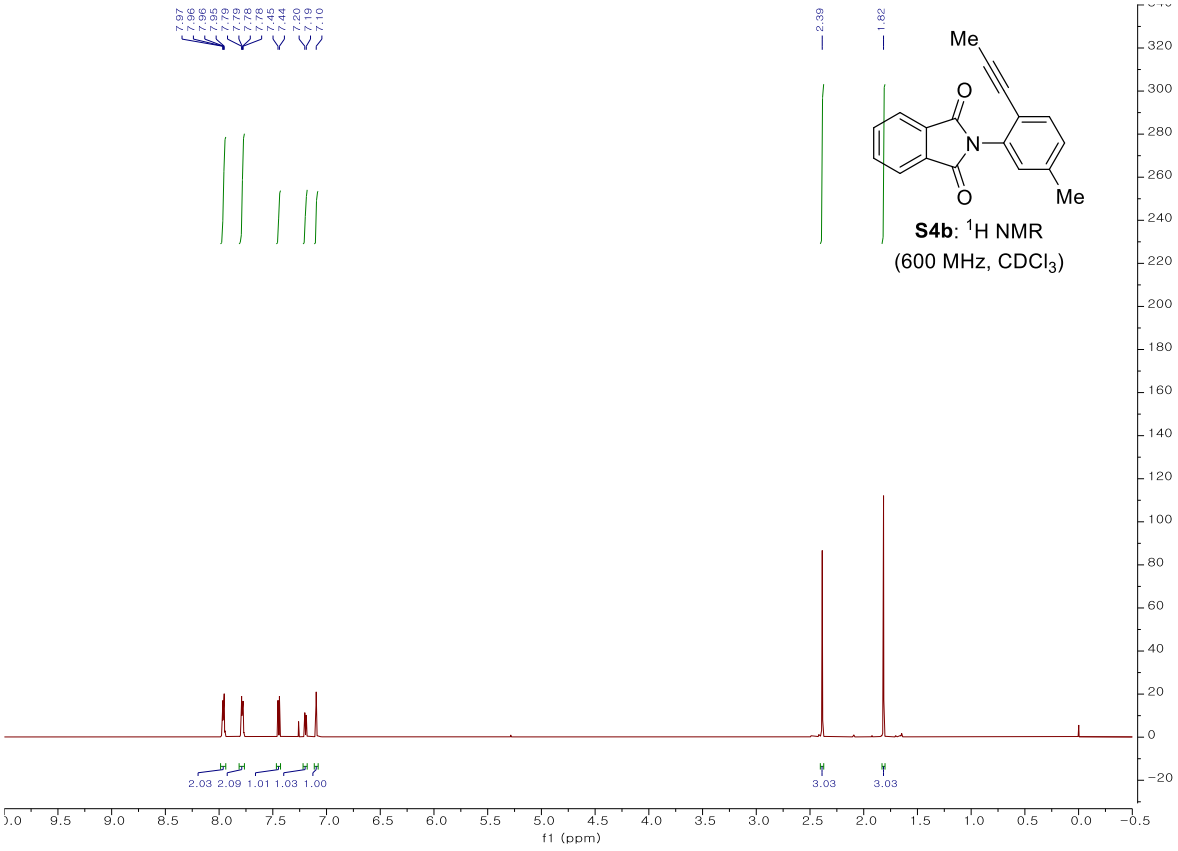

S4b: ^{1}H NMR
(600 MHz, $CDCl_3$)

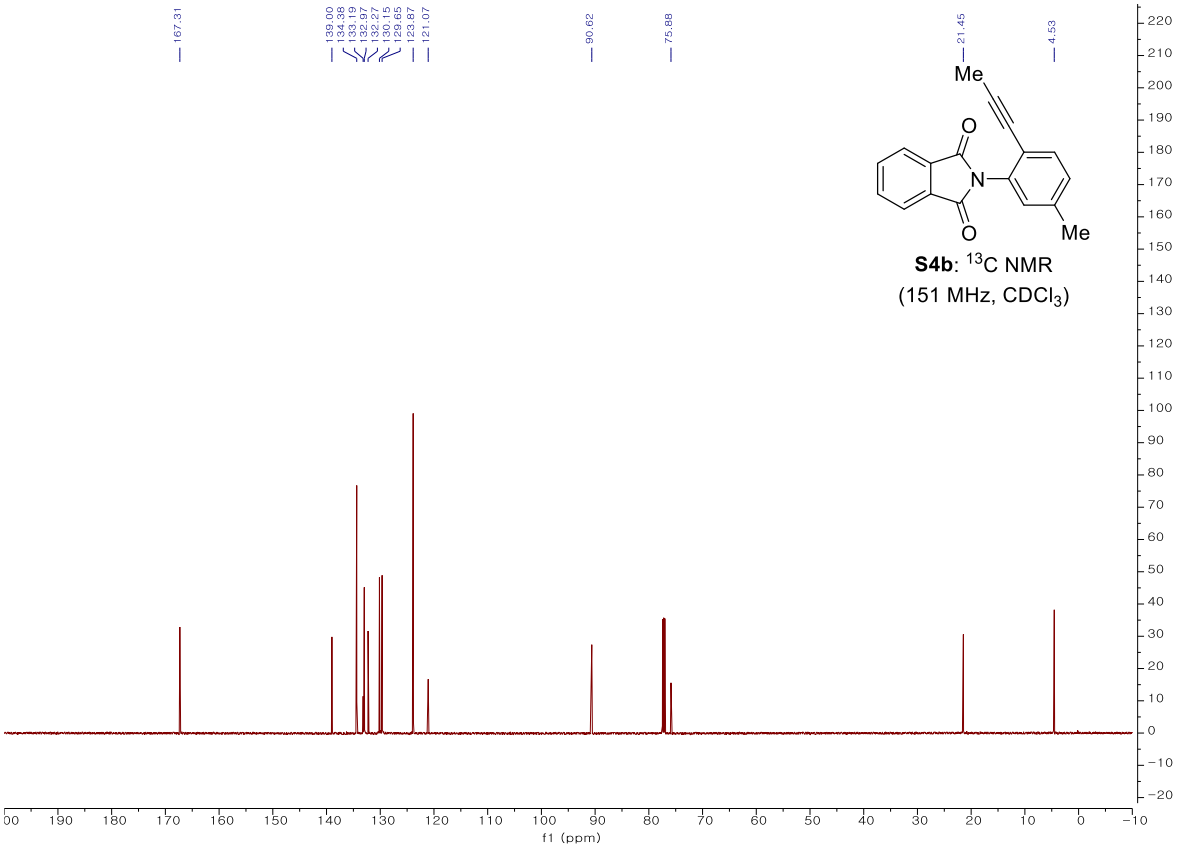

S4b: ^{13}C NMR
(151 MHz, $CDCl_3$)

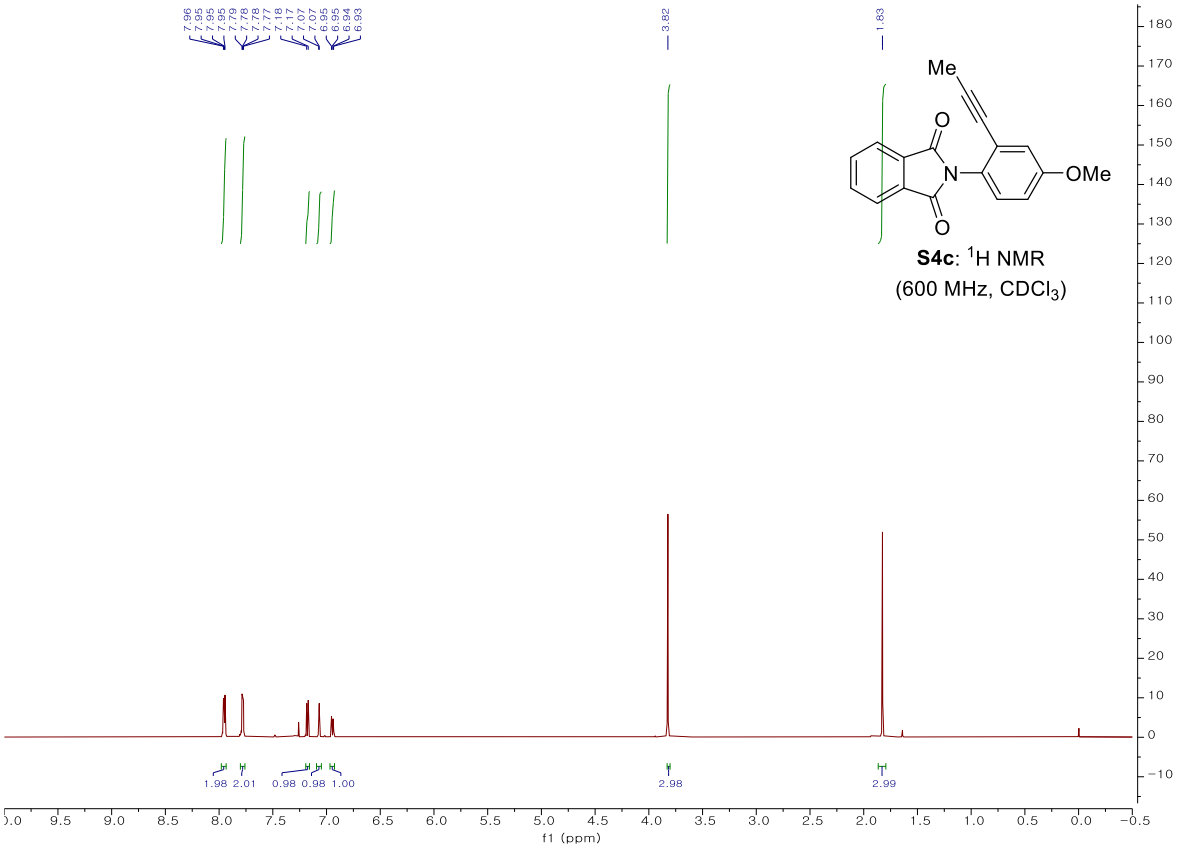

S4c: ^{1}H NMR
(600 MHz, $CDCl_3$)

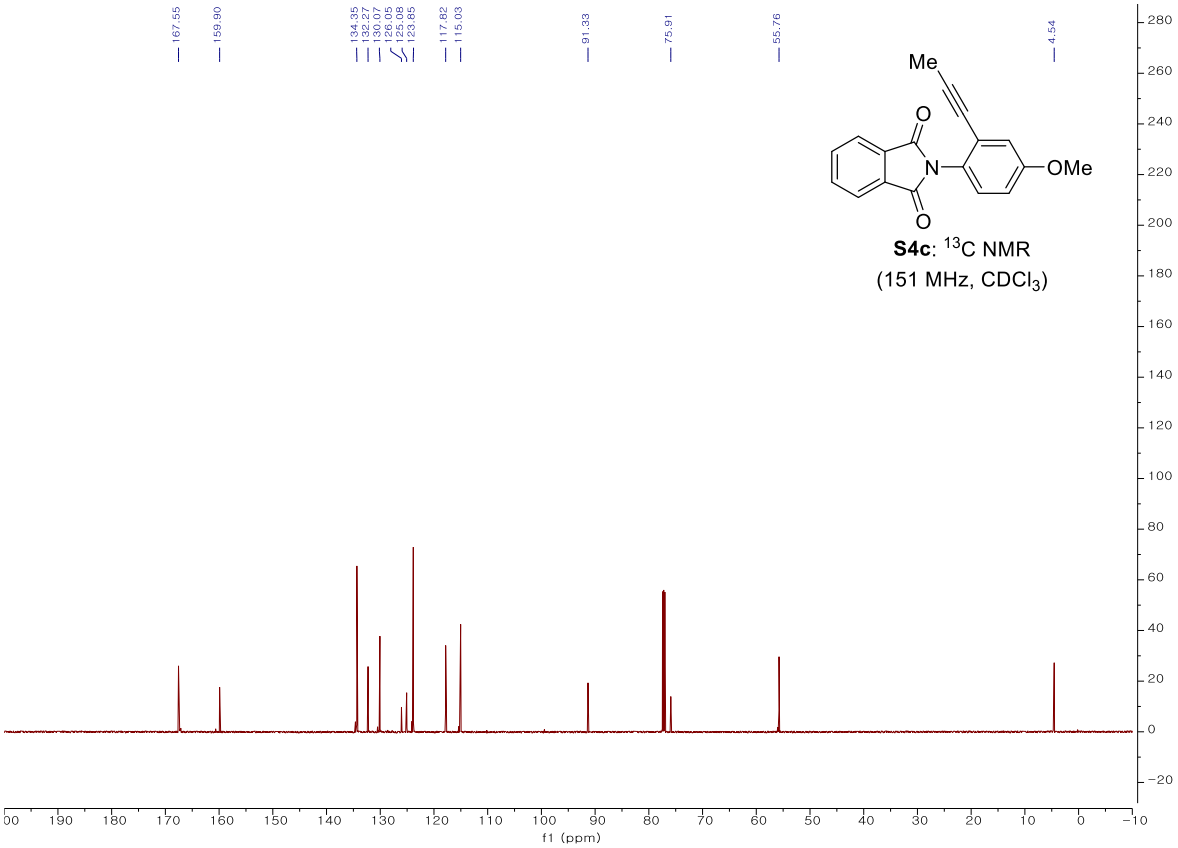

S4c: ^{13}C NMR
(151 MHz, $CDCl_3$)

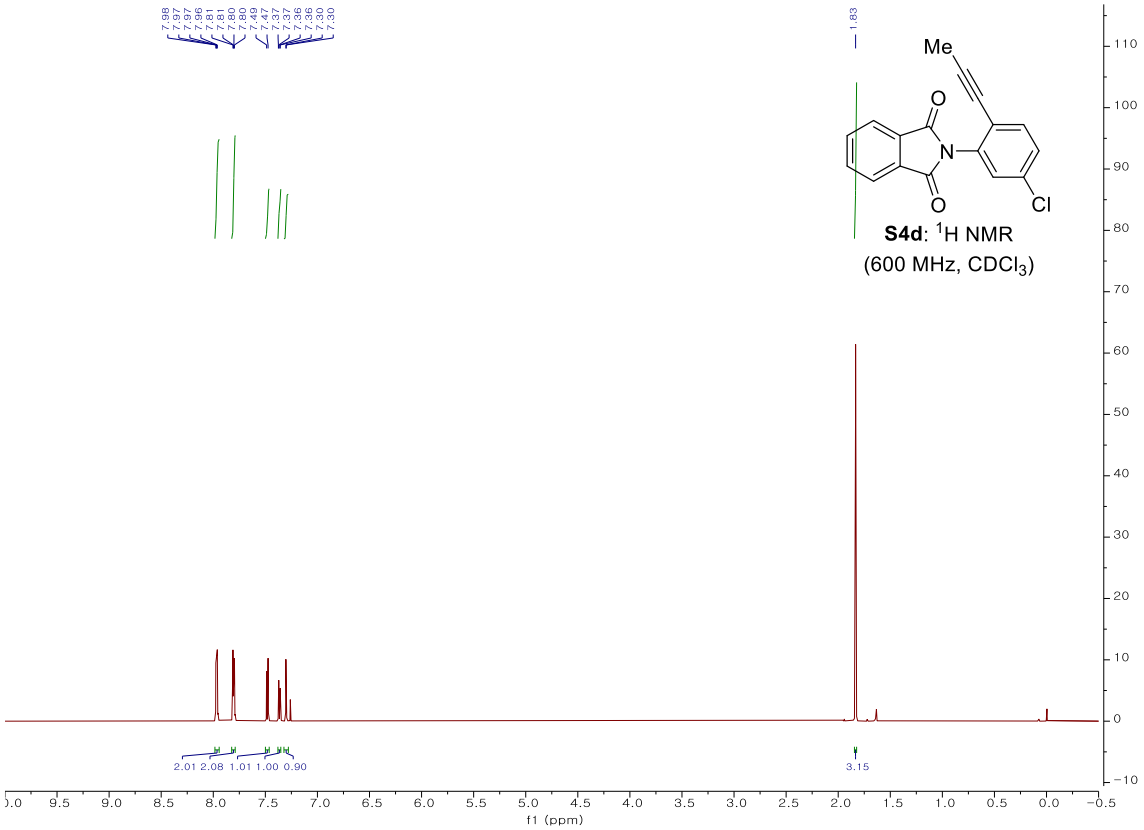

S4d: ^{1}H NMR
(600 MHz, $CDCl_3$)

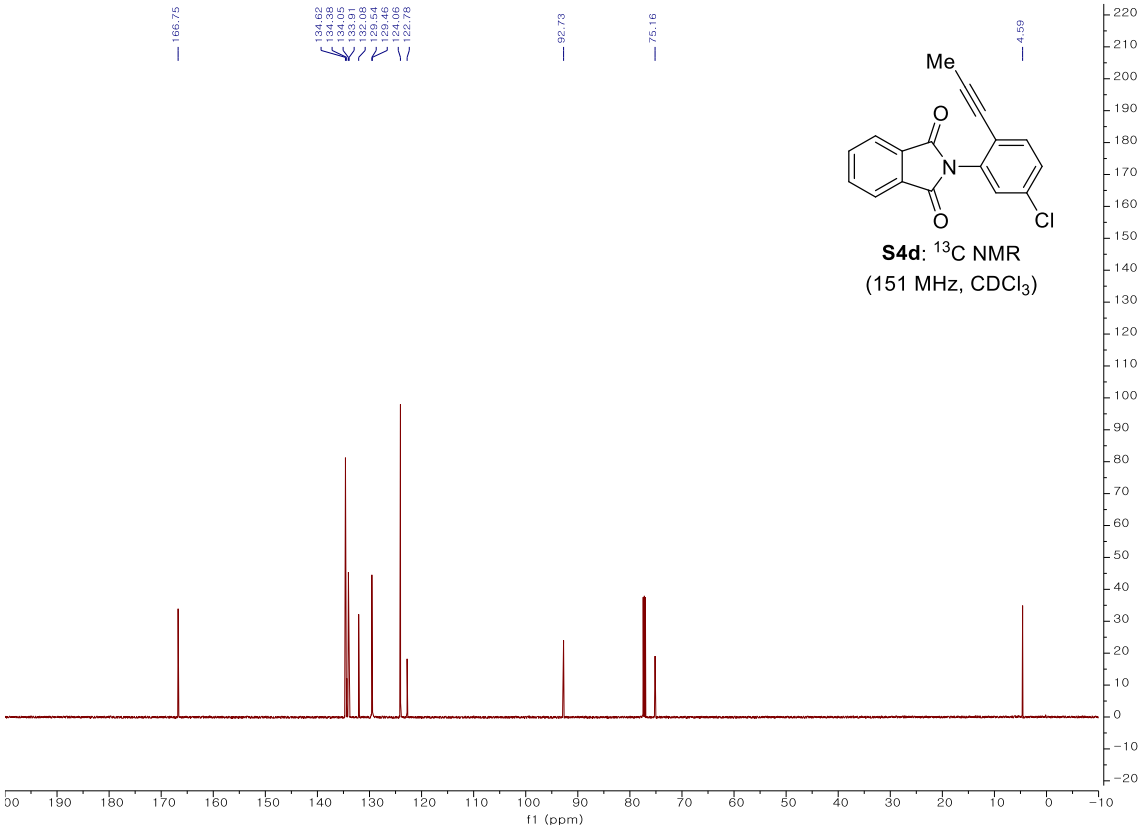

S4d: ^{13}C NMR
(151 MHz, $CDCl_3$)

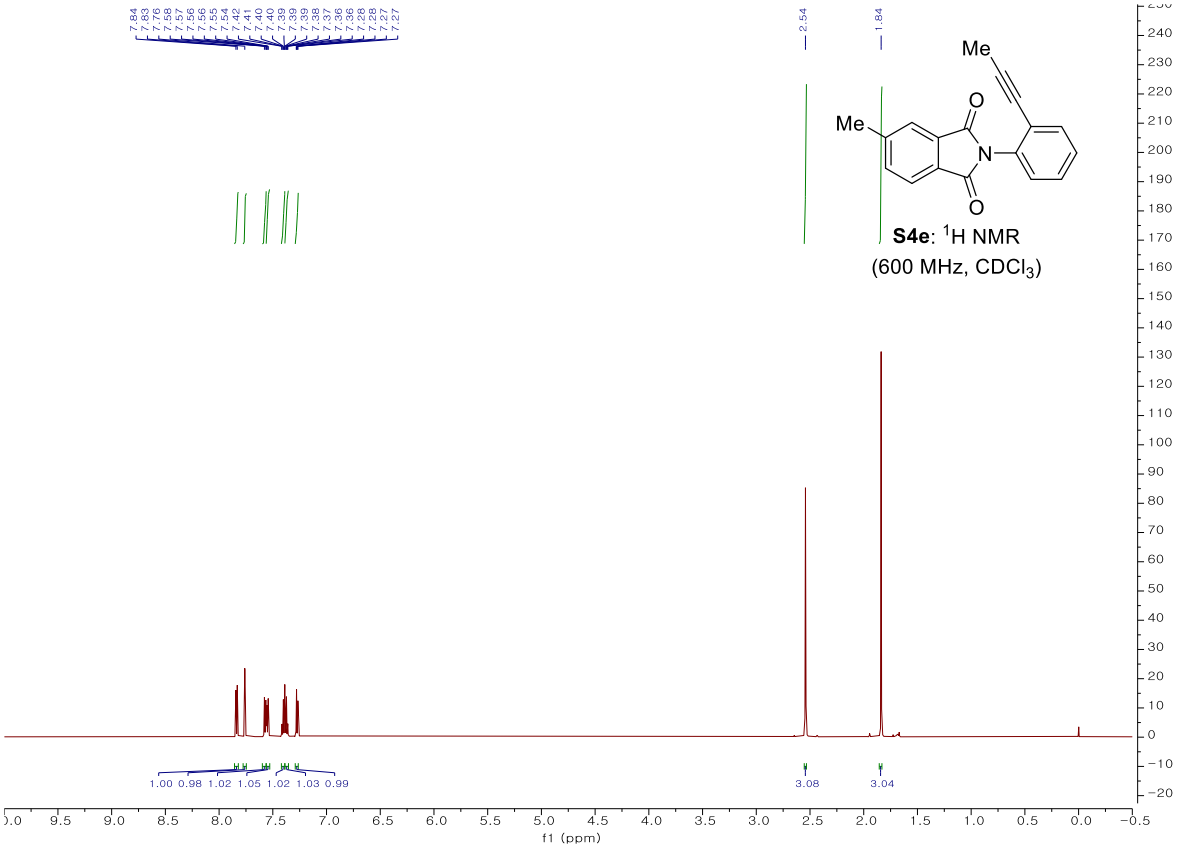

S4e: ^{1}H NMR
(600 MHz, $CDCl_3$)

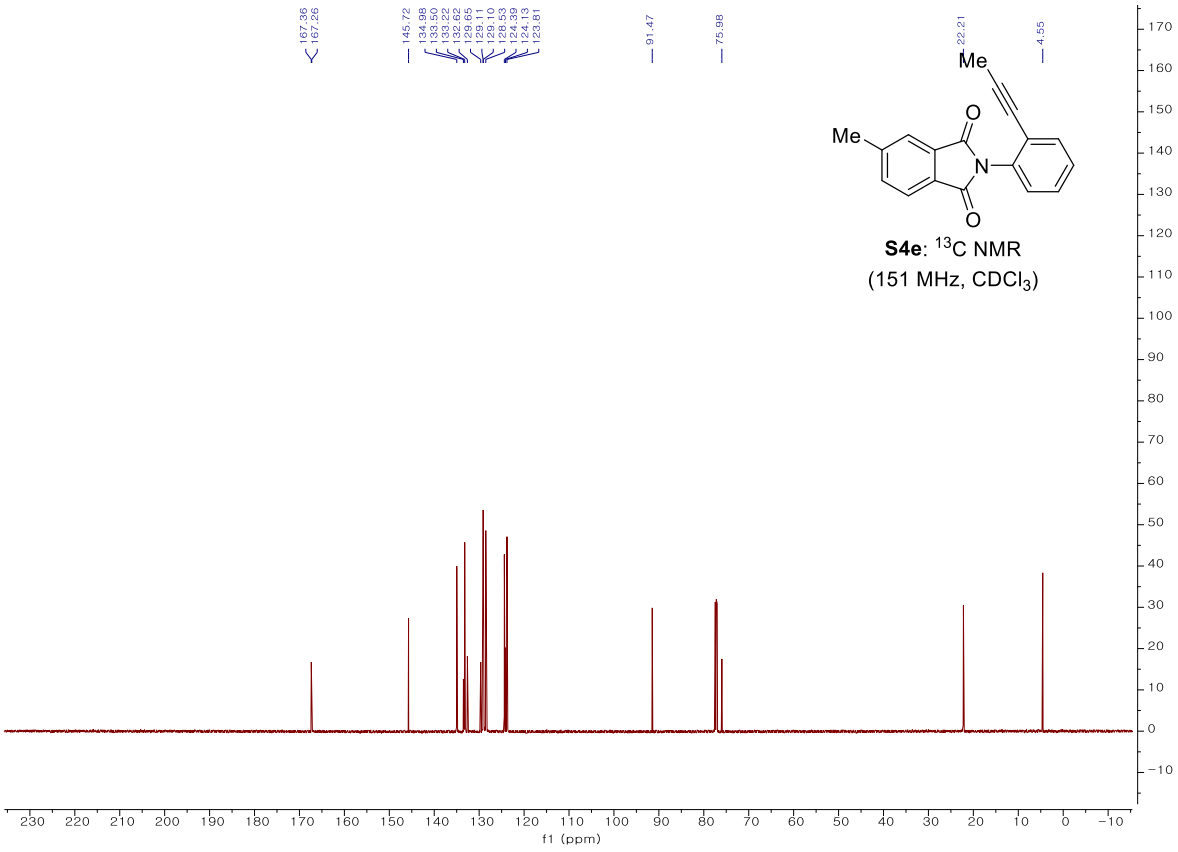

S4e: ^{13}C NMR
(151 MHz, $CDCl_3$)

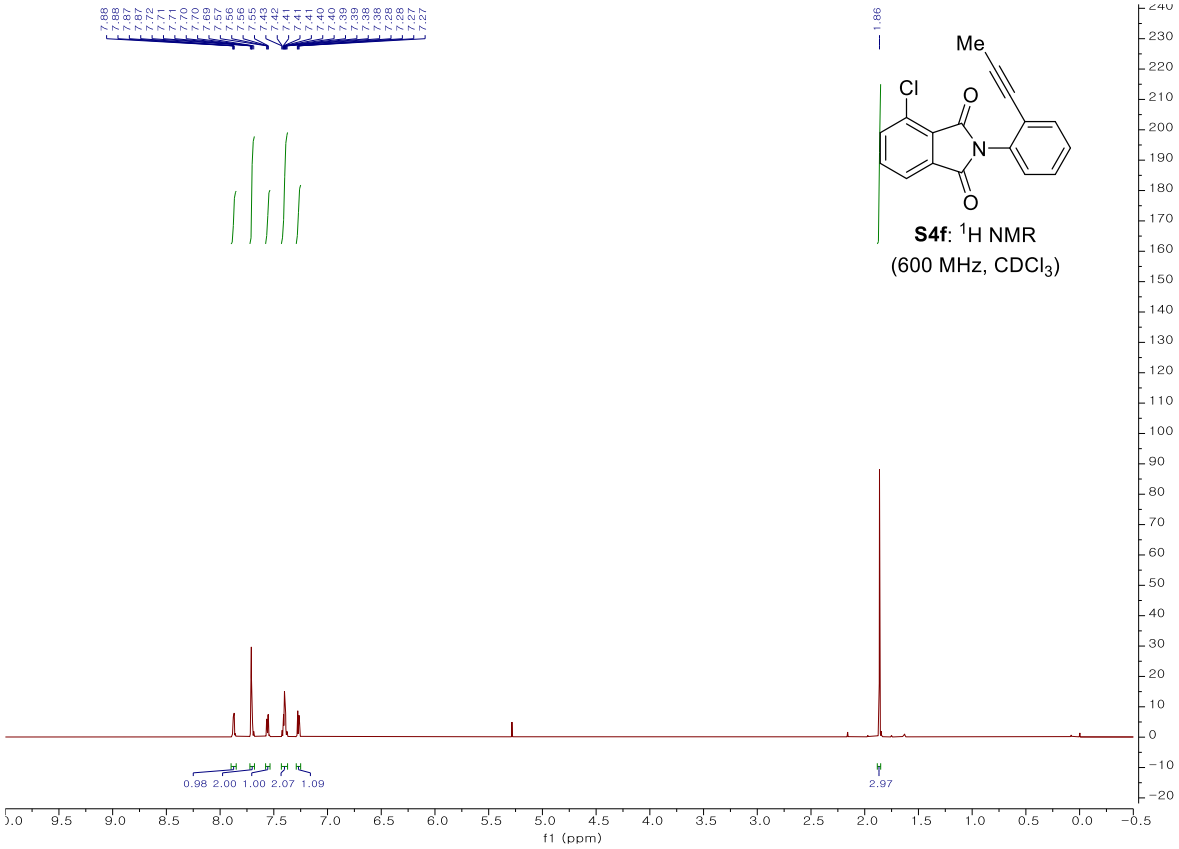

S4f: ^{1}H NMR
(600 MHz, $CDCl_3$)

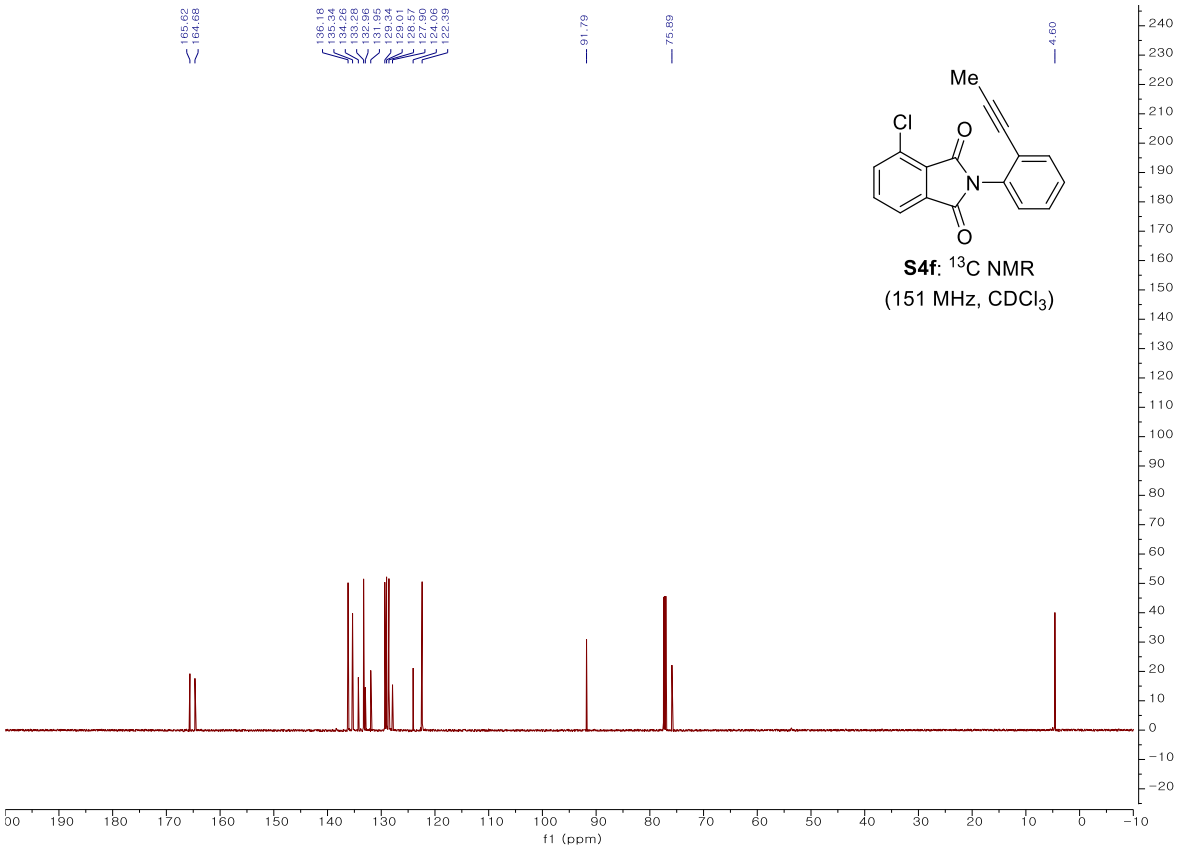

S4f: ^{13}C NMR
(151 MHz, $CDCl_3$)

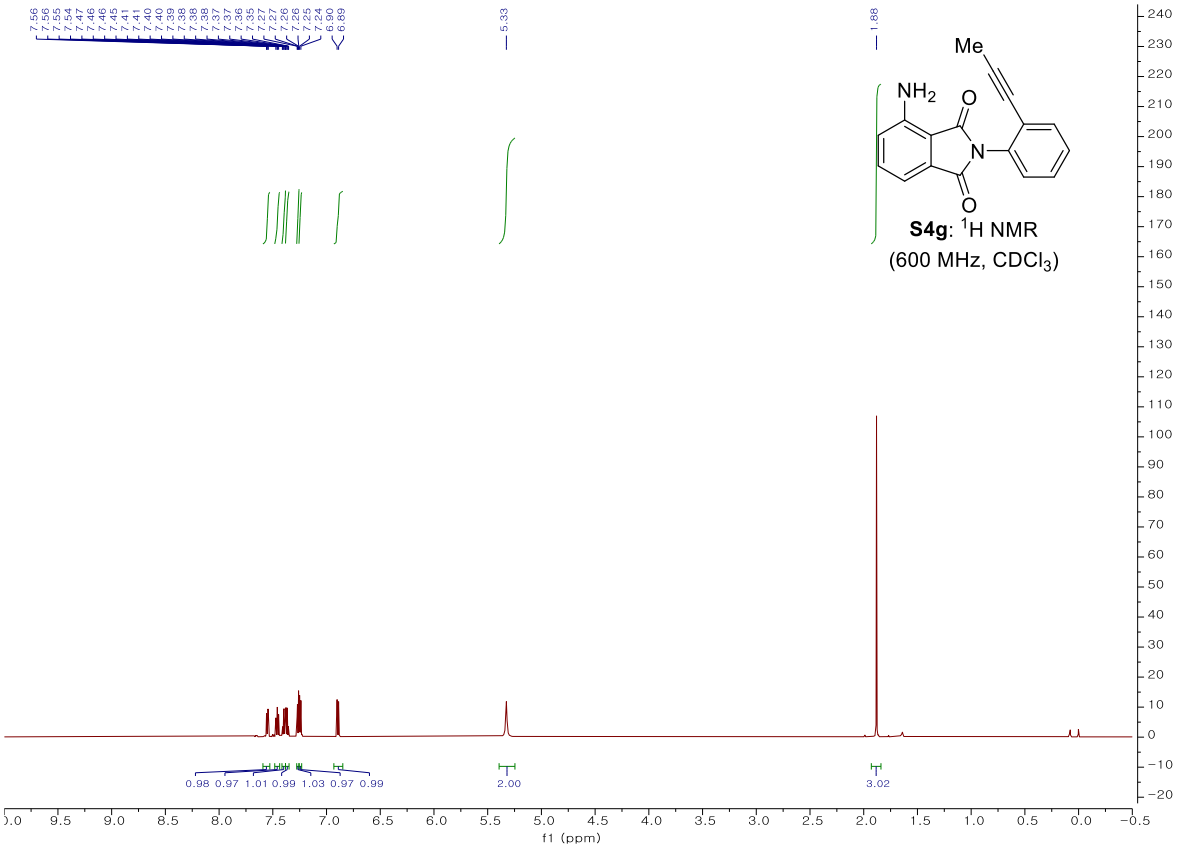

S4g: ^{1}H NMR
(600 MHz, $CDCl_3$)

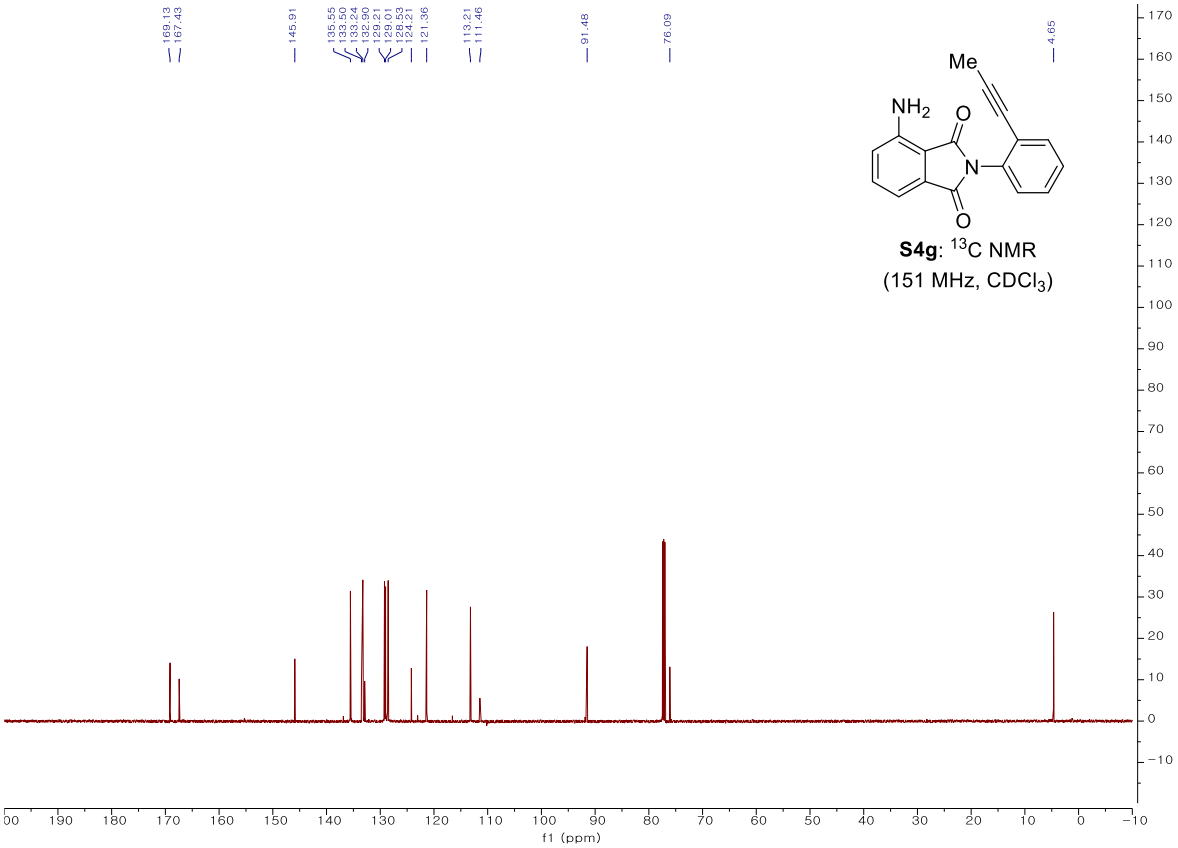

S4g: ^{13}C NMR
(151 MHz, $CDCl_3$)

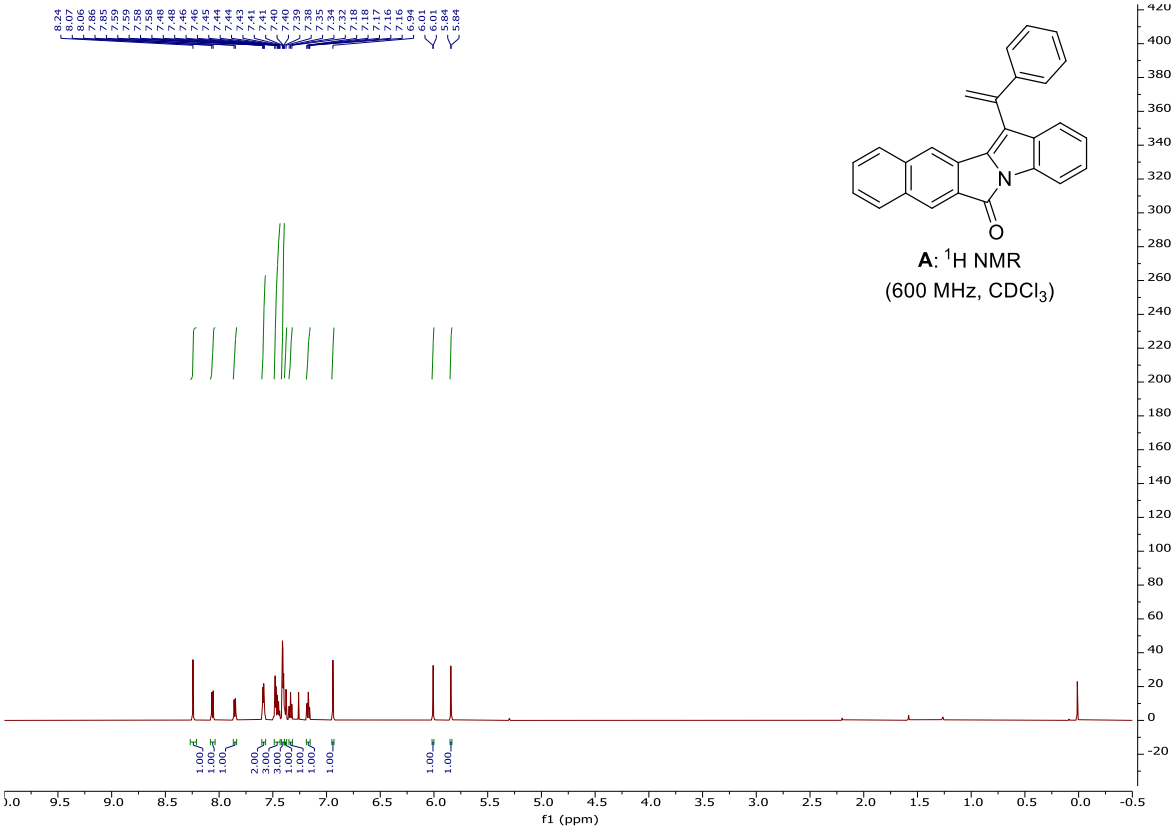

A: ^{1}H NMR
(600 MHz, $CDCl_3$)

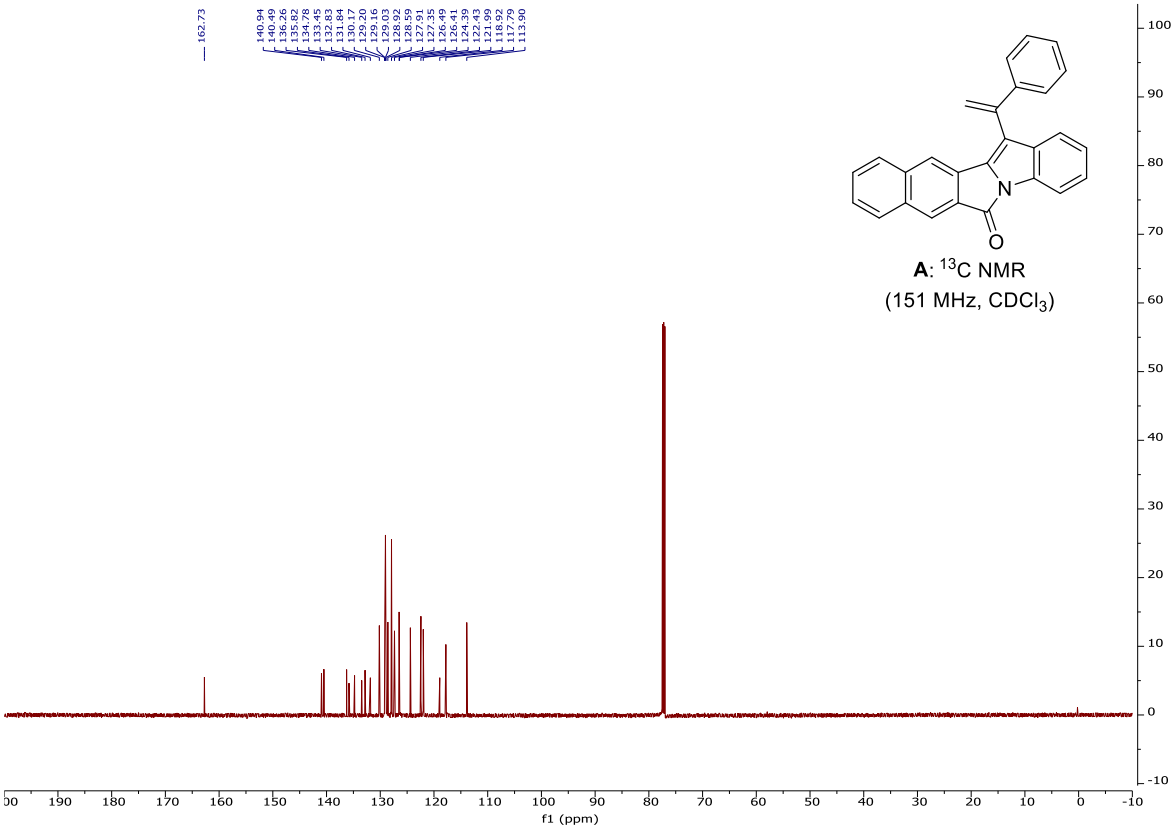

A: ^{13}C NMR
(151 MHz, $CDCl_3$)

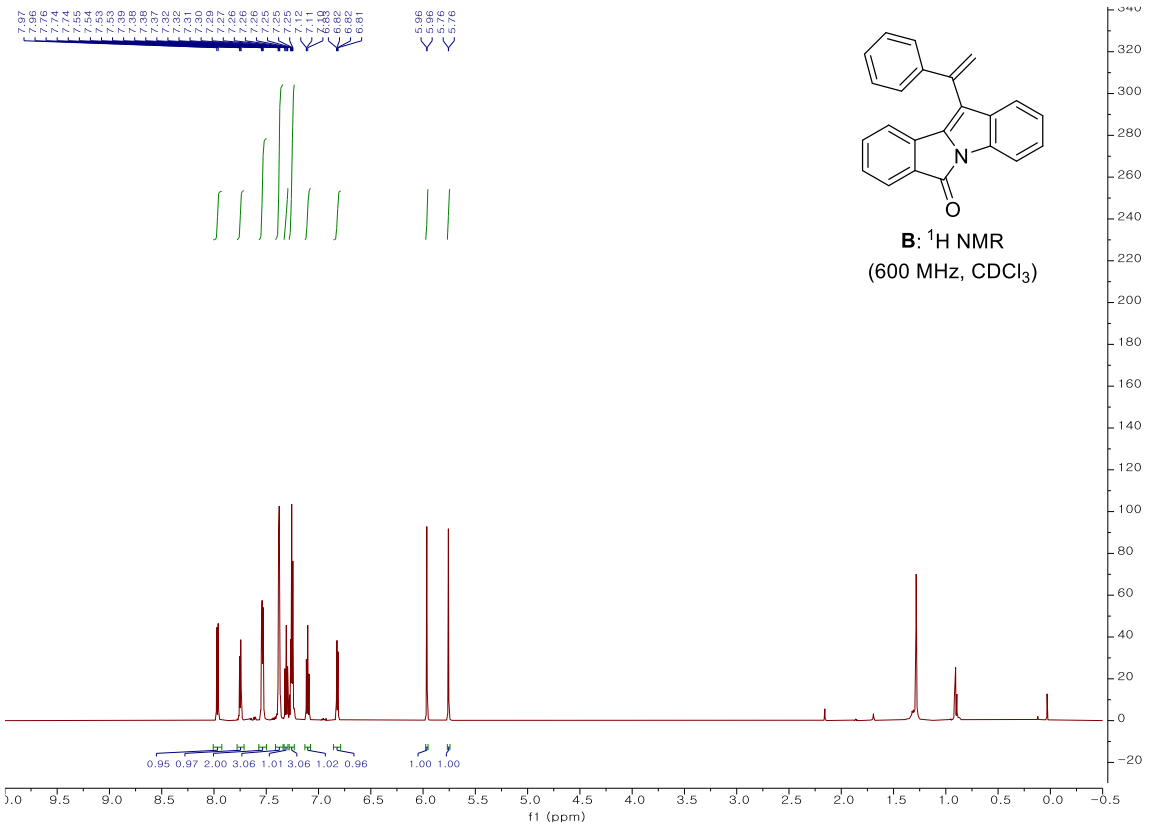

B: ^{1}H NMR
(600 MHz, $CDCl_3$)

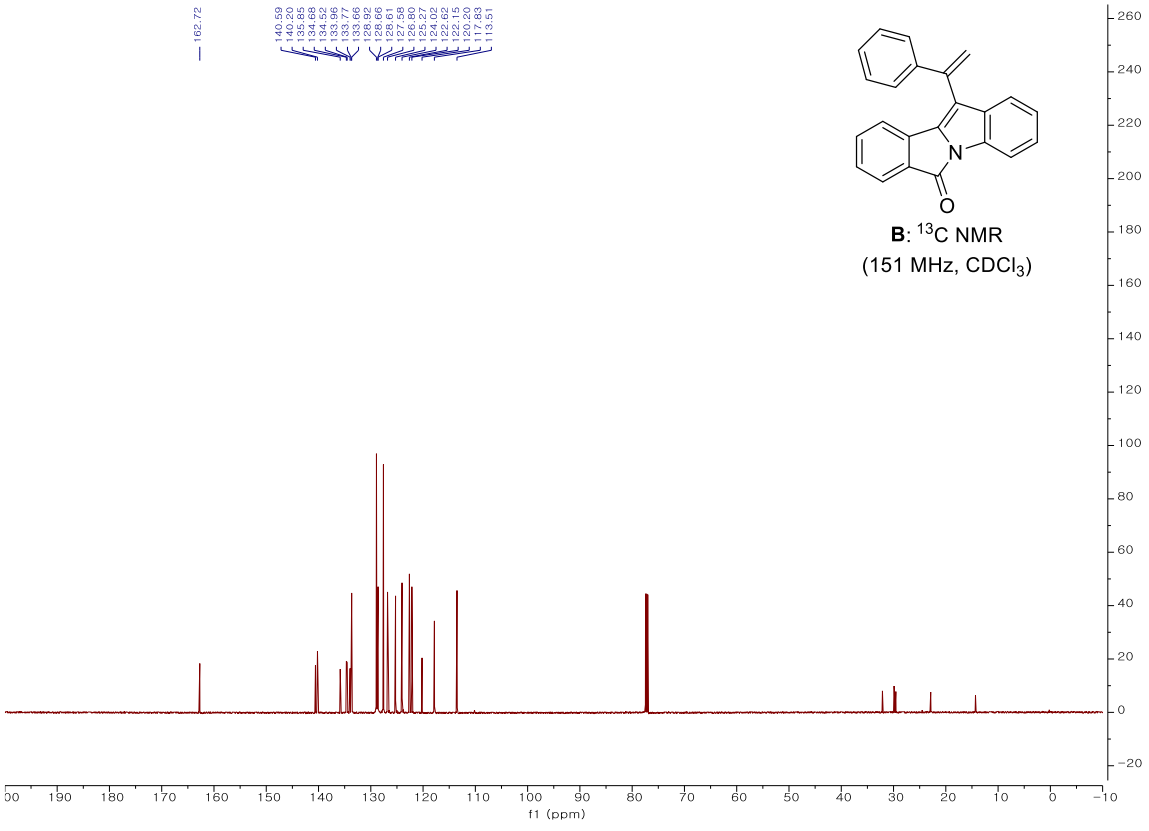

B: ^{13}C NMR
(151 MHz, $CDCl_3$)

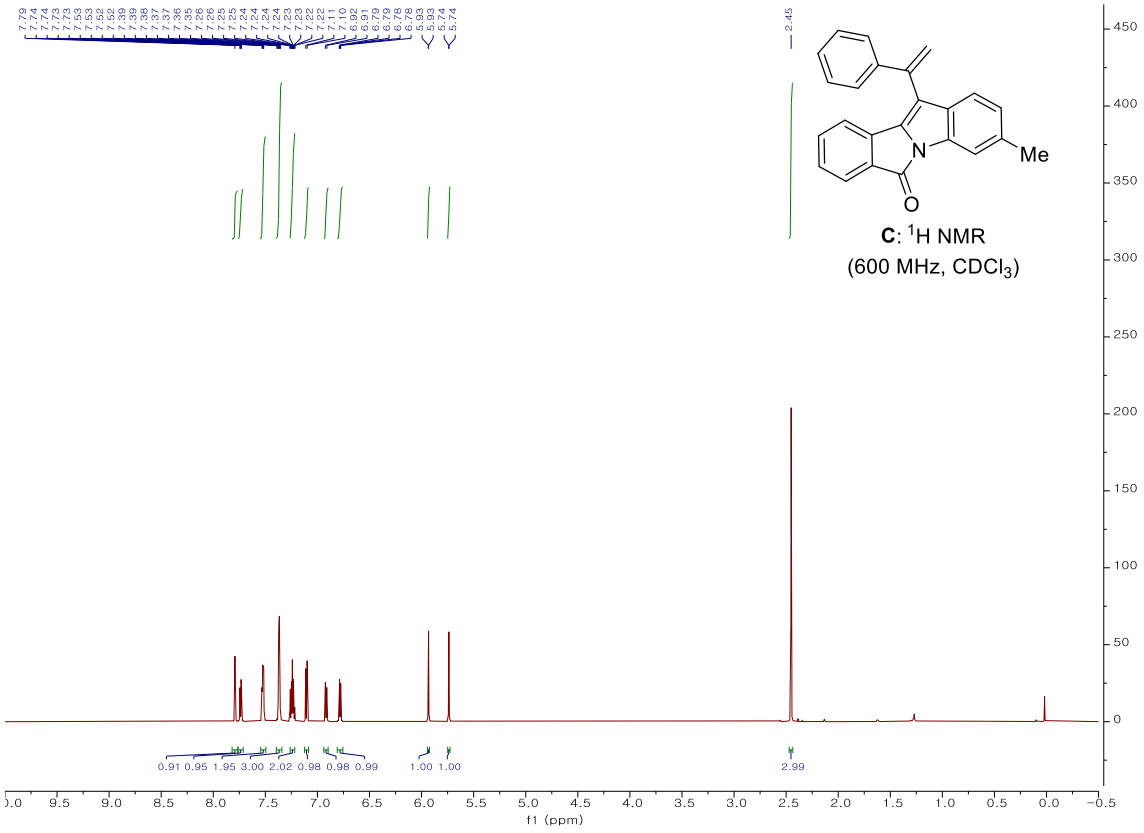
Me
O
C: 1H NMR
(600 MHz, CDCl3)
f1 (ppm)

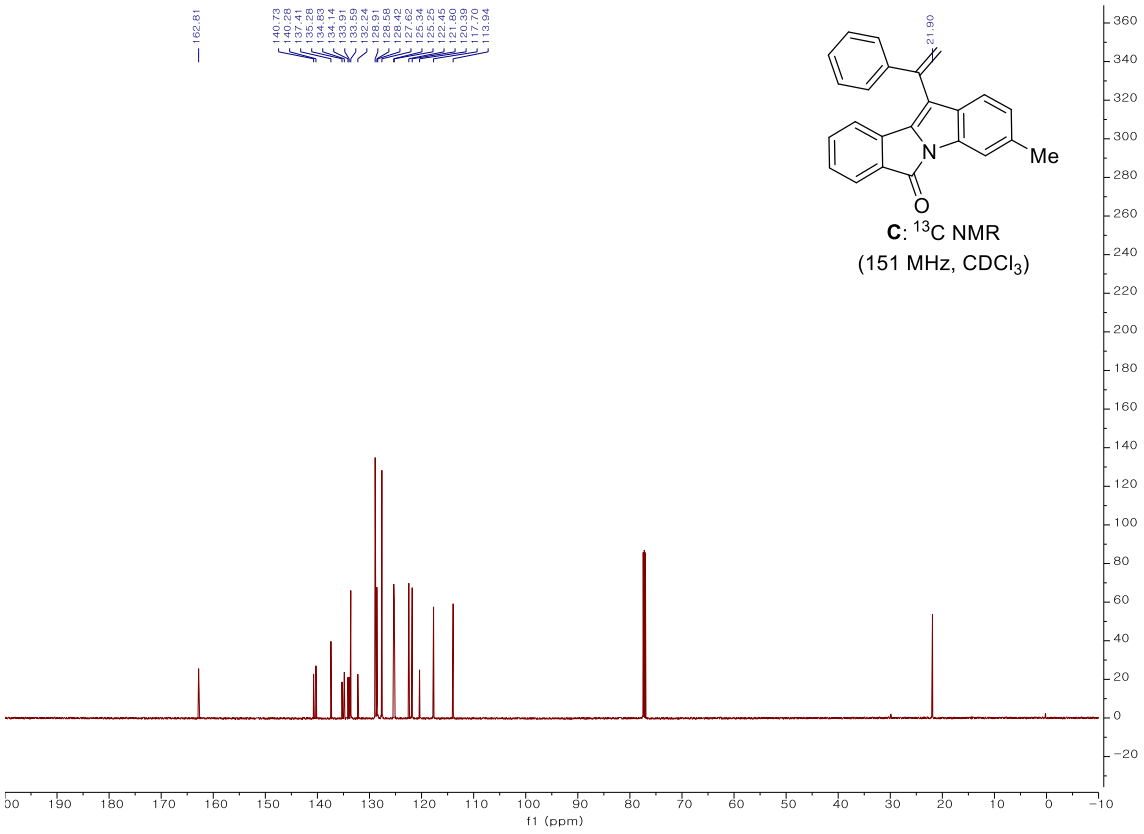
Me
O
C: 13C NMR
(151 MHz, CDCl3)
f1 (ppm)

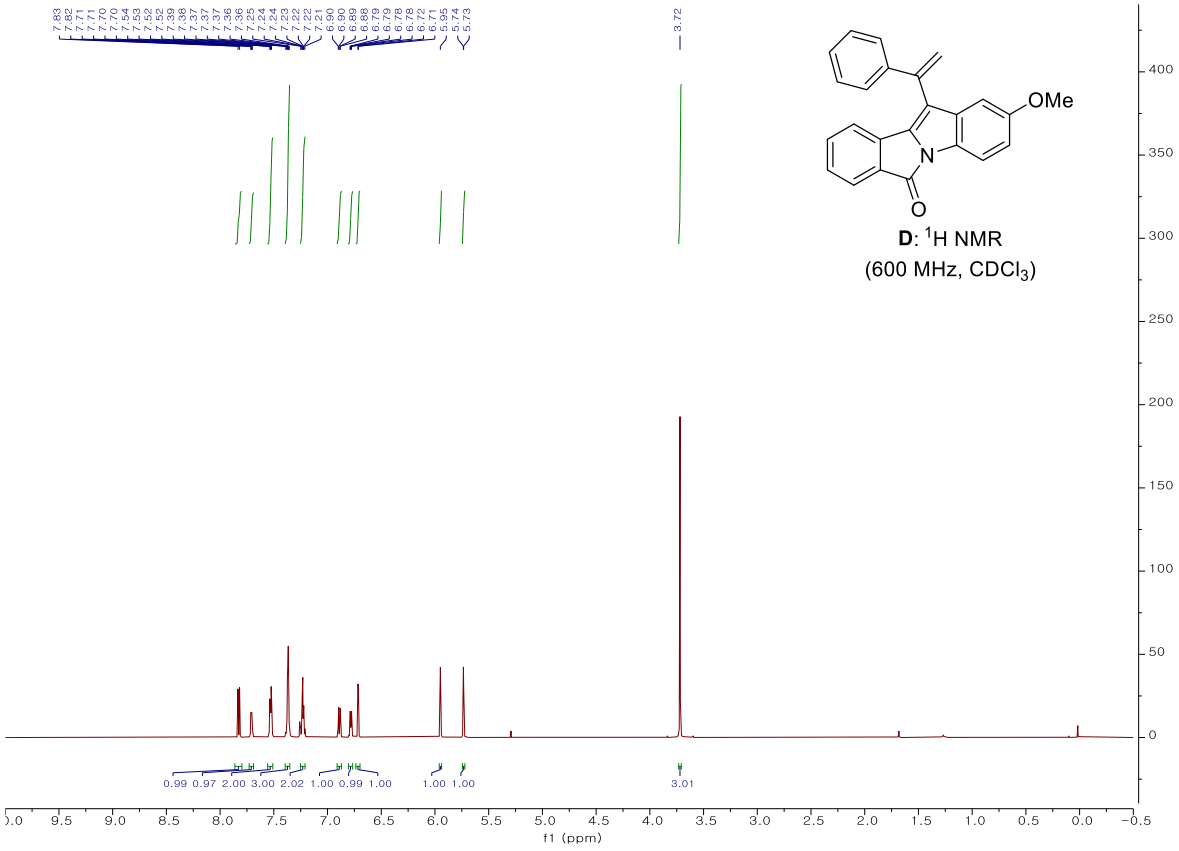

D: ^{1}H NMR
(600 MHz, $CDCl_3$)

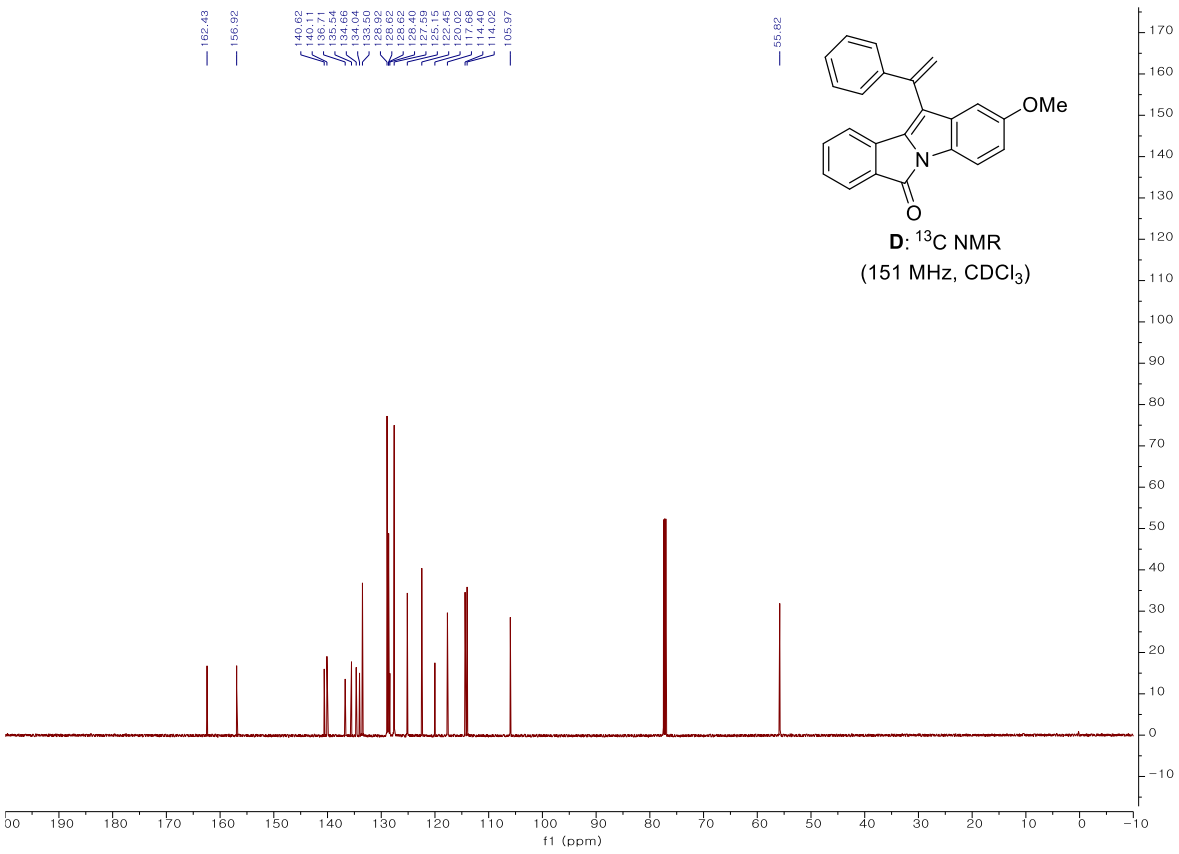

D: ^{13}C NMR
(151 MHz, $CDCl_3$)

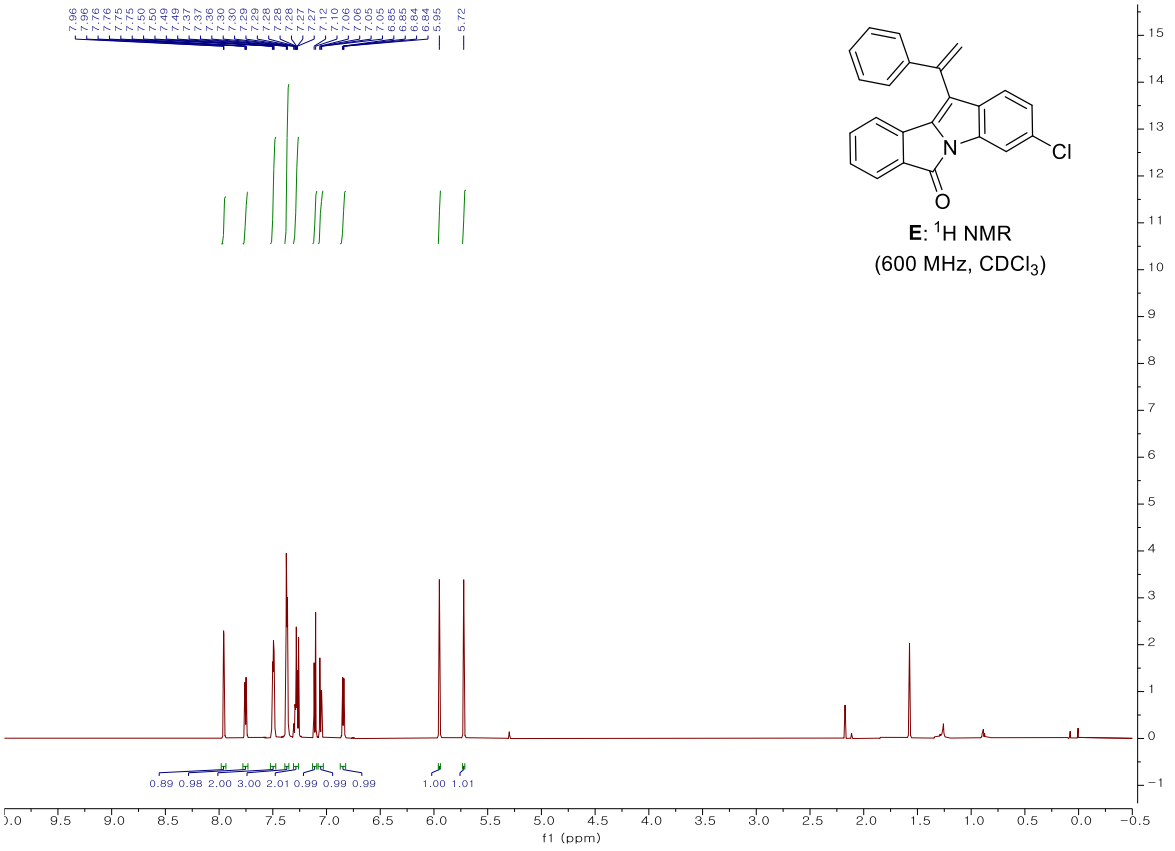

E: ^{1}H NMR
(600 MHz, $CDCl_3$)

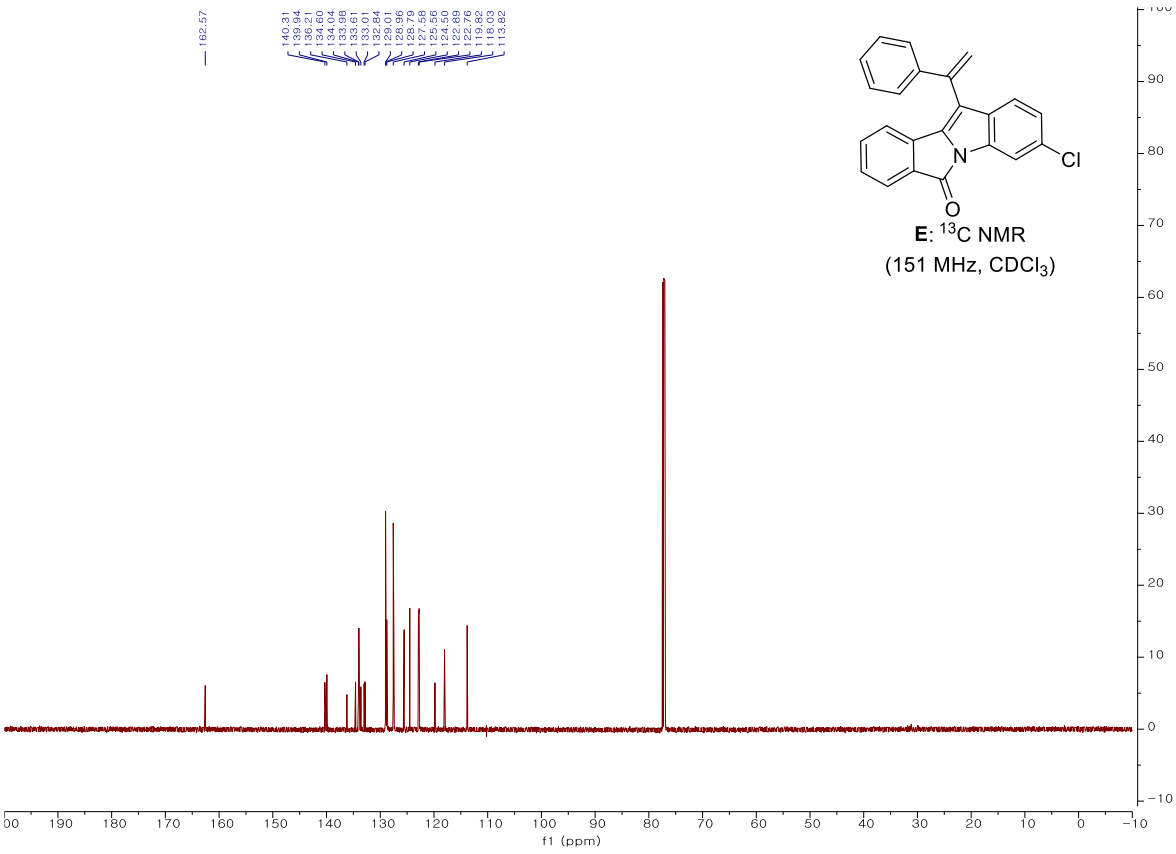

E: ^{13}C NMR
(151 MHz, $CDCl_3$)

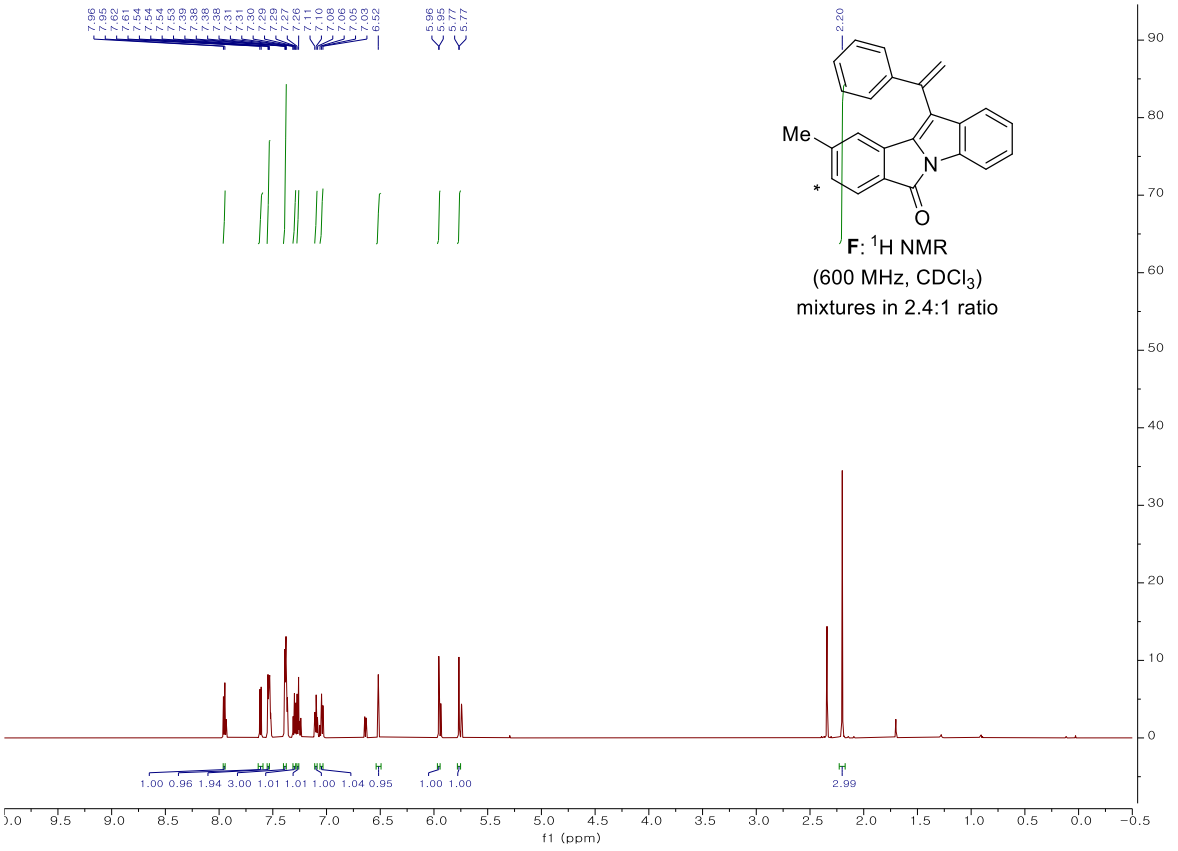
Me
N
O
*
F: 1H NMR
(600 MHz, CDCl3)
mixtures in 2.4:1 ratio
f1 (ppm)

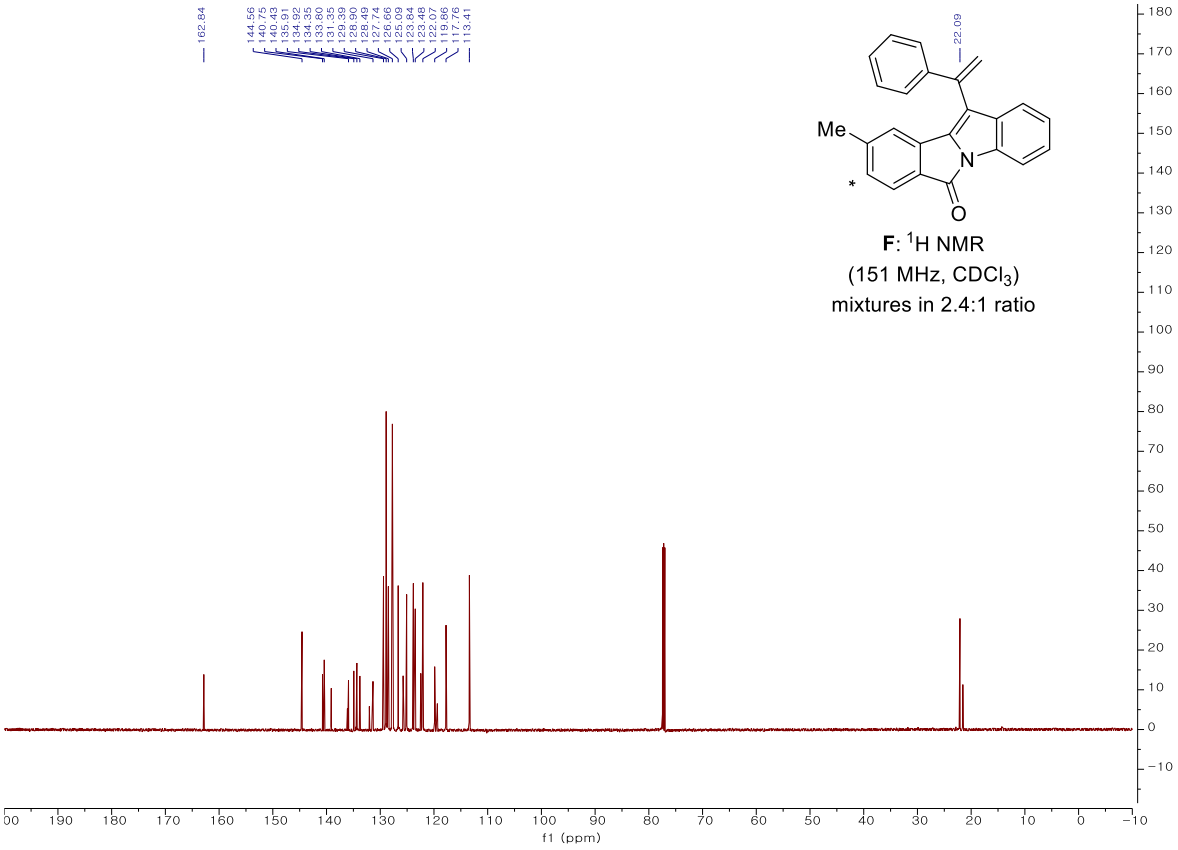
Me
N
O
*
F: 1H NMR
(151 MHz, CDCl3)
mixtures in 2.4:1 ratio
f1 (ppm)

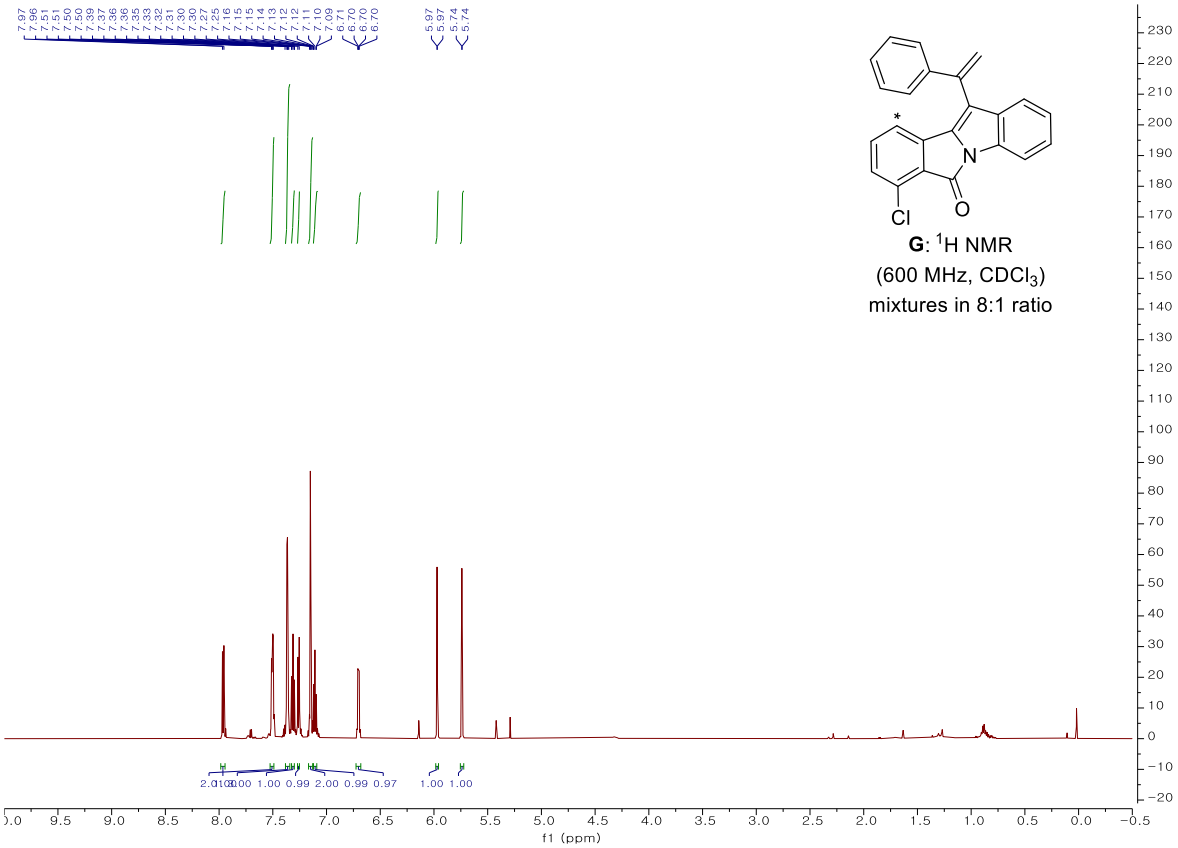

G: ^{1}H NMR
(600 MHz, $CDCl_3$)
mixtures in 8:1 ratio

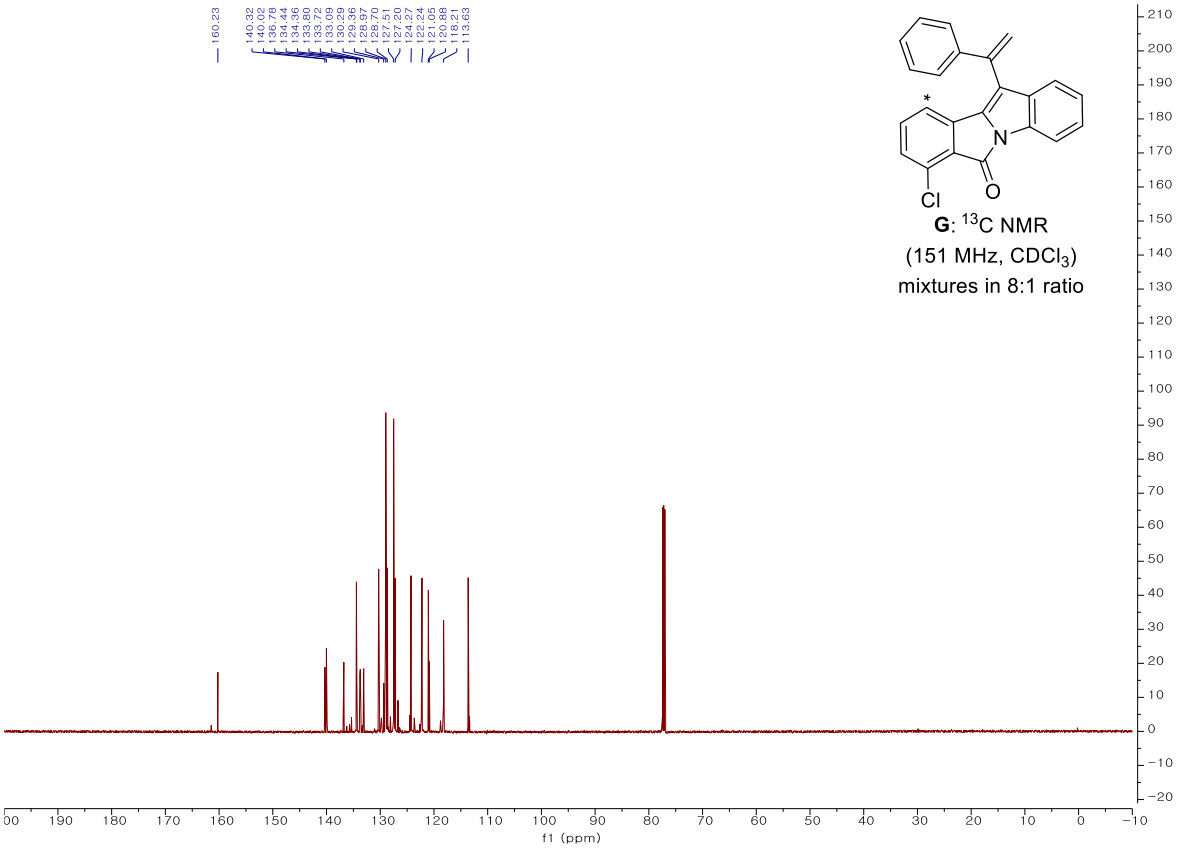

G: ^{13}C NMR
(151 MHz, $CDCl_3$)
mixtures in 8:1 ratio

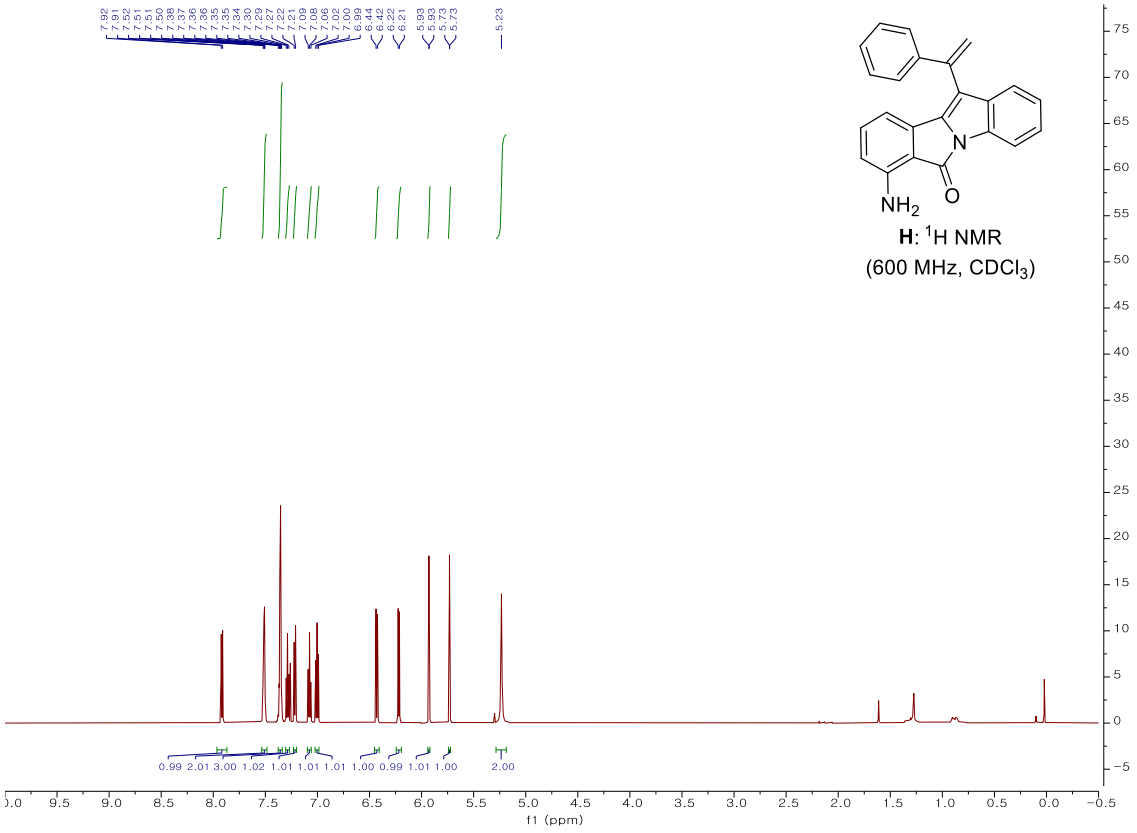

H: ^{1}H NMR
(600 MHz, $CDCl_3$)

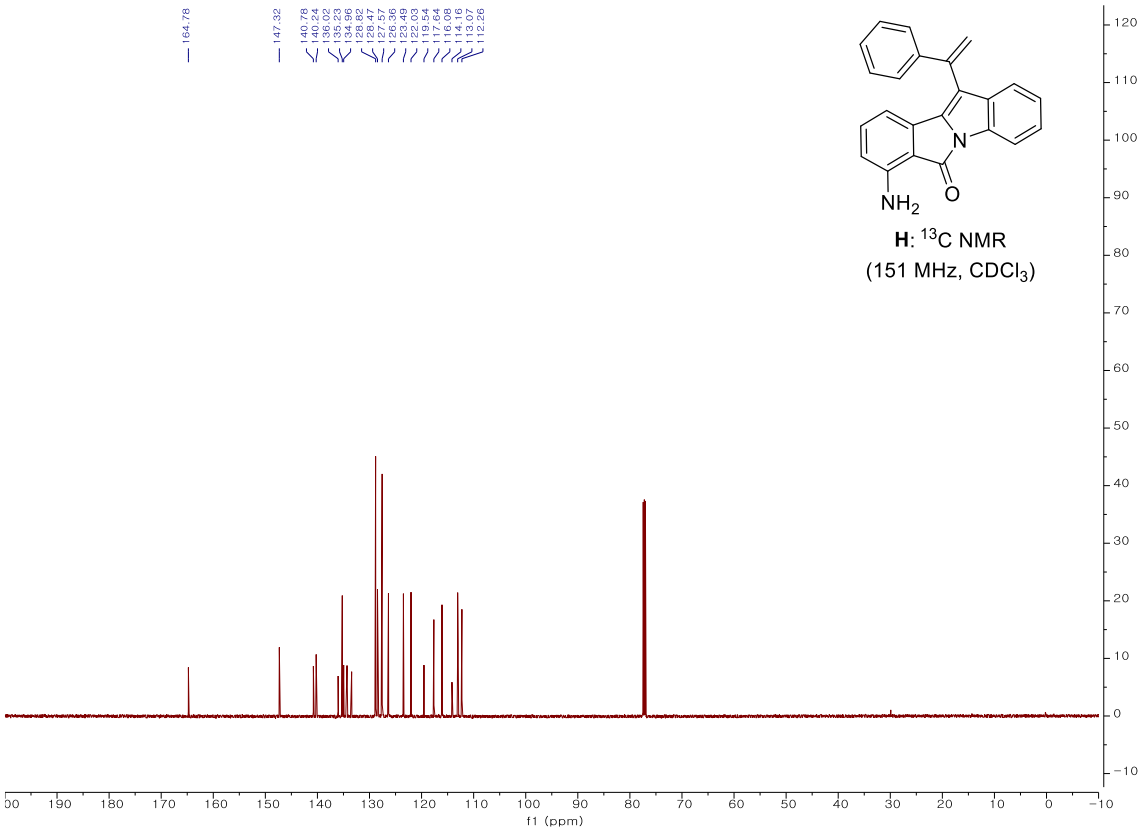

H: ^{13}C NMR
(151 MHz, $CDCl_3$)

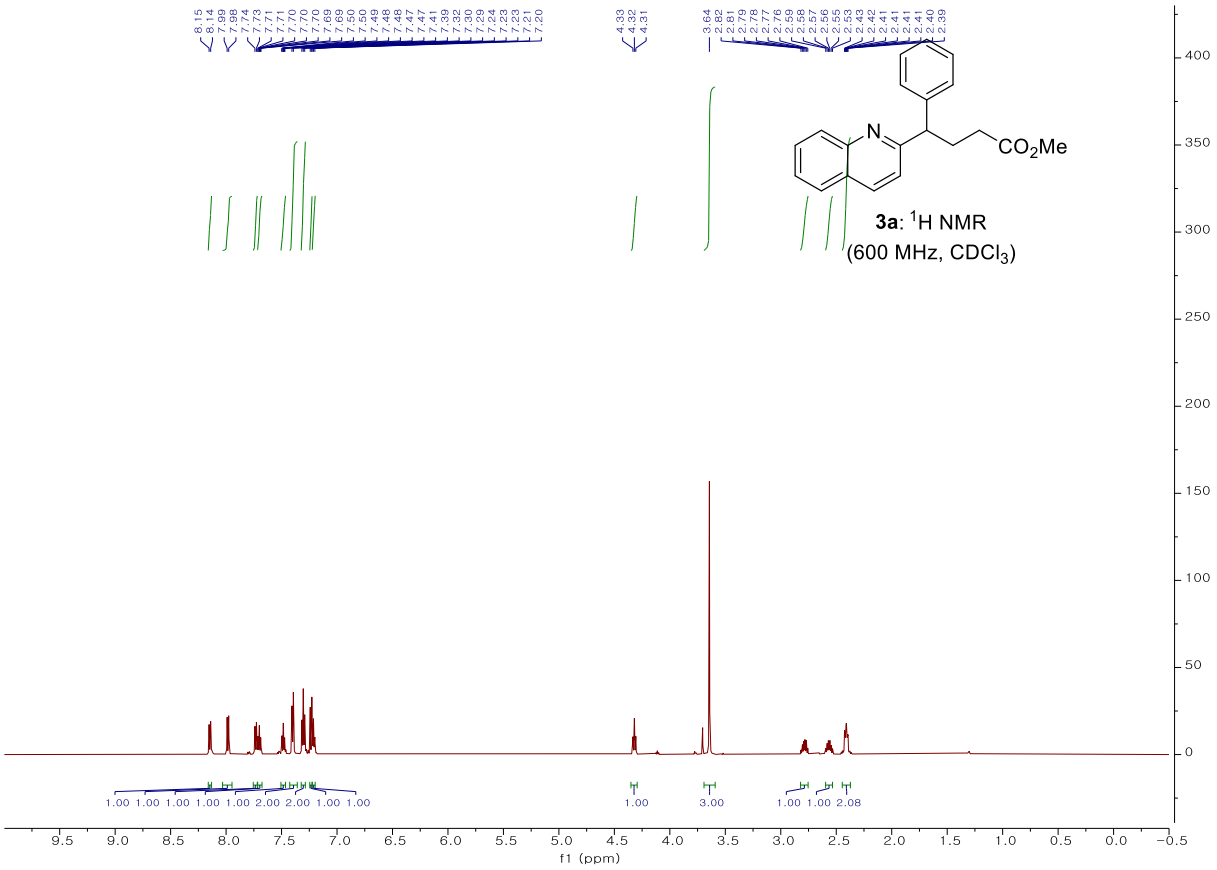
8.15
8.14
7.99
7.98
7.74
7.73
7.71
7.70
7.70
7.70
7.69
7.69
7.50
7.50
7.49
7.48
7.48
7.47
7.47
7.41
7.39
7.32
7.30
7.29
7.24
7.23
7.21
7.20
4.33
4.32
4.31
3.64
2.82
2.81
2.79
2.78
2.77
2.76
2.59
2.58
2.57
2.56
2.55
2.53
2.43
2.42
2.41
2.41
2.41
2.40
2.39
N
CO2Me
3a: 1H NMR
(600 MHz, CDCl3)
1.00 1.00 1.00 1.00 1.00 2.00 2.00 1.00 1.00
1.00
3.00
1.00 1.00 2.08
f1 (ppm)

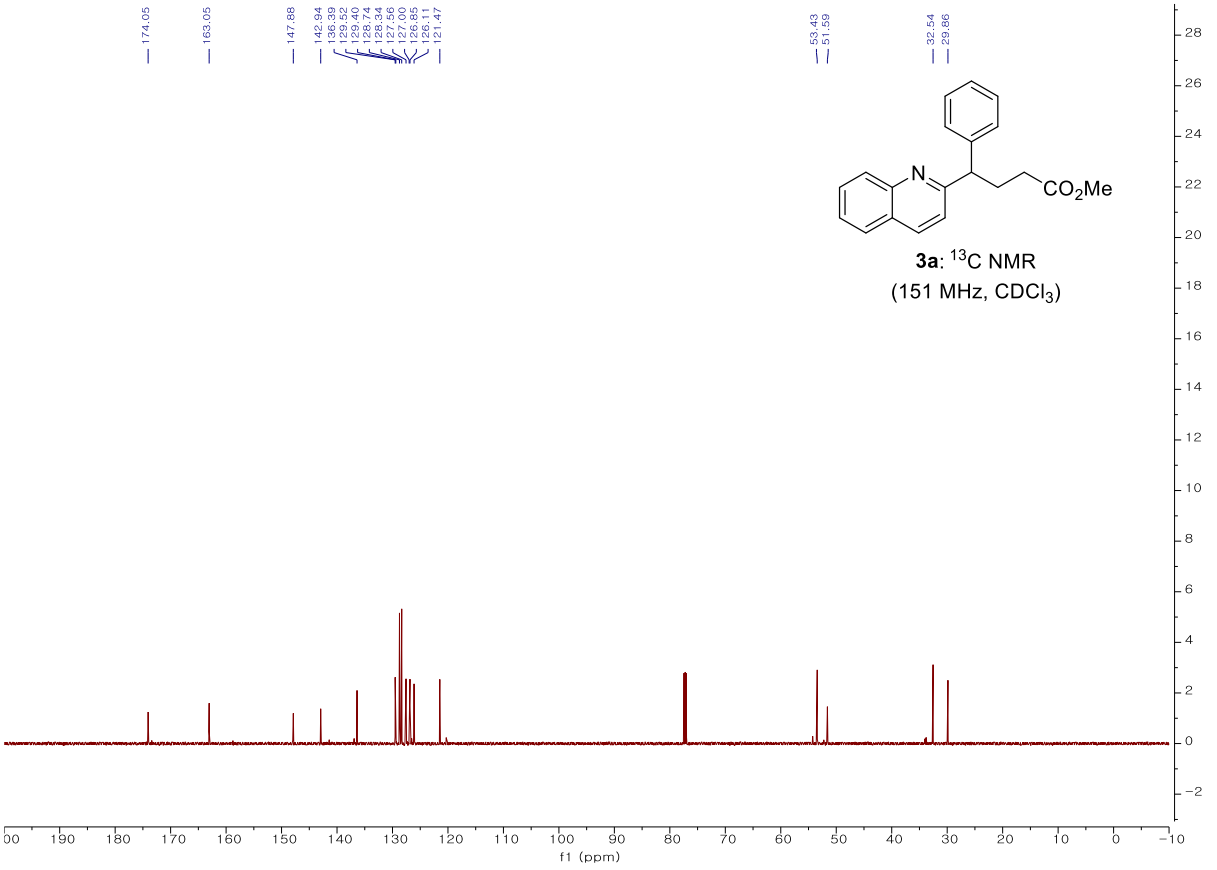
174.05
163.05
147.88
142.94
136.59
129.82
129.40
128.74
128.34
127.56
127.00
126.55
126.11
121.47
53.43
51.59
32.54
29.86
N
CO2Me
3a: 13C NMR
(151 MHz, CDCl3)
f1 (ppm)

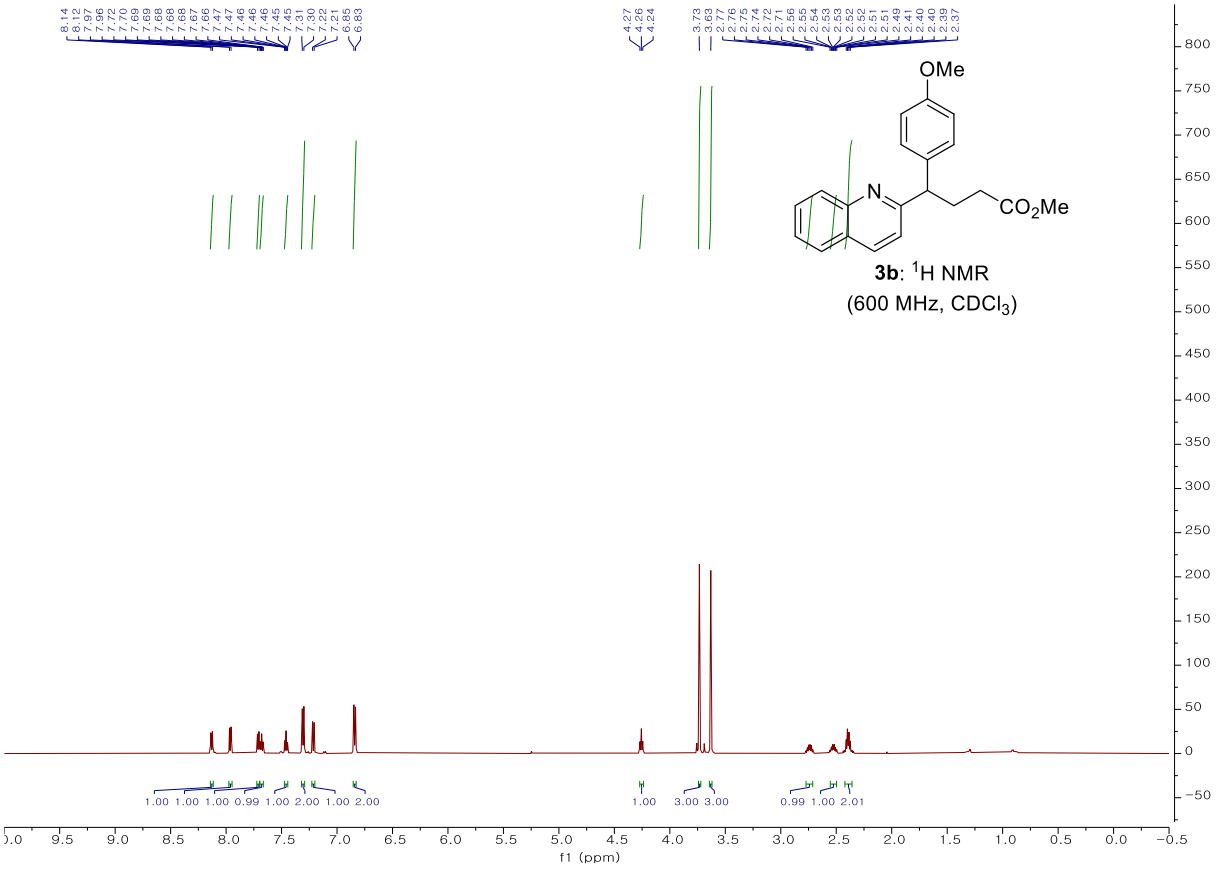

3b: ^{1}H NMR
(600 MHz, $CDCl_3$)

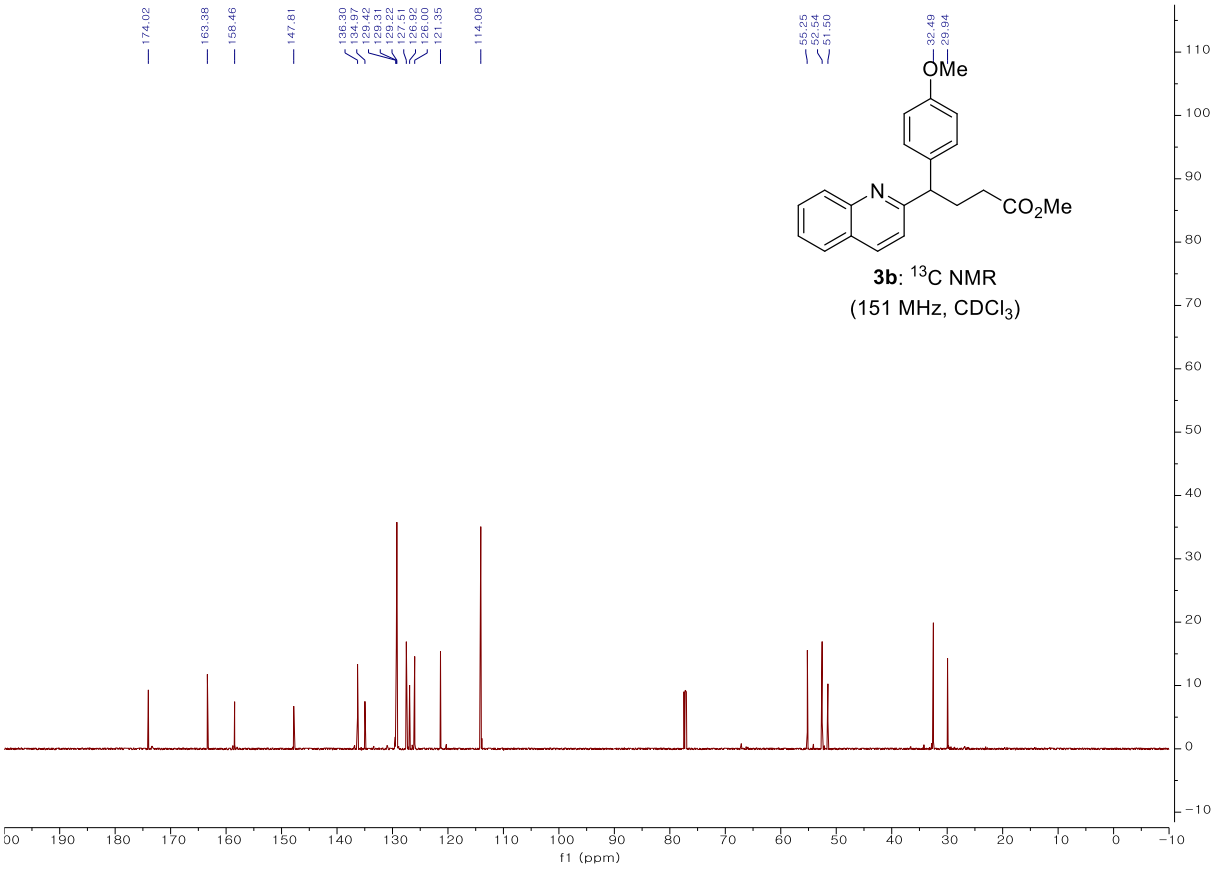

3b: ^{13}C NMR
(151 MHz, $CDCl_3$)

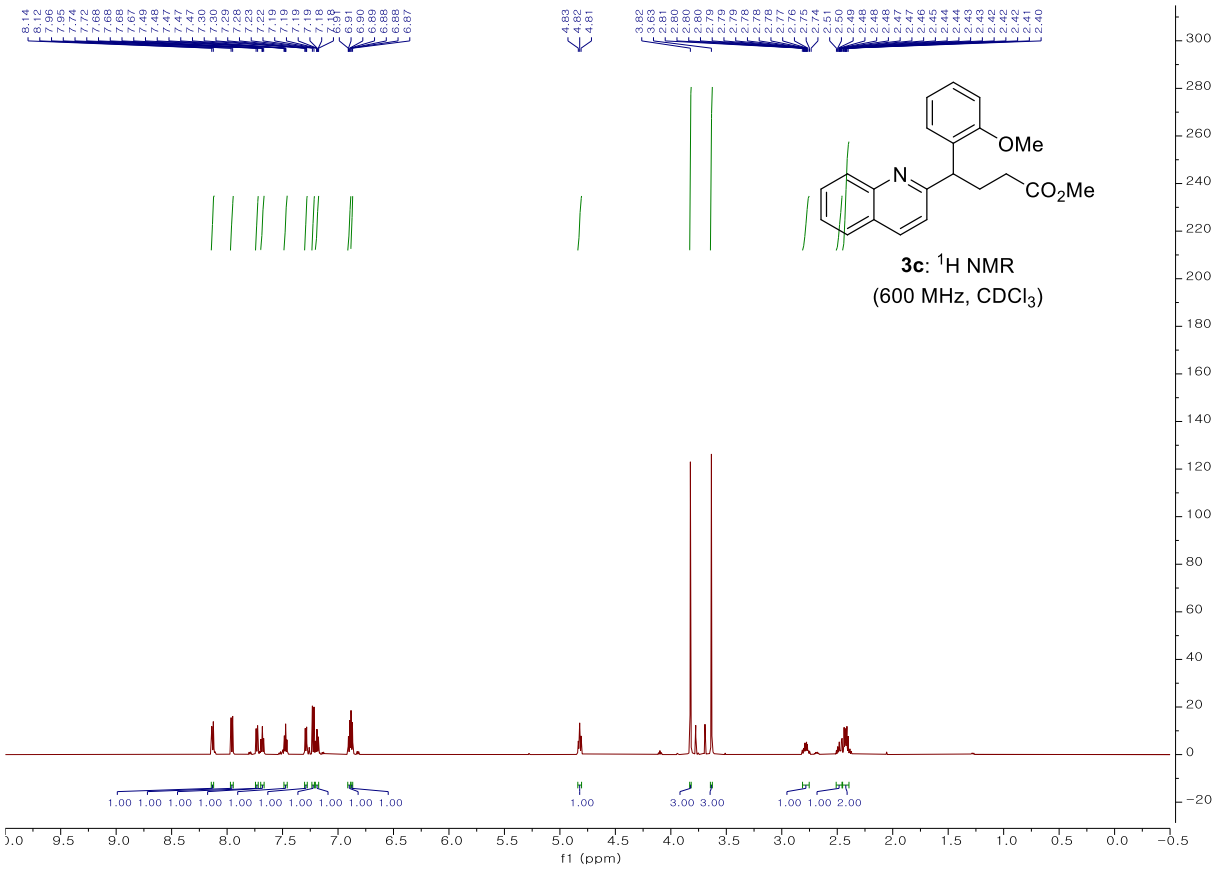

3c: ^{1}H NMR
(600 MHz, $CDCl_3$)

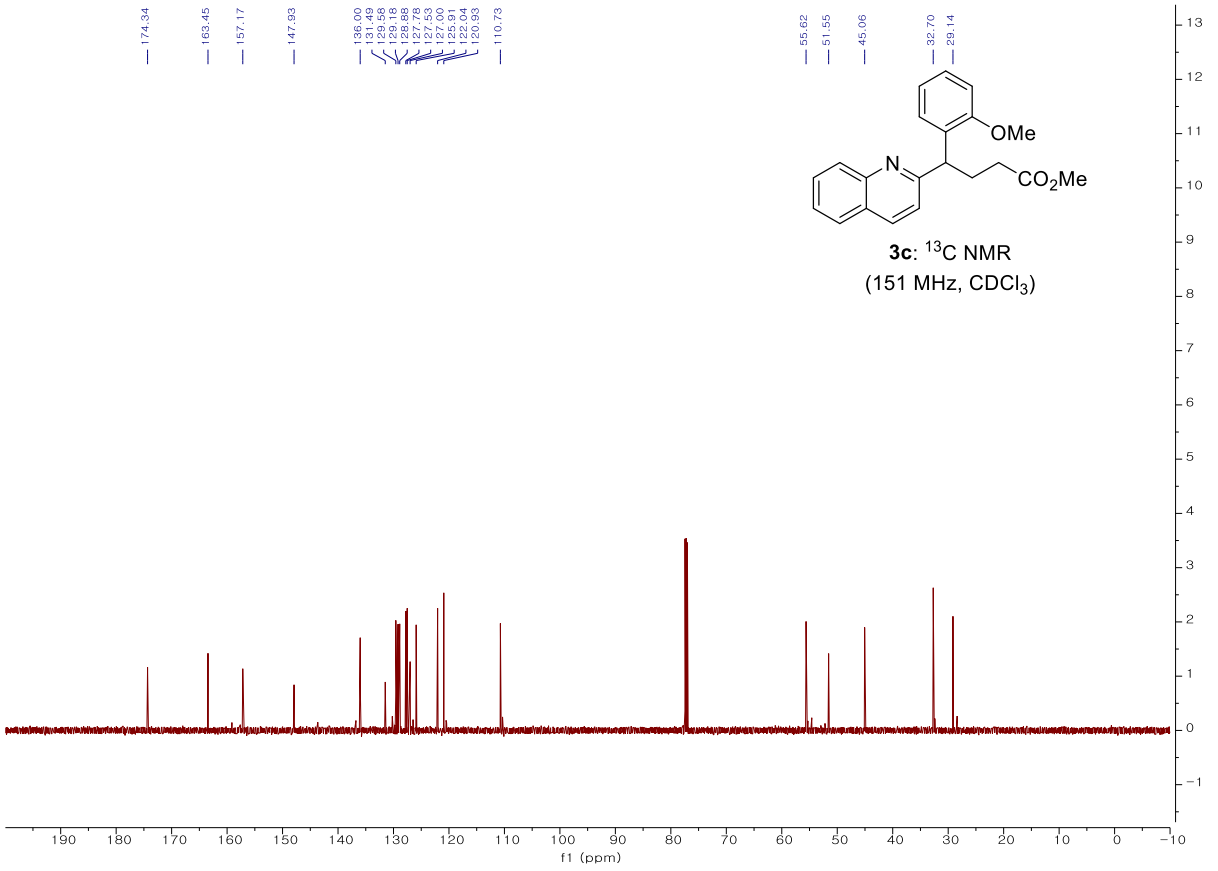

3c: ^{13}C NMR
(151 MHz, $CDCl_3$)

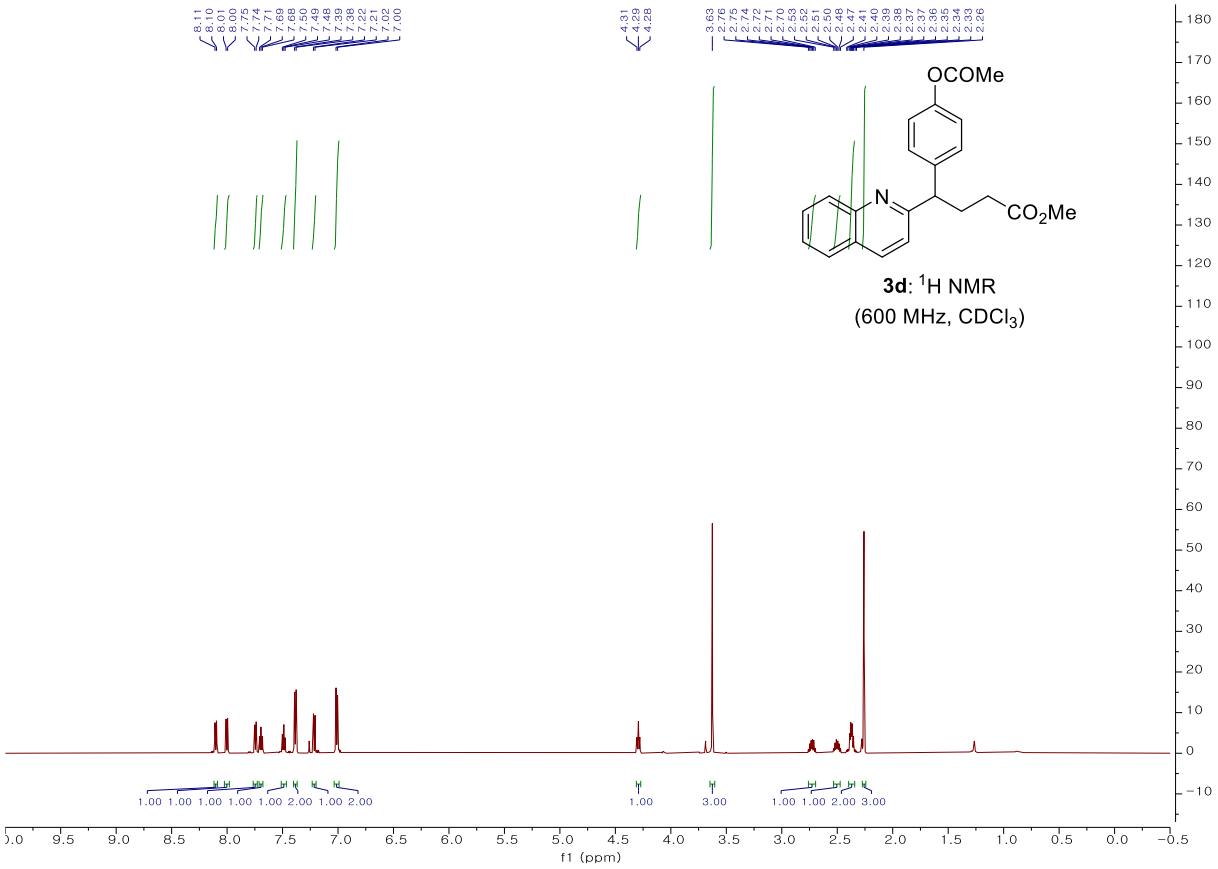
OCOMe
N
CO2Me
3d: 1H NMR
(600 MHz, CDCl3)
f1 (ppm)

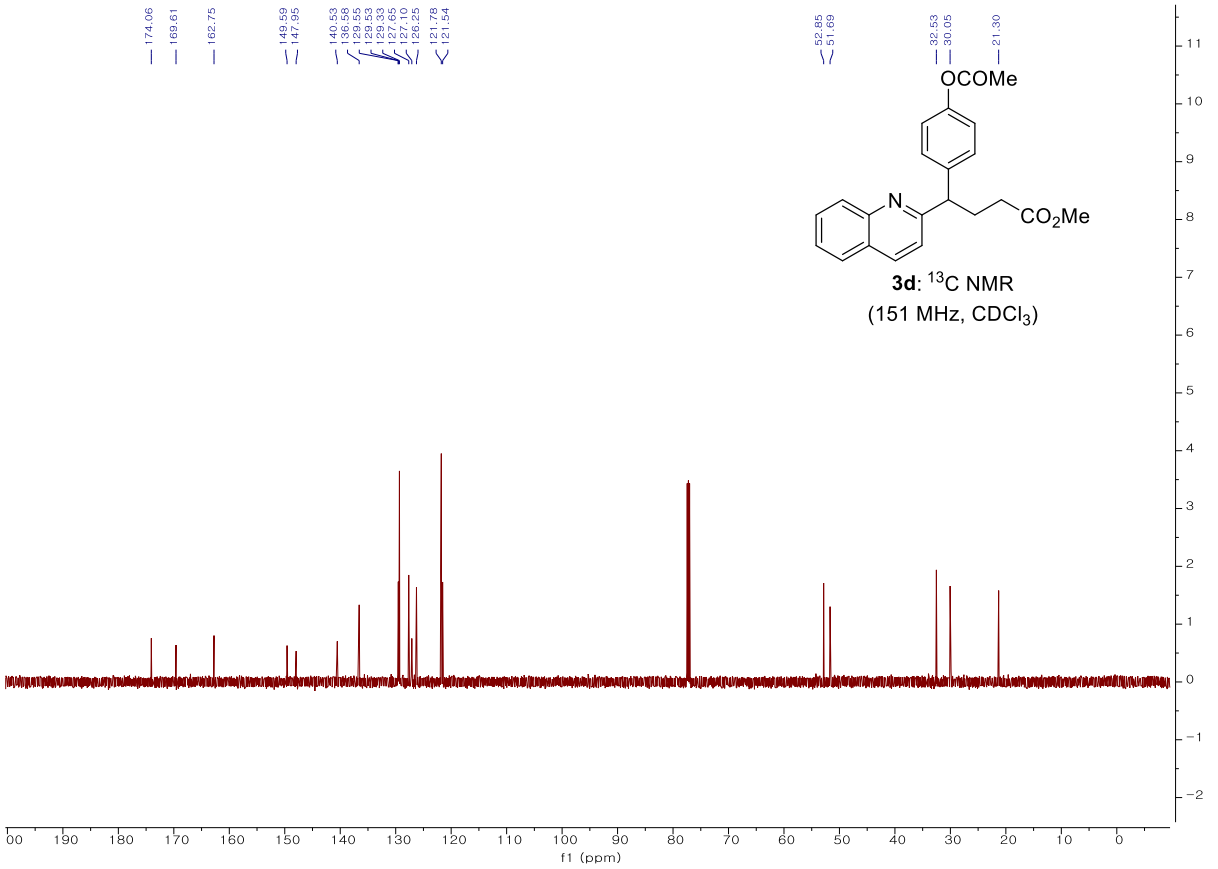
OCOMe
N
CO2Me
3d: 13C NMR
(151 MHz, CDCl3)
f1 (ppm)

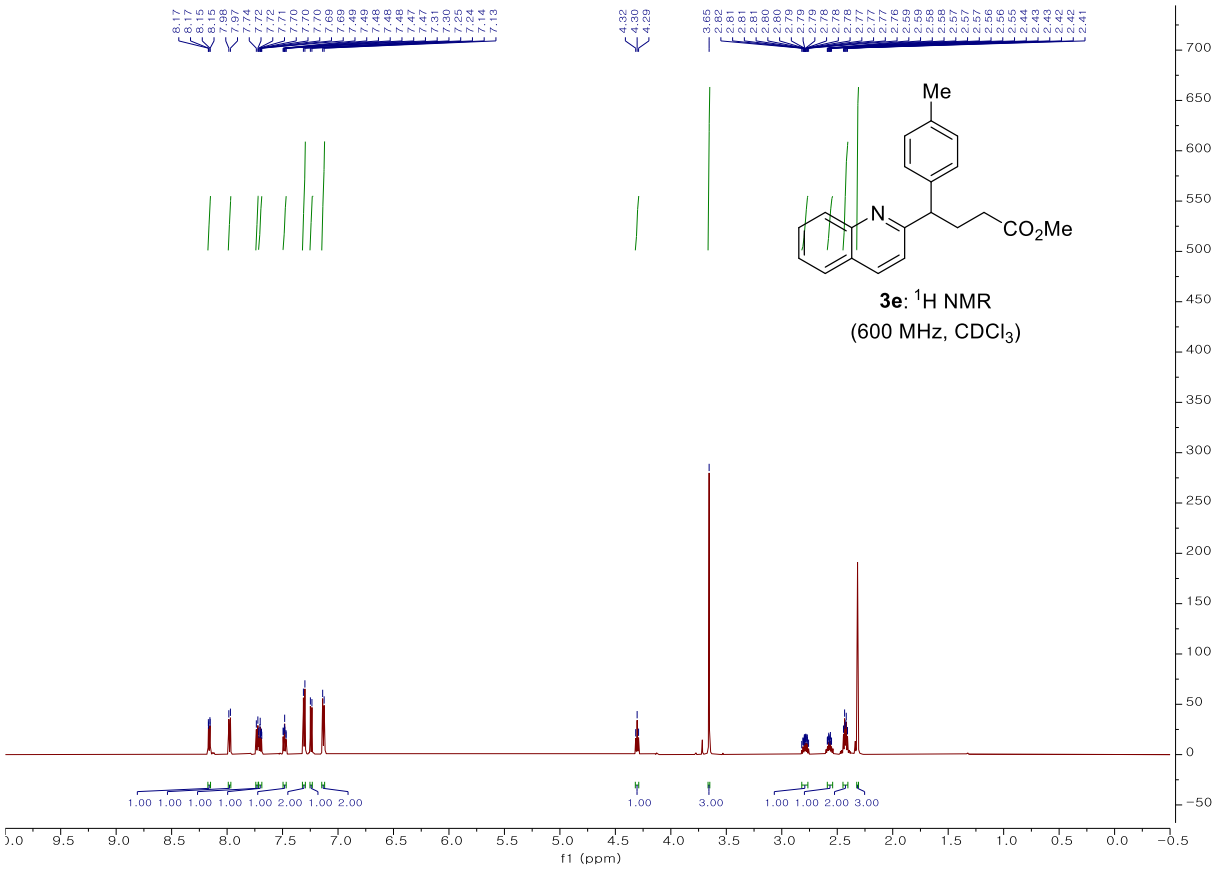

3e: ^{1}H NMR
(600 MHz, $CDCl_3$)

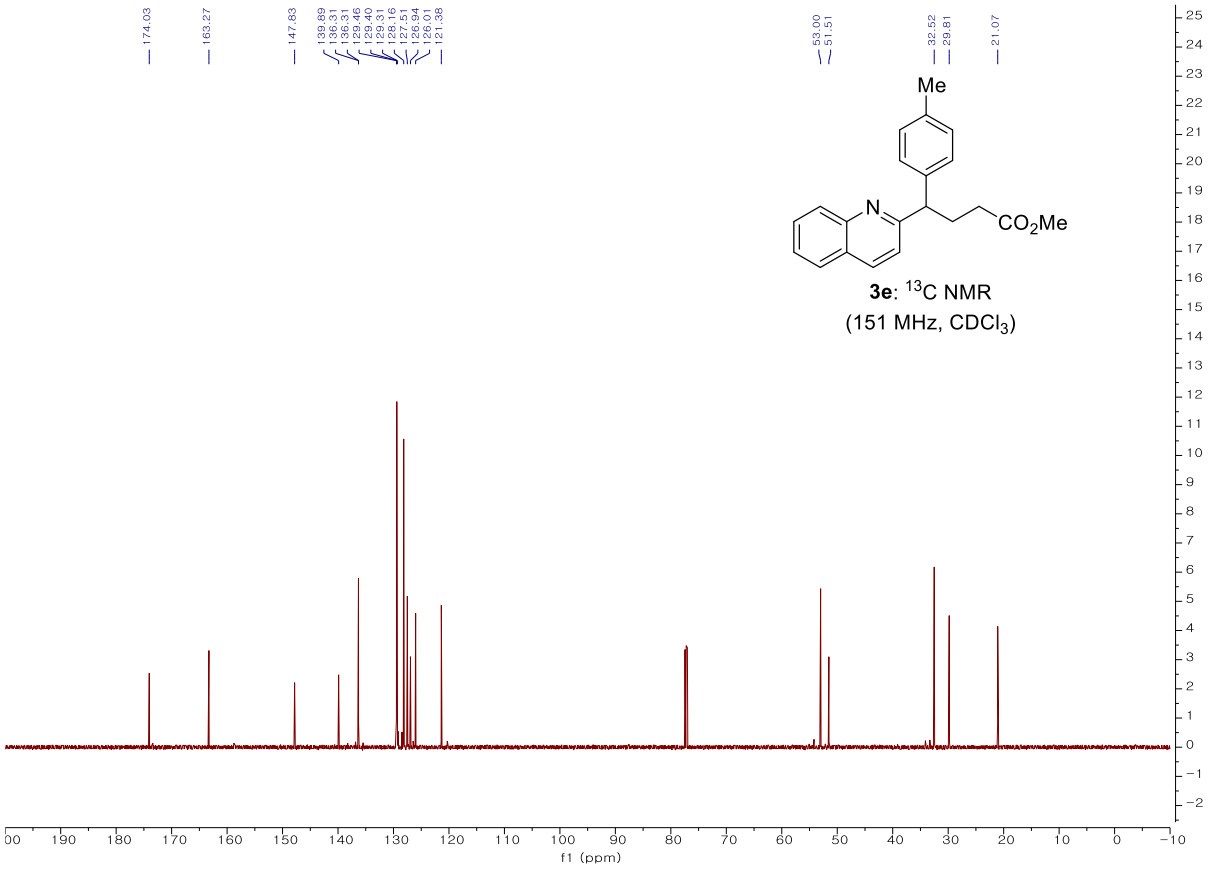

3e: ^{13}C NMR
(151 MHz, $CDCl_3$)

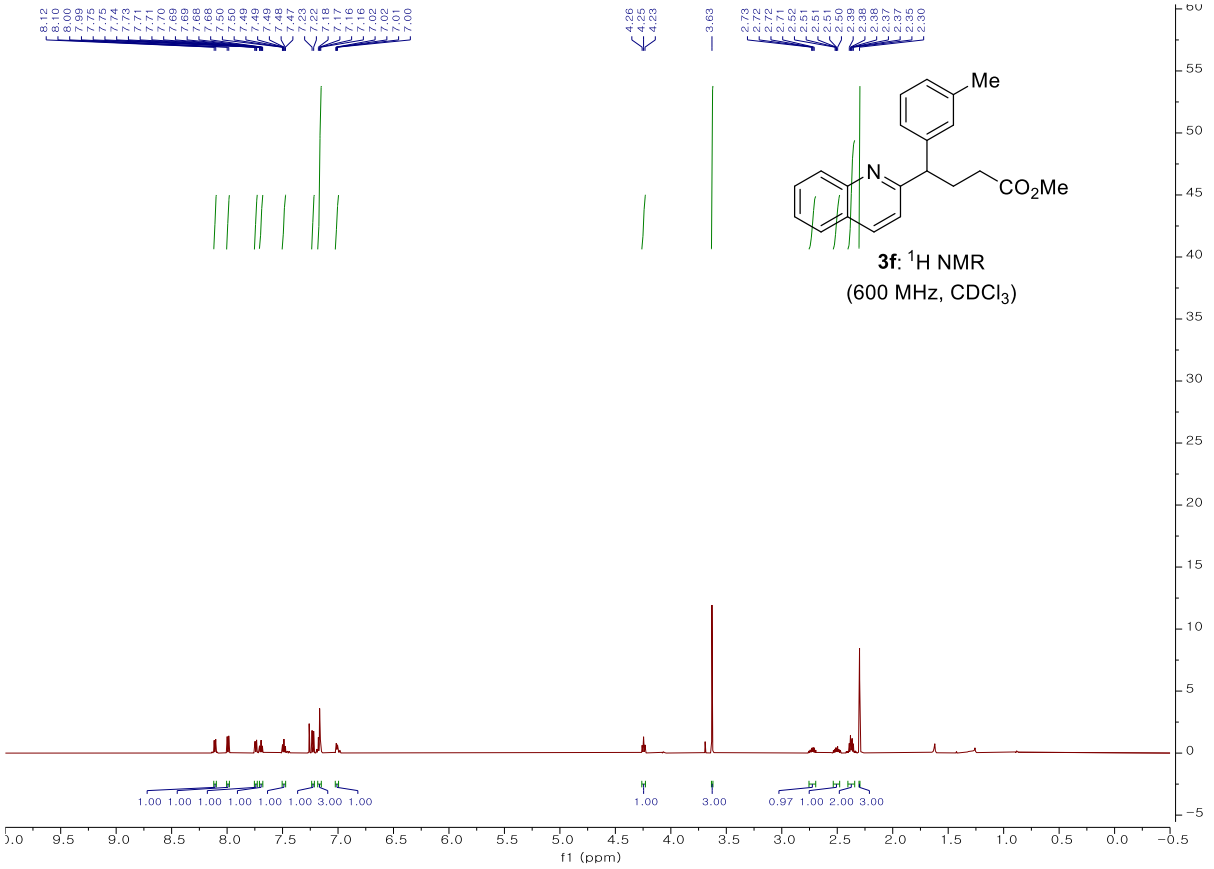

3f: ^{1}H NMR
(600 MHz, $CDCl_3$)

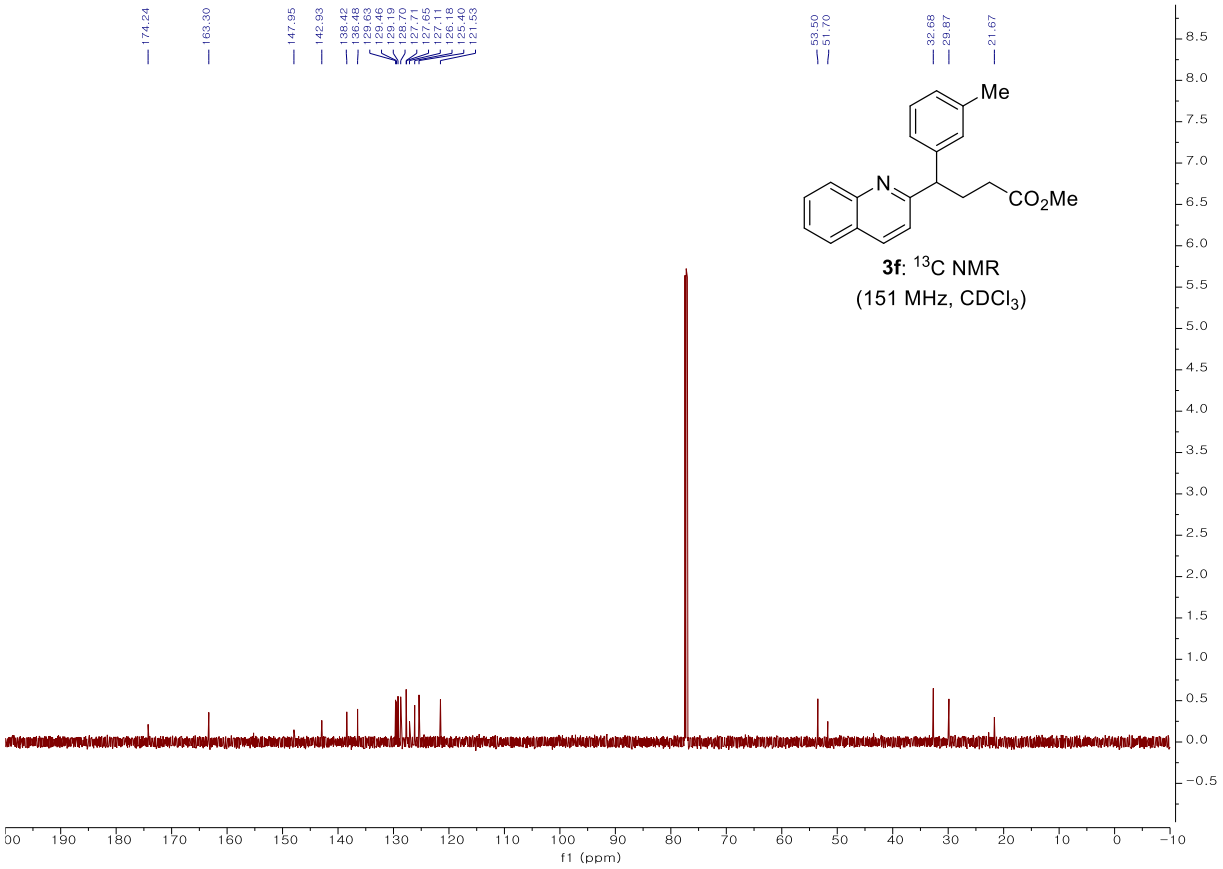

3f: ^{13}C NMR
(151 MHz, $CDCl_3$)

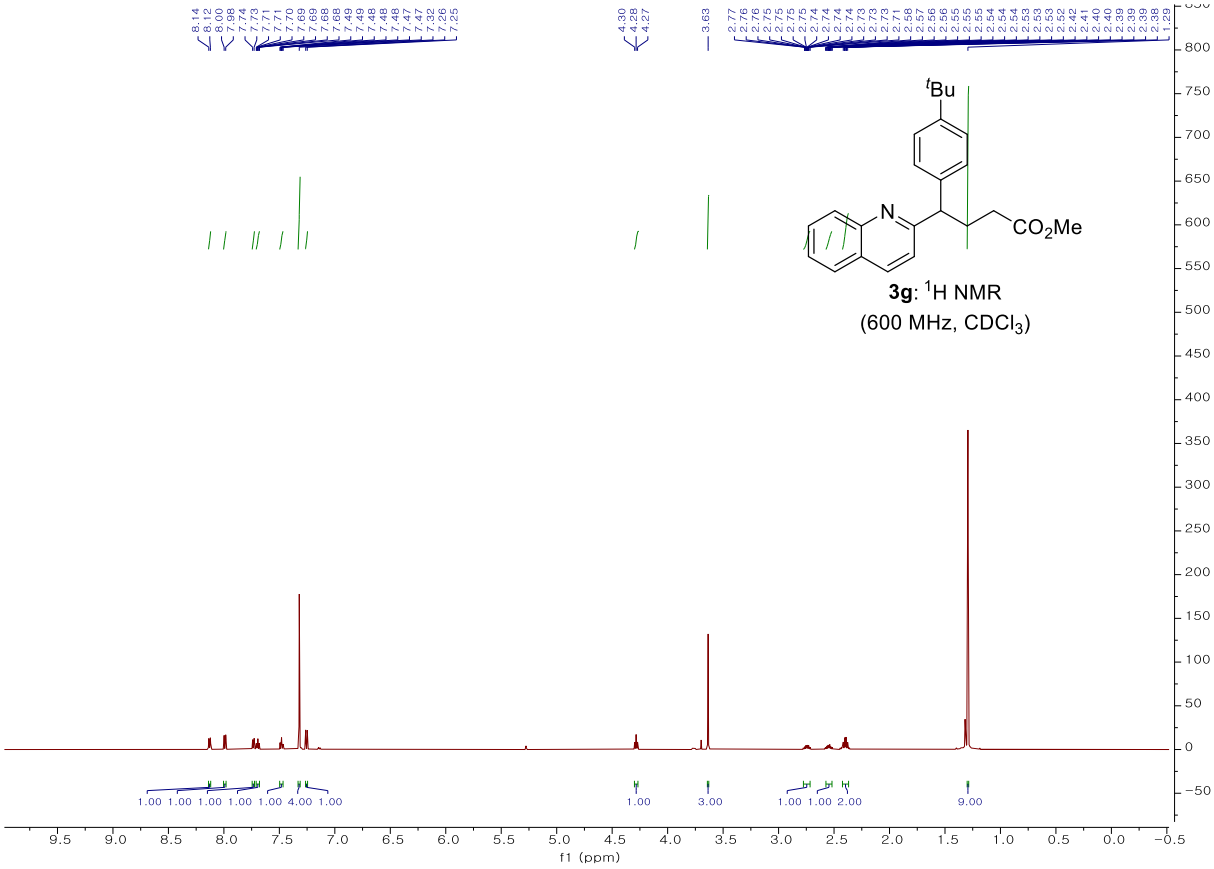

3g: ^{1}H NMR
(600 MHz, $CDCl_3$)

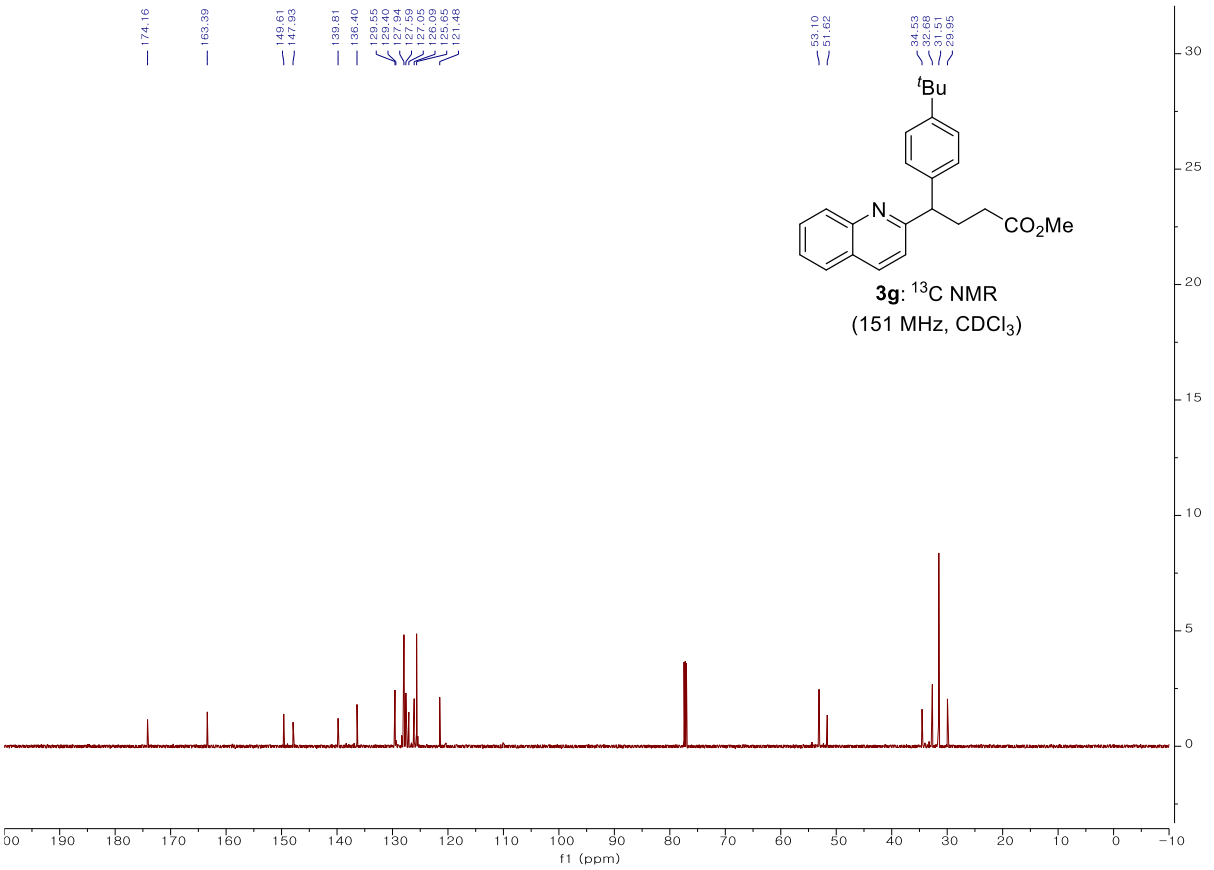

3g: ^{13}C NMR
(151 MHz, $CDCl_3$)

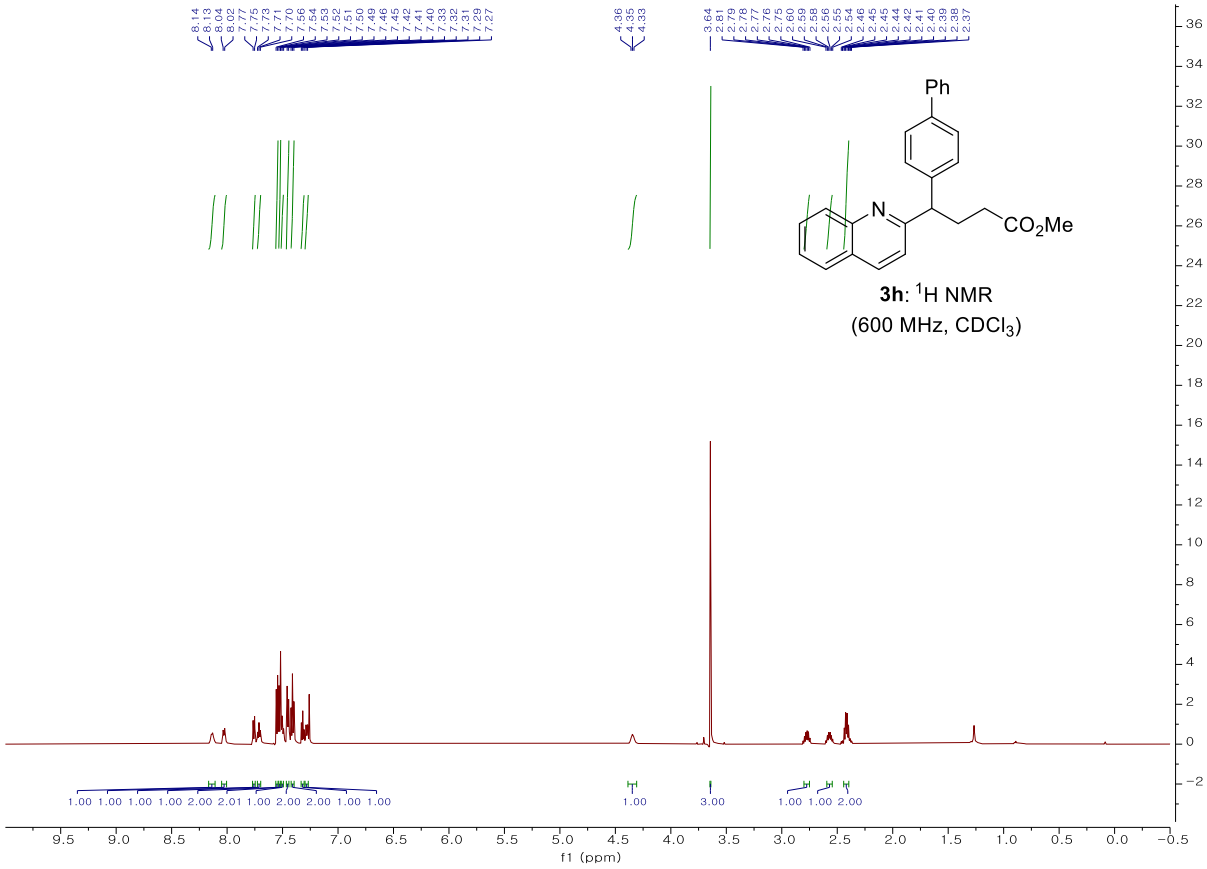

3h: ^{1}H NMR
(600 MHz, $CDCl_3$)

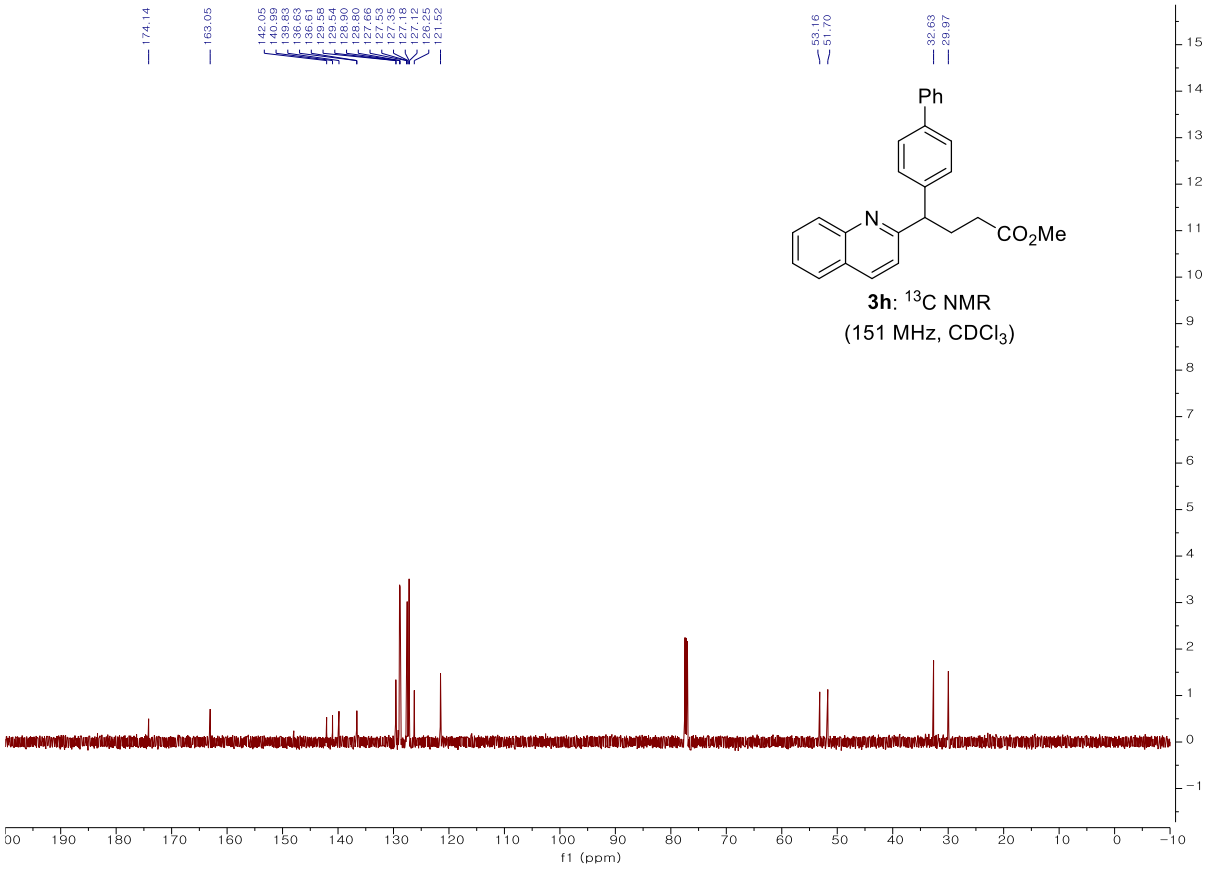

3h: ^{13}C NMR
(151 MHz, $CDCl_3$)

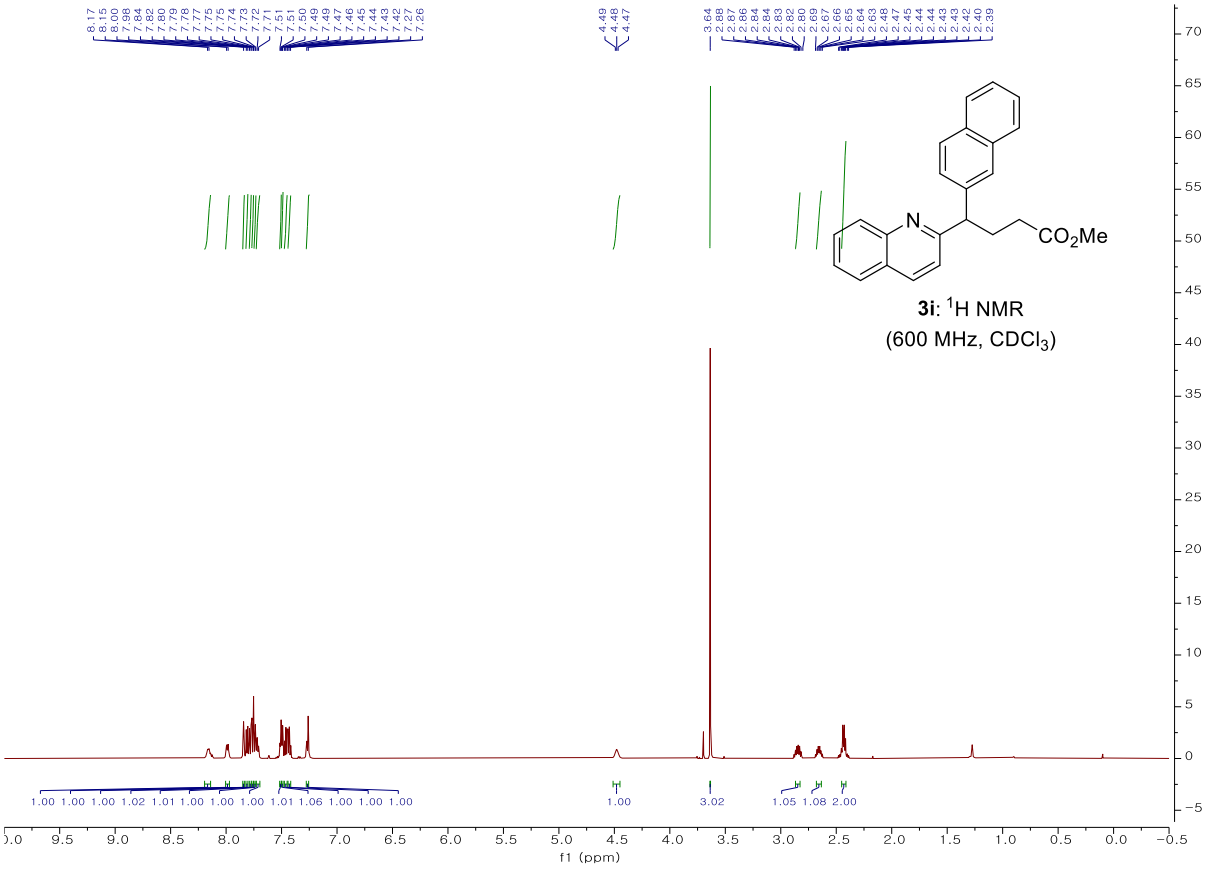

3i: ^{1}H NMR
(600 MHz, $CDCl_3$)

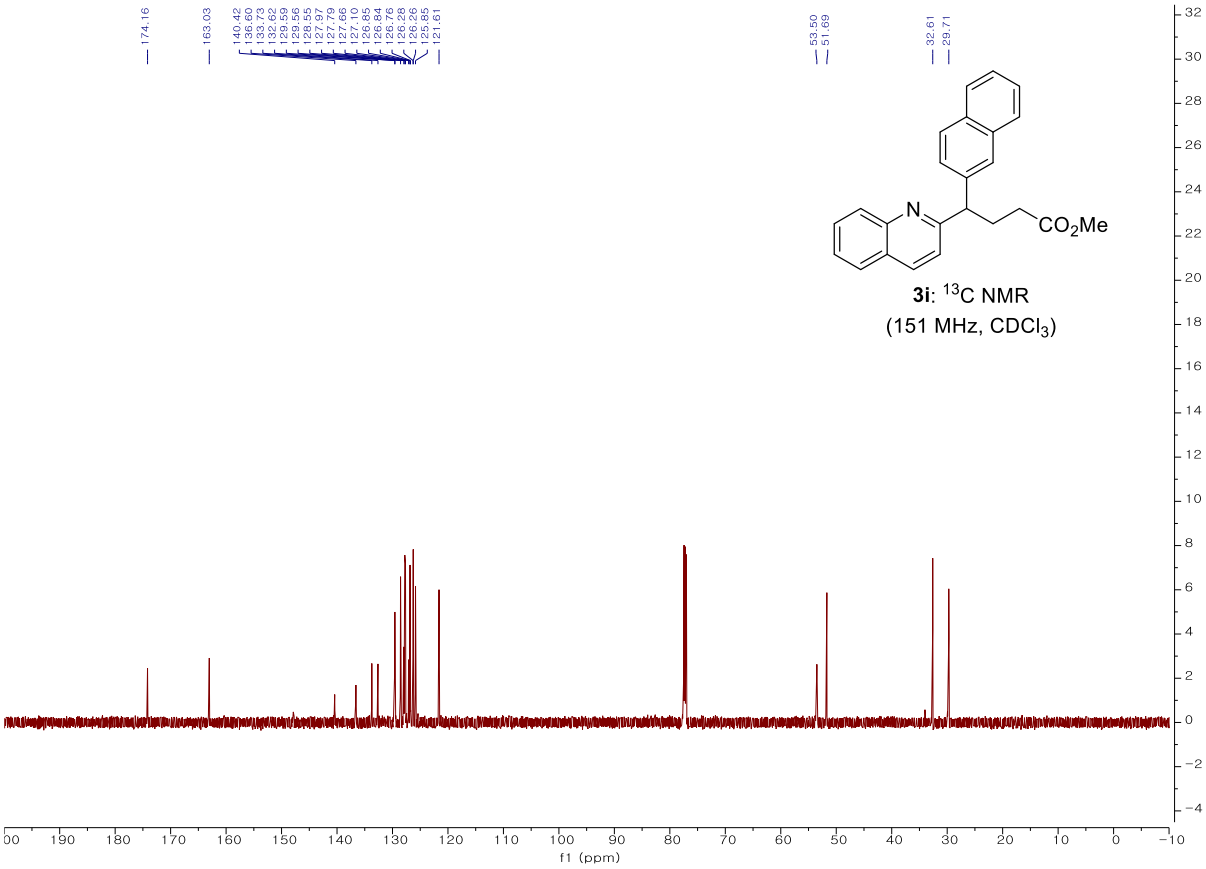

3i: ^{13}C NMR
(151 MHz, $CDCl_3$)

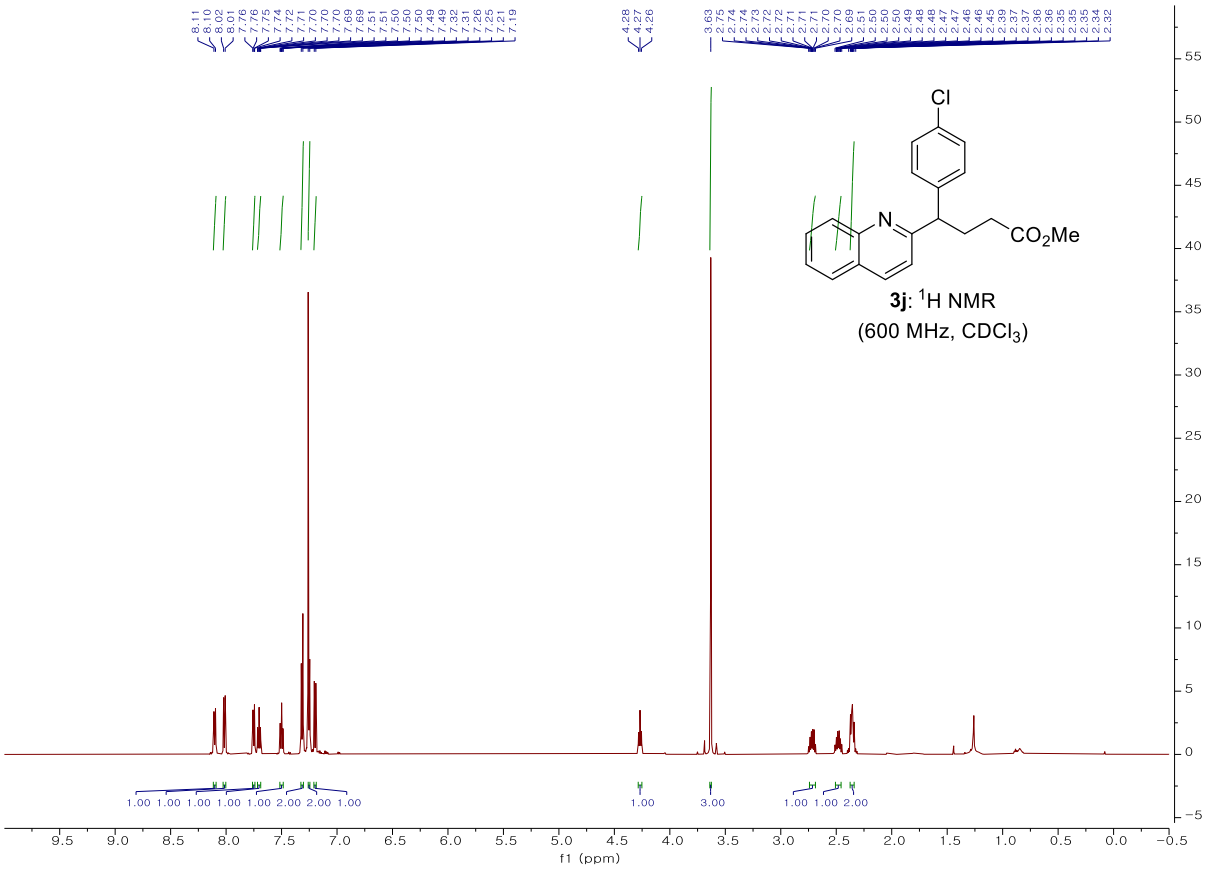
Cl
N
CO2Me
3j: 1H NMR
(600 MHz, CDCl3)
f1 (ppm)

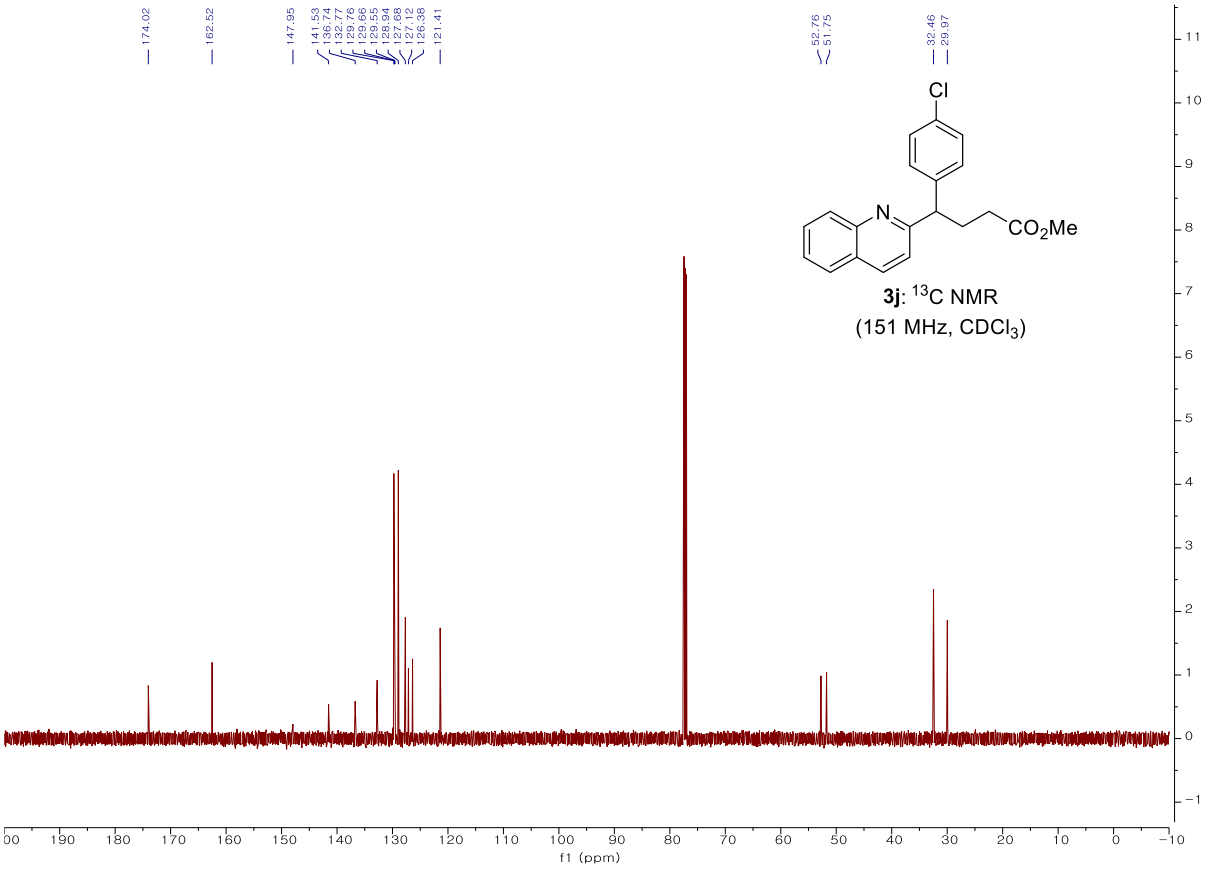
Cl
N
CO2Me
3j: 13C NMR
(151 MHz, CDCl3)
f1 (ppm)

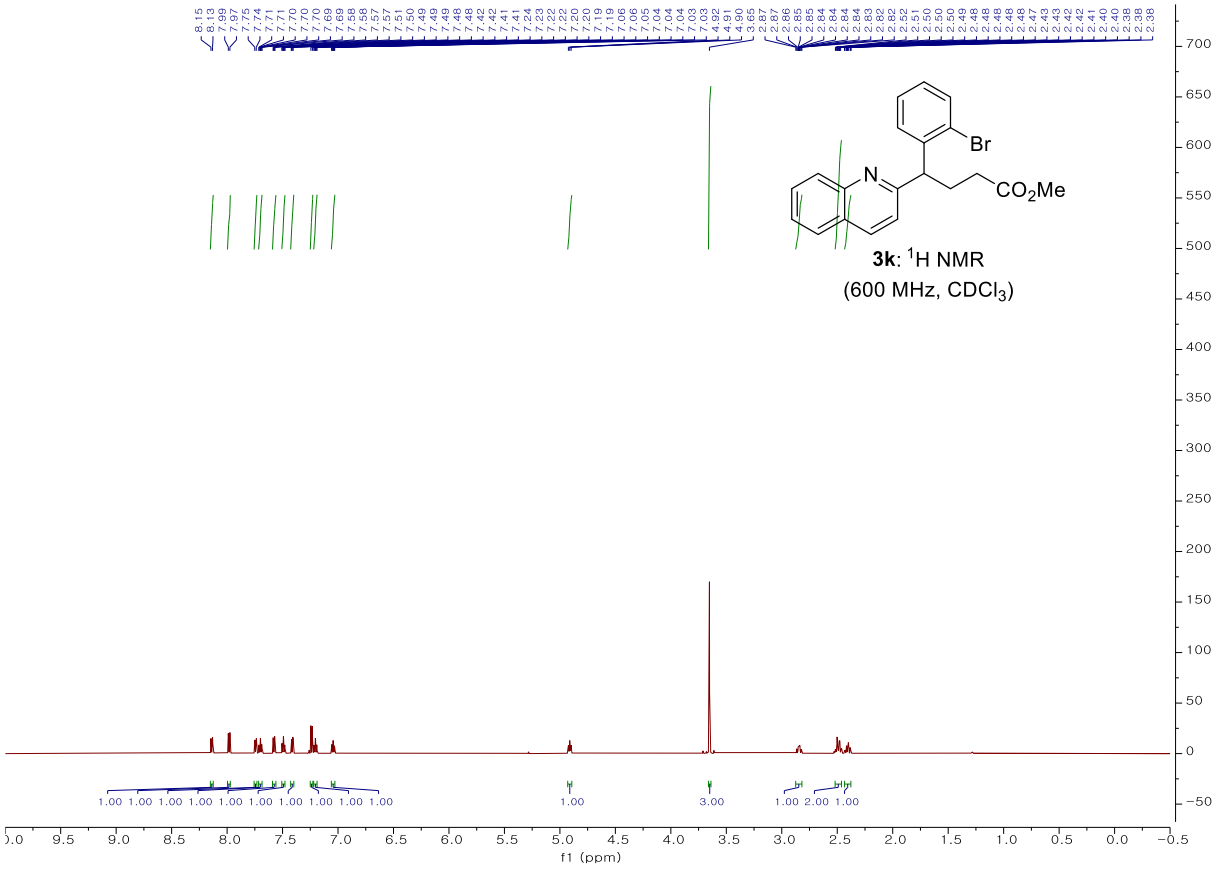

3k: ^{1}H NMR
(600 MHz, $CDCl_3$)

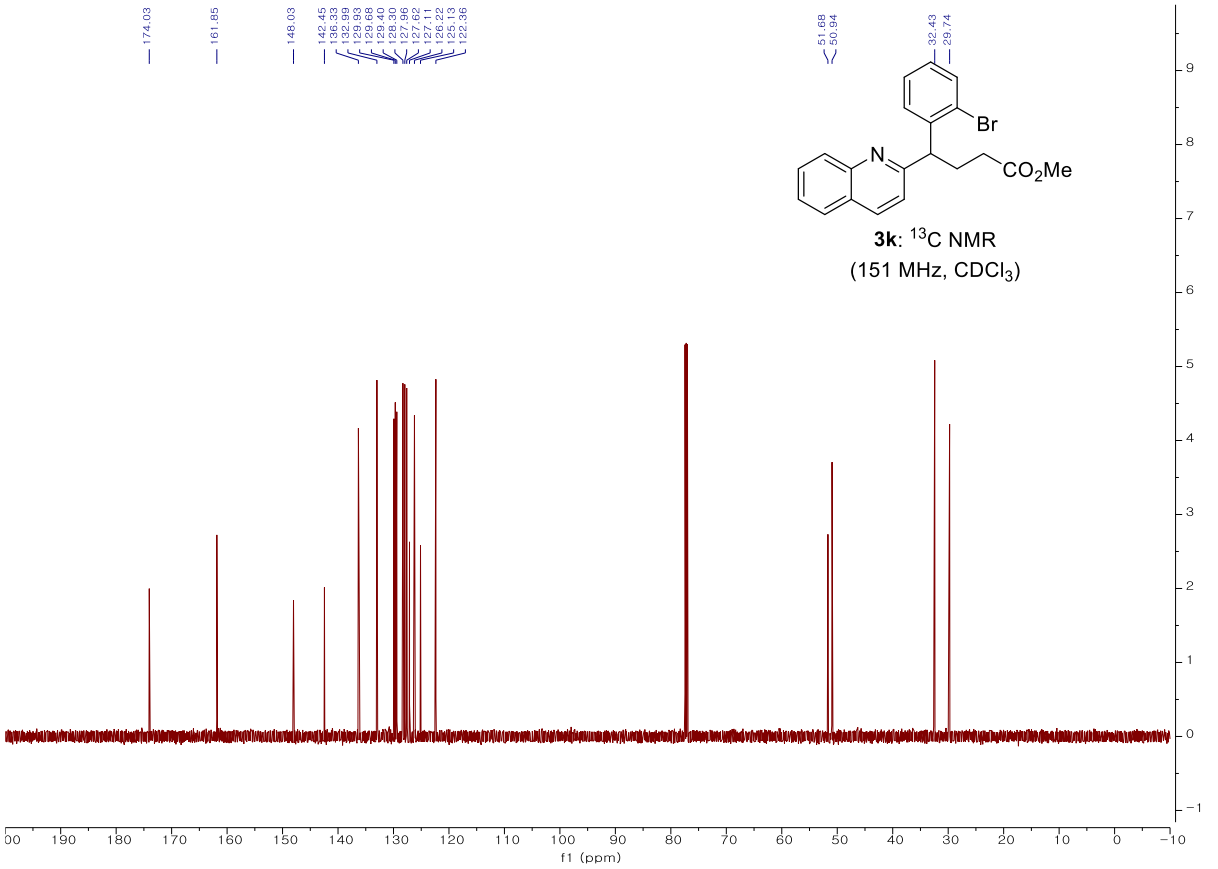

3k: ^{13}C NMR
(151 MHz, $CDCl_3$)

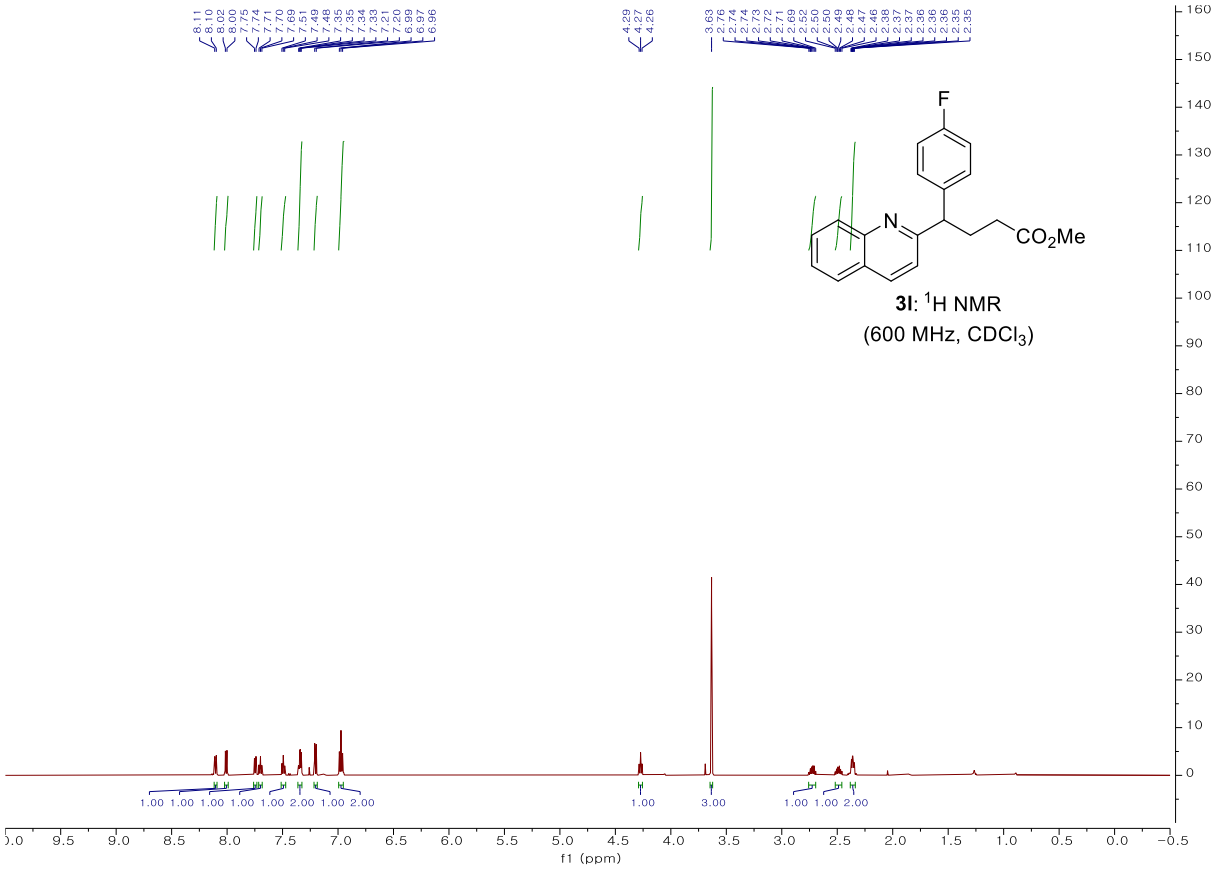
F
N
CO2Me
3I: 1H NMR
(600 MHz, CDCl3)
f1 (ppm)

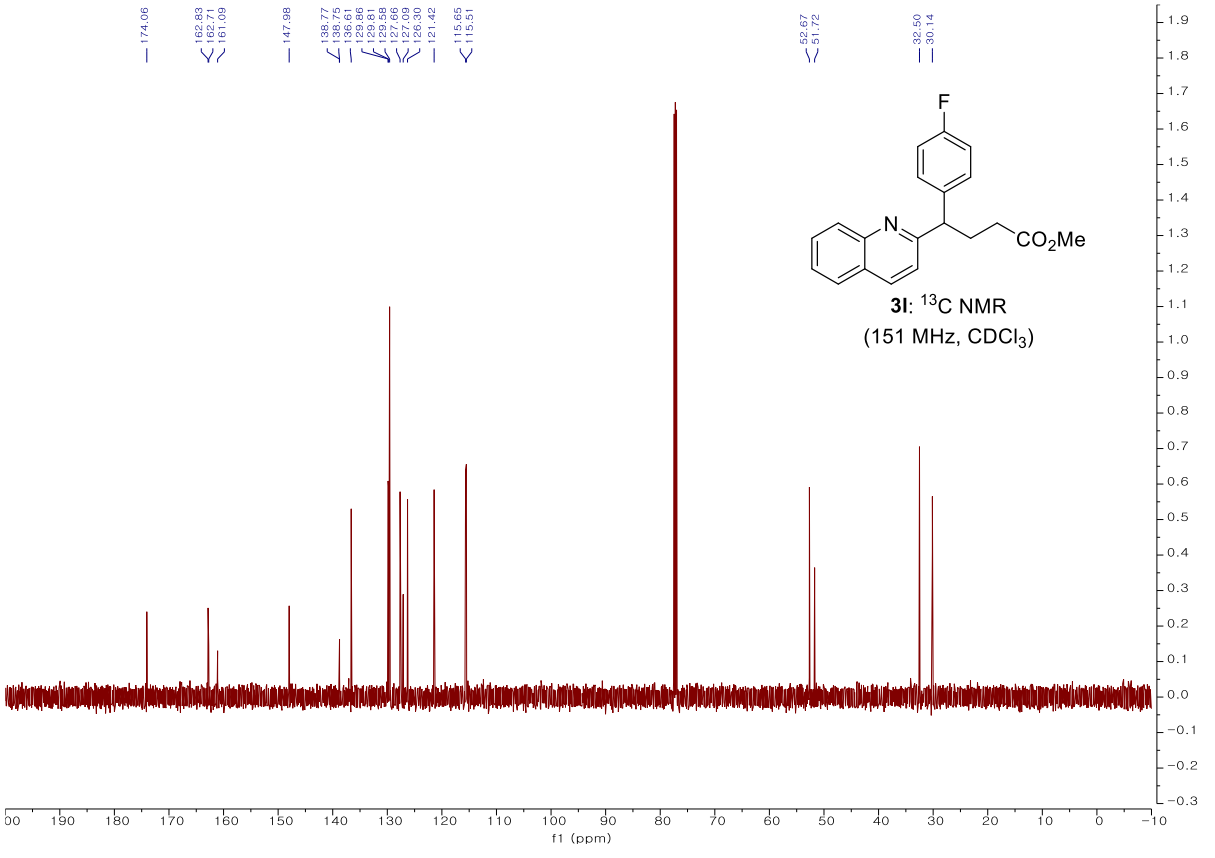
F
N
CO2Me
3I: 13C NMR
(151 MHz, CDCl3)
f1 (ppm)

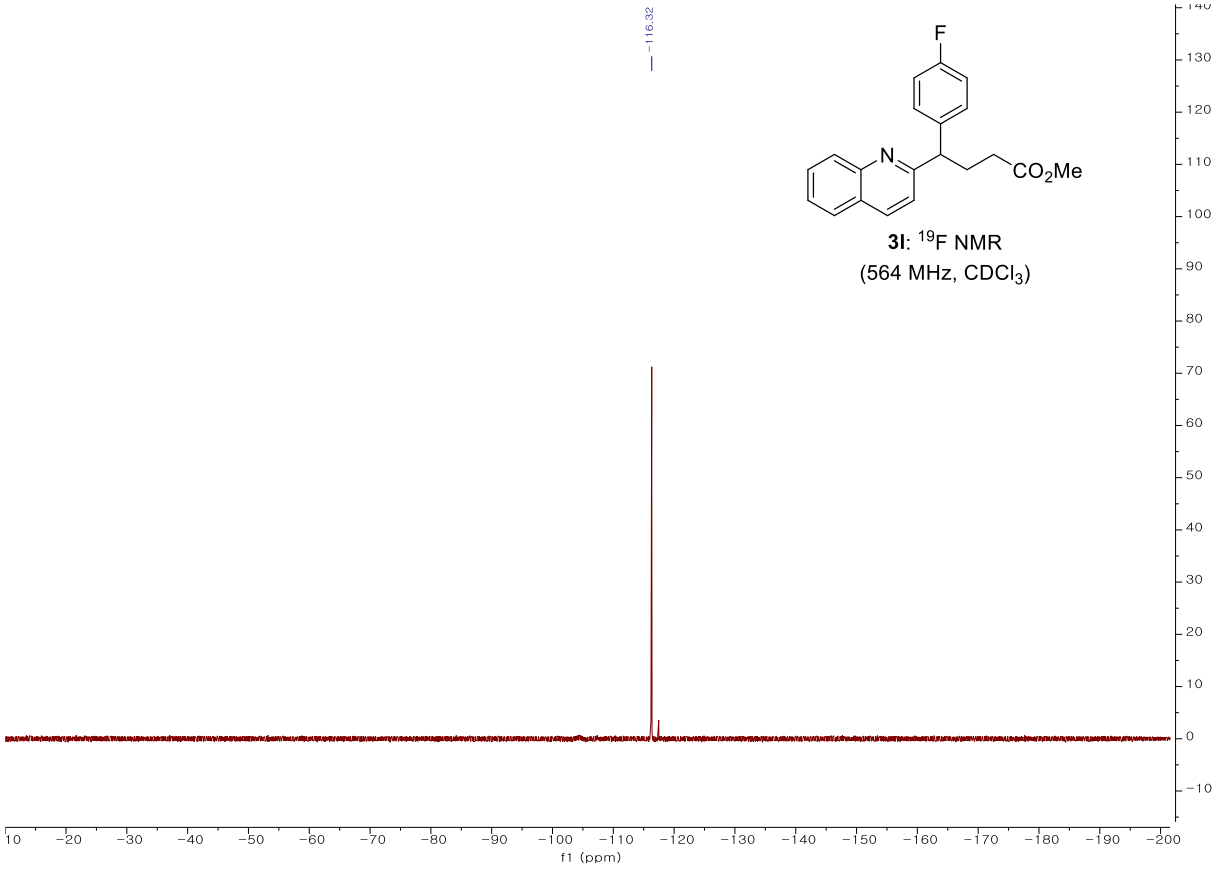
−116.32
F
N
CO2Me
3I: 19F NMR
(564 MHz, CDCl3)
f1 (ppm)

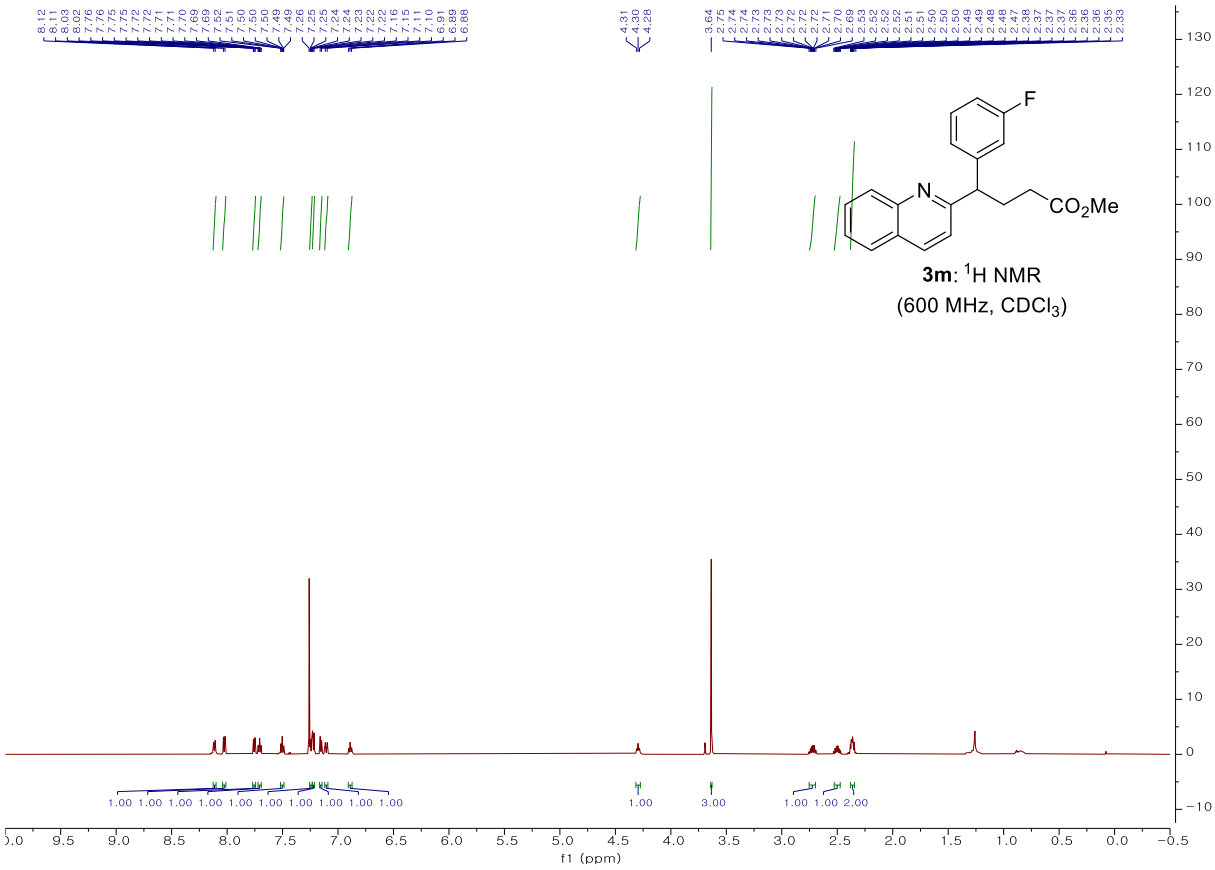
F
N
CO2Me
3m: 1H NMR
(600 MHz, CDCl3)
f1 (ppm)

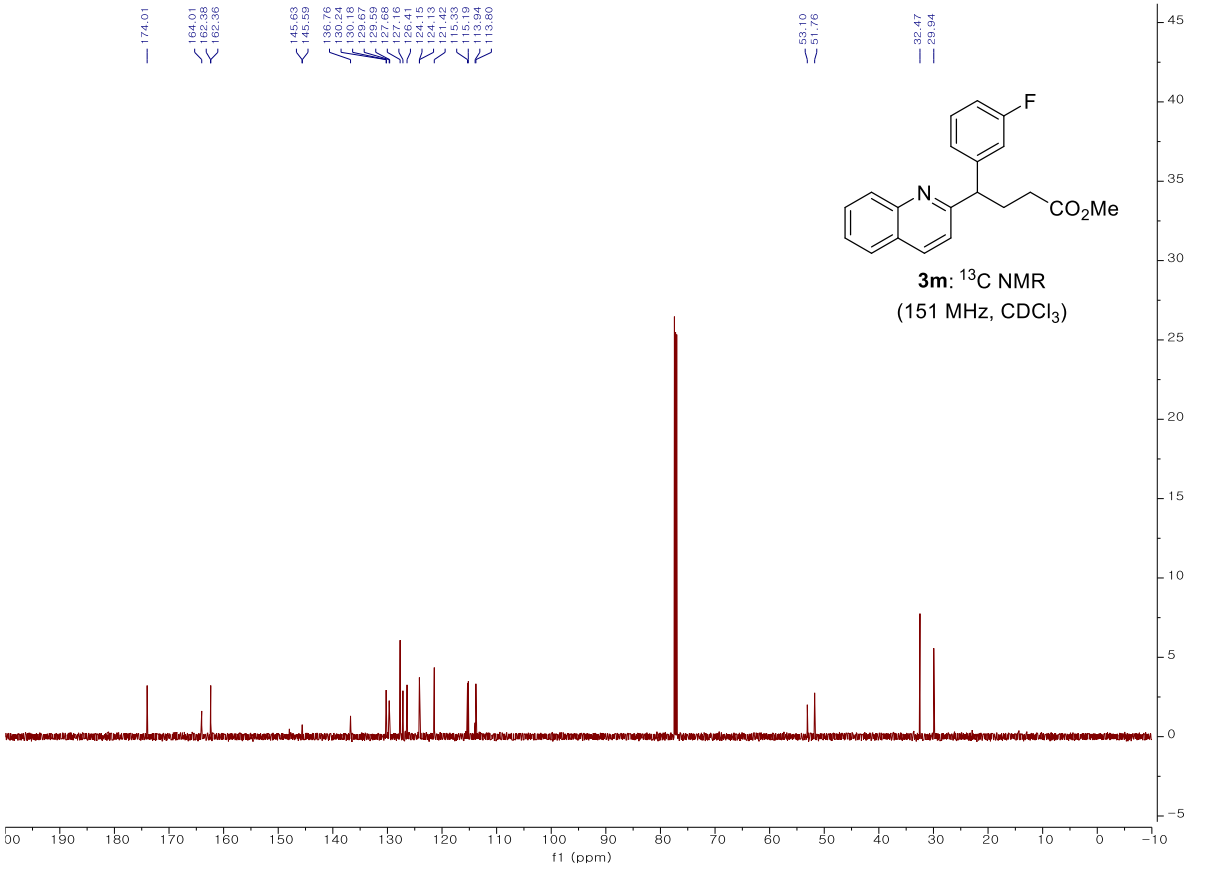
F
N
CO2Me
3m: 13C NMR
(151 MHz, CDCl3)
f1 (ppm)

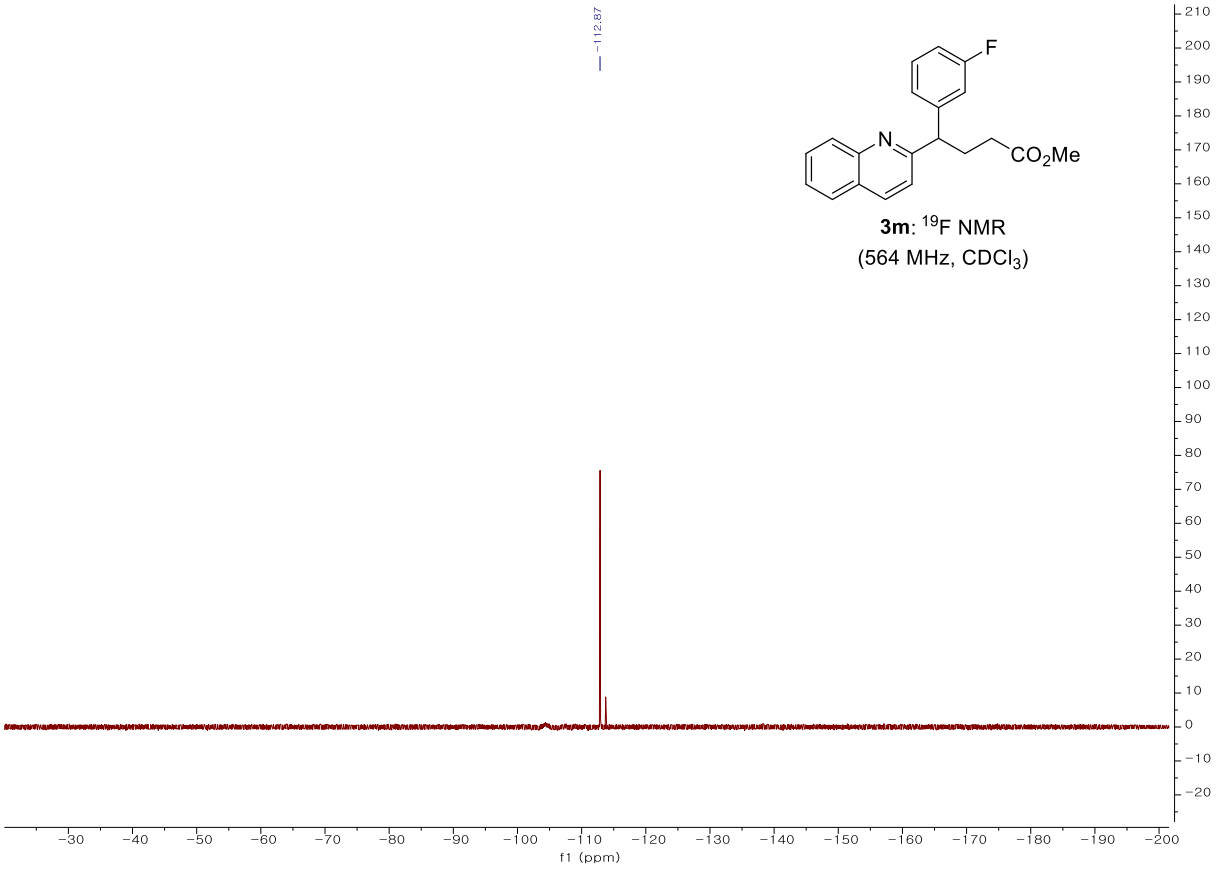
−112.87
F
N
CO2Me
3m: 19F NMR
(564 MHz, CDCl3)
f1 (ppm)

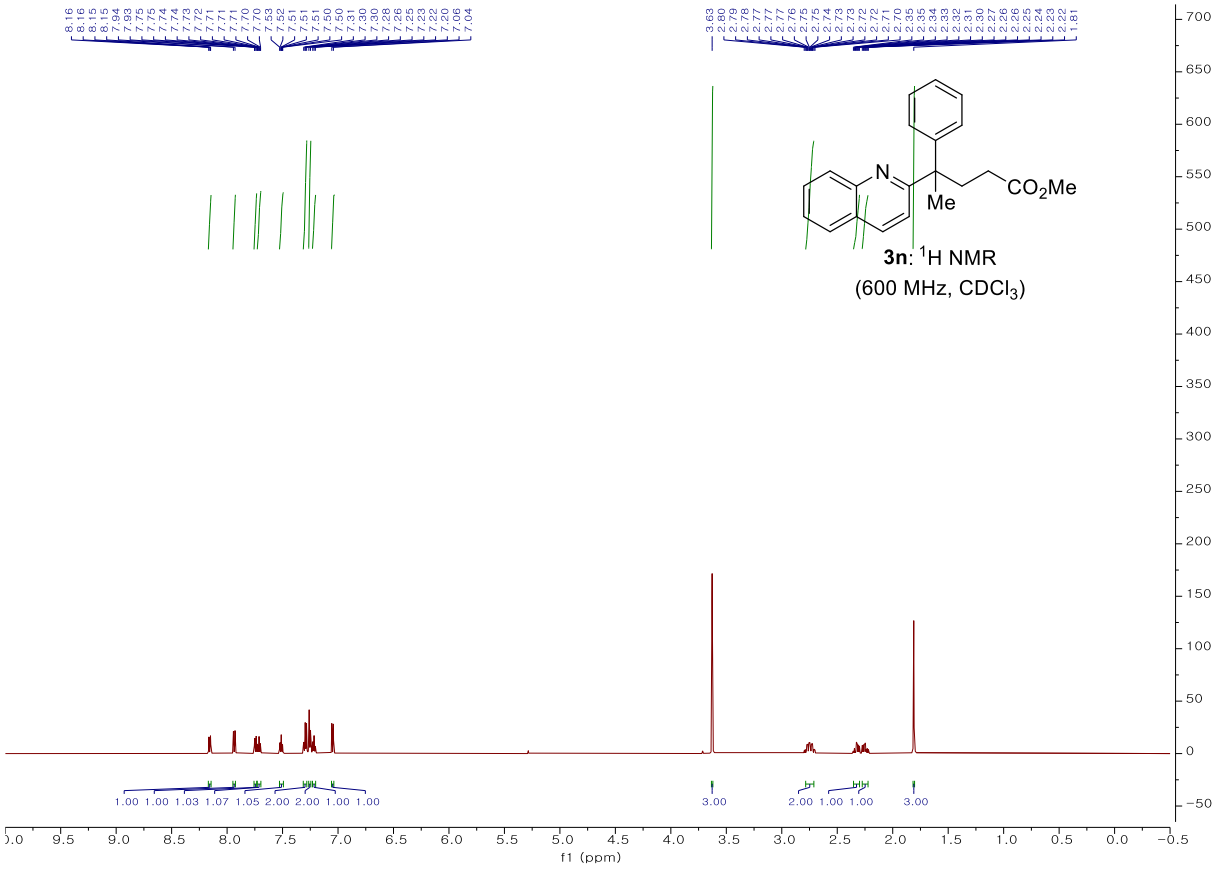

3n: ^{1}H NMR
(600 MHz, $CDCl_3$)

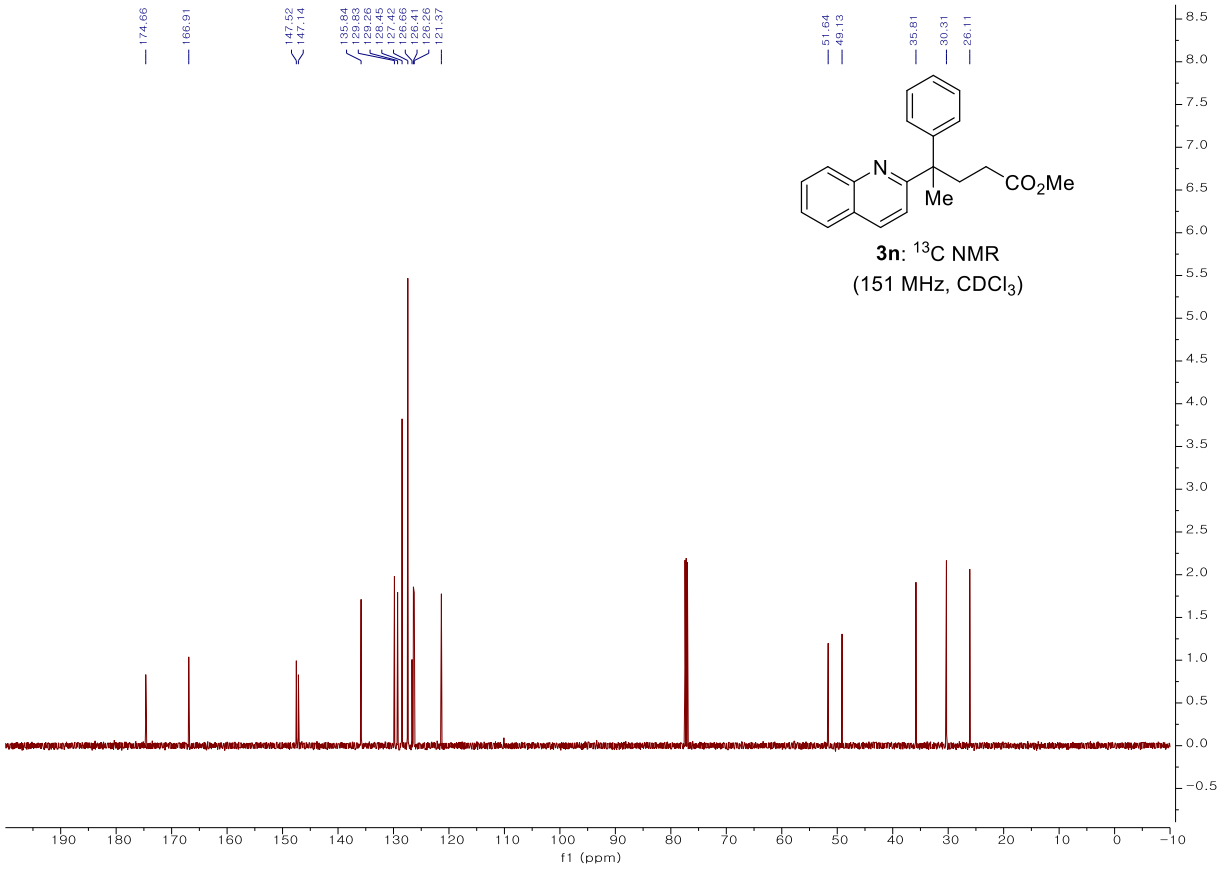

3n: ^{13}C NMR
(151 MHz, $CDCl_3$)

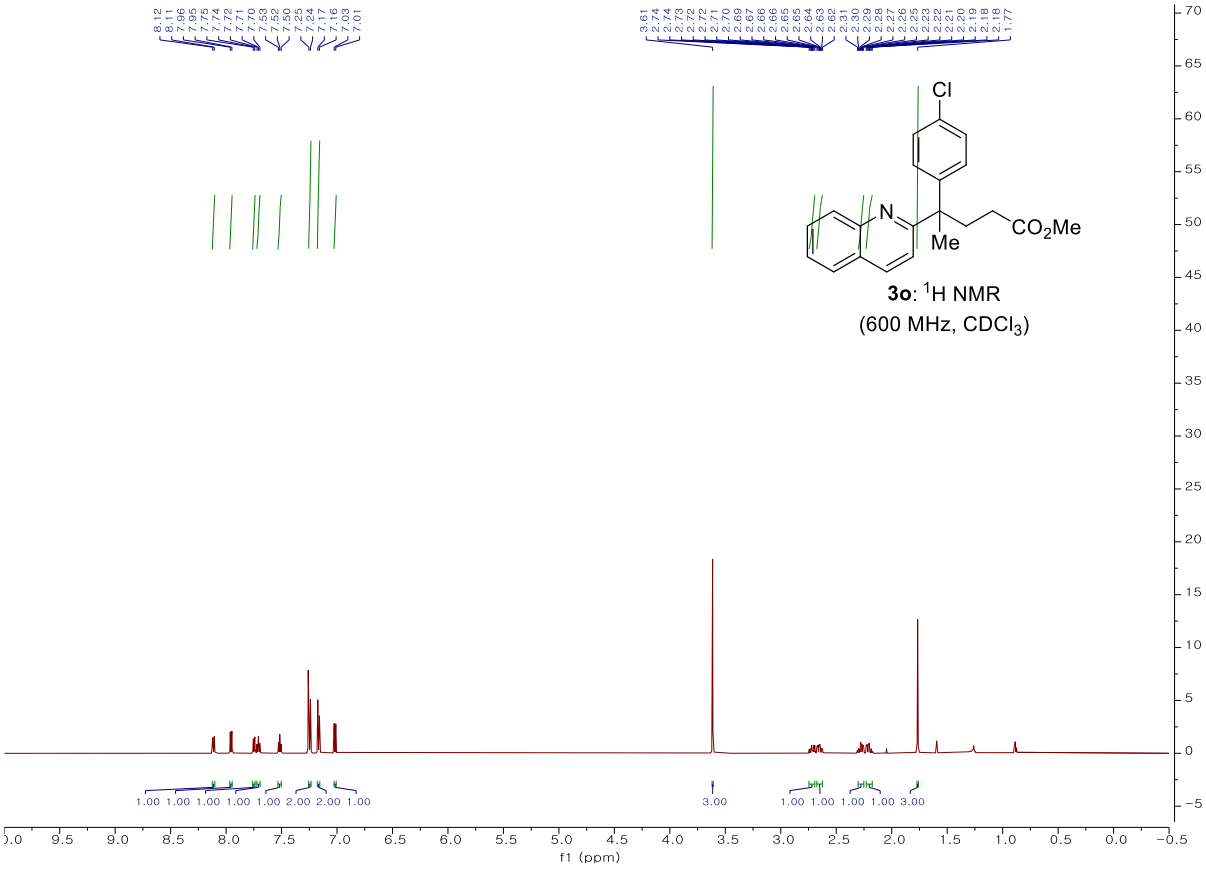

3o: ^{1}H NMR
(600 MHz, $CDCl_3$)

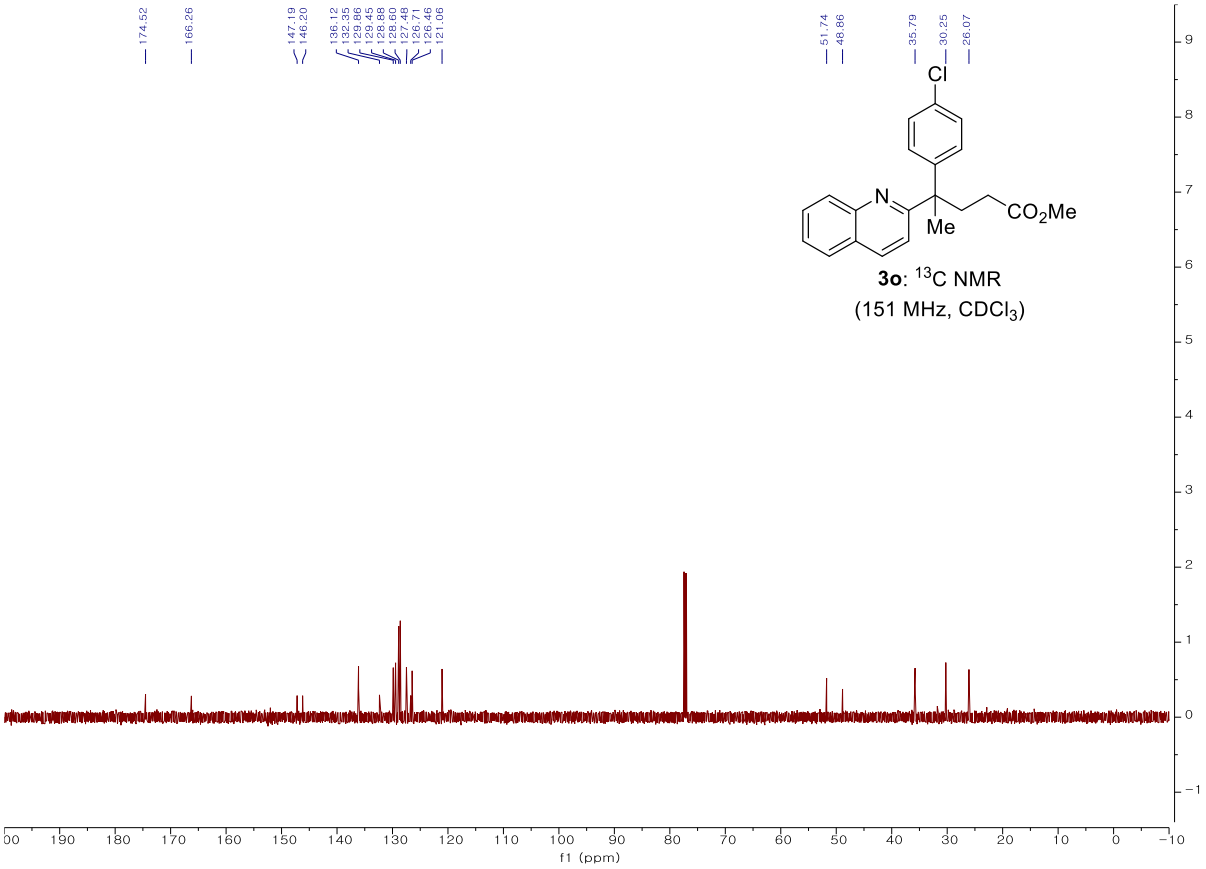

3o: ^{13}C NMR
(151 MHz, $CDCl_3$)

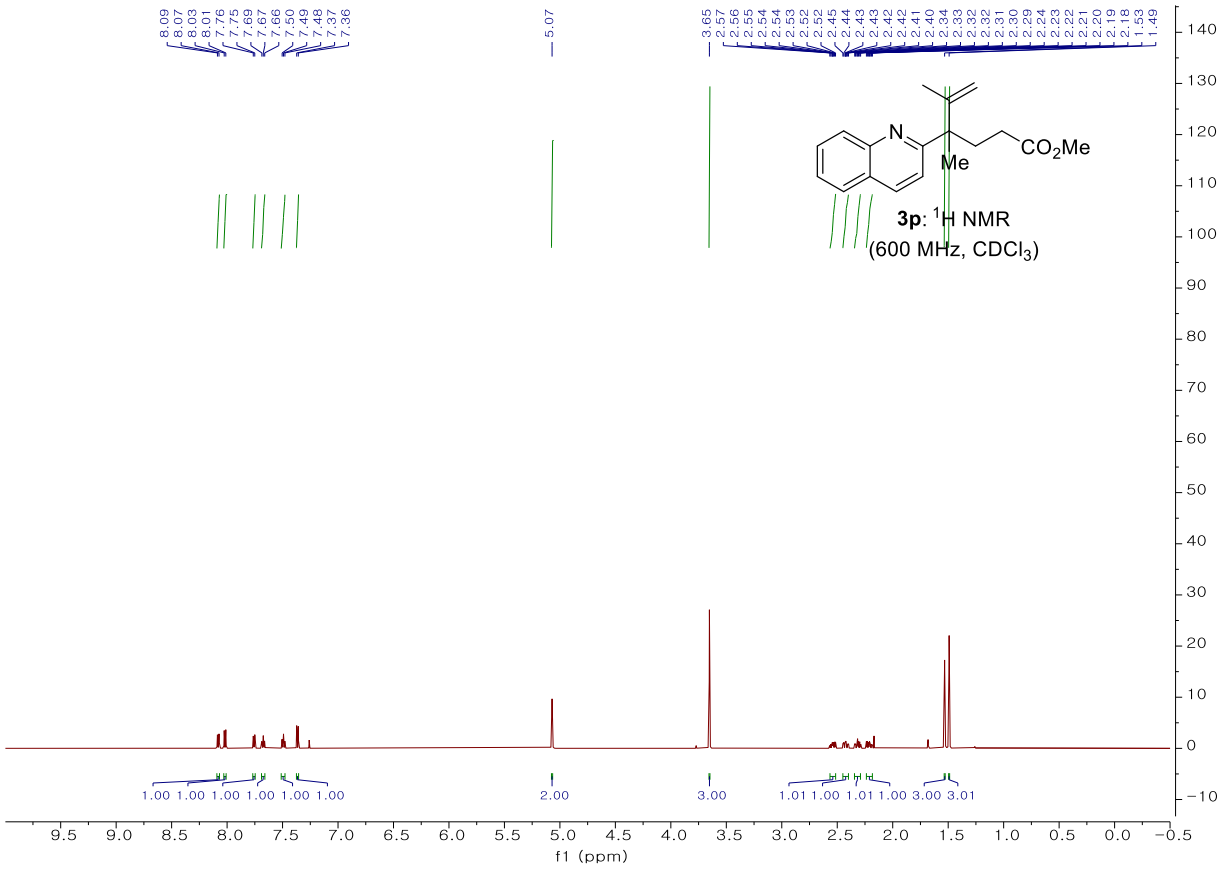
8.09
8.07
8.03
8.01
7.76
7.75
7.69
7.67
7.66
7.50
7.49
7.48
7.37
7.36
5.07
3.65
2.57
2.56
2.55
2.54
2.54
2.53
2.52
2.52
2.45
2.44
2.43
2.43
2.42
2.42
2.41
2.40
2.34
2.33
2.32
2.32
2.31
2.30
2.29
2.24
2.23
2.22
2.21
2.20
2.19
2.18
1.53
1.49
N
Me
CO2Me
3p: 1H NMR
(600 MHz, CDCl3)
1.00 1.00 1.00 1.00 1.00 1.00
2.00
3.00
1.01 1.00 1.01 1.00 3.00 3.01
f1 (ppm)

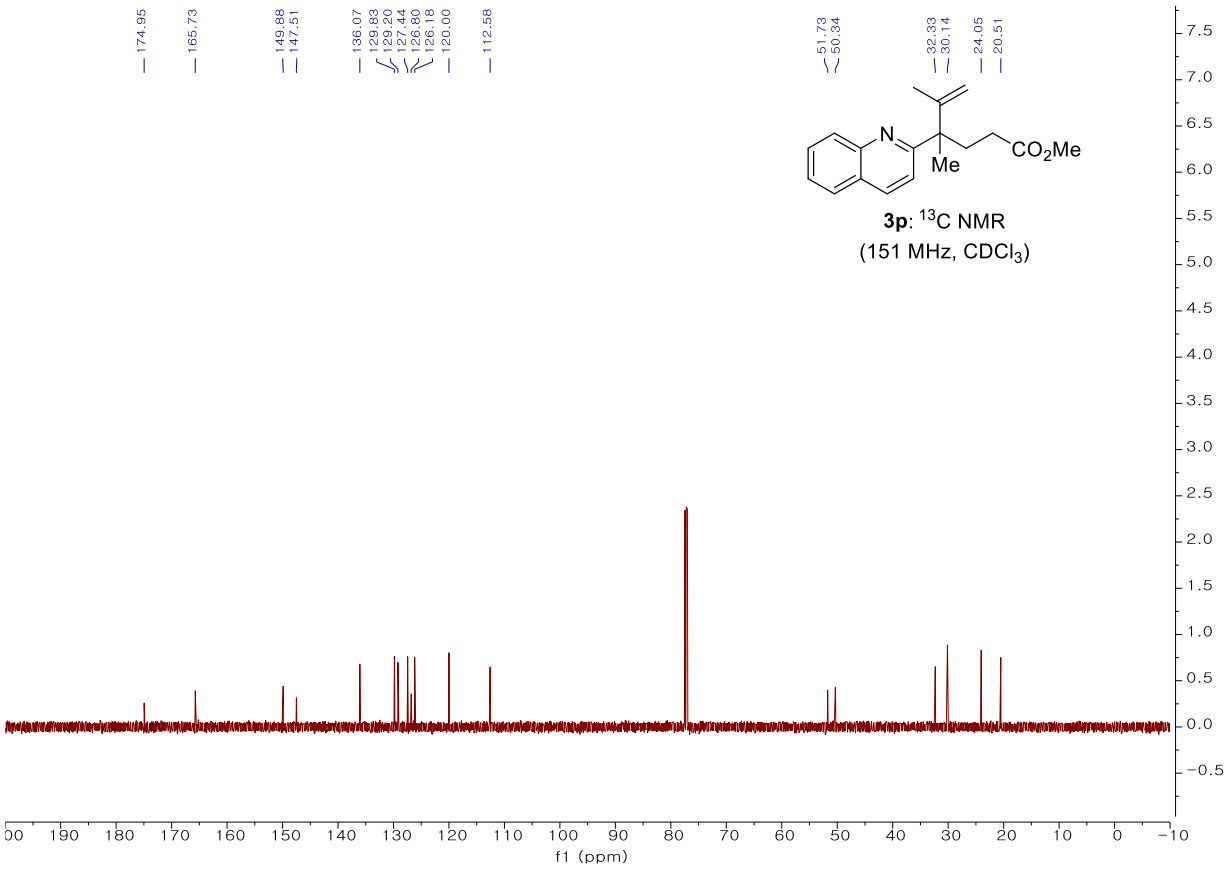
174.95
165.73
149.88
147.51
136.07
129.83
129.20
127.44
126.80
126.18
120.00
112.58
51.73
50.34
32.33
30.14
24.05
20.51
N
Me
CO2Me
3p: 13C NMR
(151 MHz, CDCl3)
f1 (ppm)

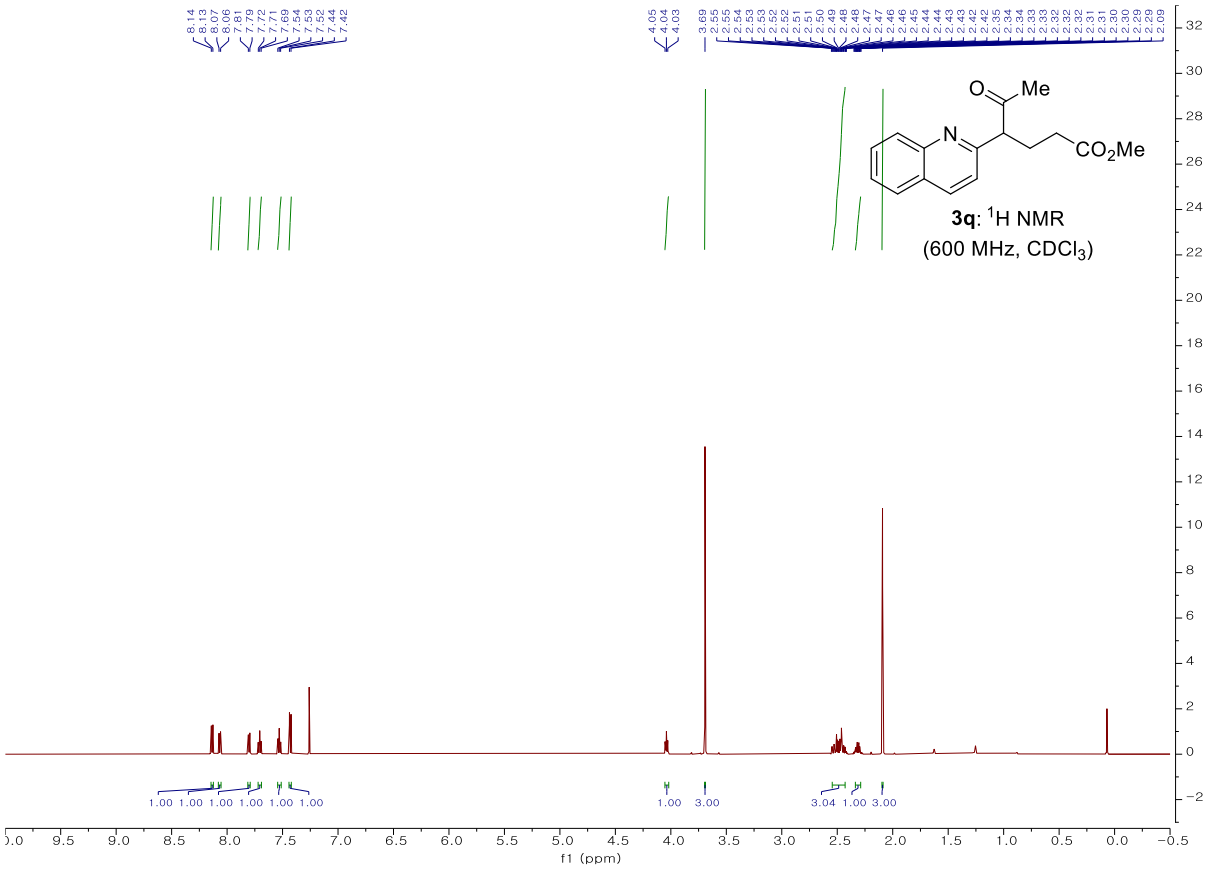
8.14
8.13
8.07
8.06
7.81
7.79
7.72
7.71
7.69
7.54
7.53
7.52
7.44
7.42
4.05
4.04
4.03
3.69
2.55
2.54
2.53
2.52
2.51
2.50
2.49
2.48
2.47
2.46
2.45
2.44
2.43
2.42
2.35
2.34
2.33
2.32
2.31
2.30
2.29
2.09
O
Me
N
CO2Me
3q: 1H NMR
(600 MHz, CDCl3)
1.00 1.00 1.00 1.00 1.00 1.00
1.00 3.00
3.04 1.00 3.00
f1 (ppm)

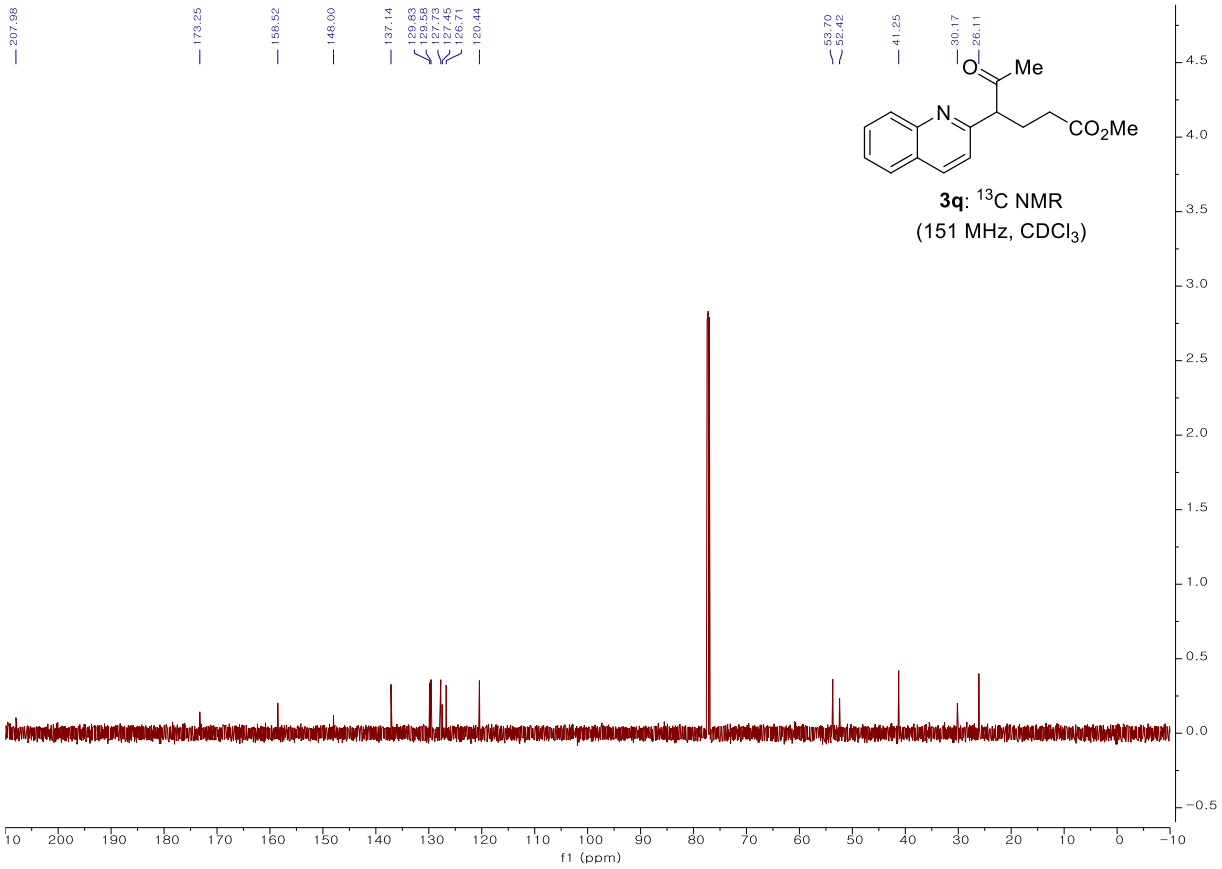
207.98
173.25
158.52
148.00
137.14
129.83
129.58
127.73
127.45
126.71
120.44
53.70
52.42
41.25
30.17
26.11
O
Me
N
CO2Me
3q: 13C NMR
(151 MHz, CDCl3)
f1 (ppm)

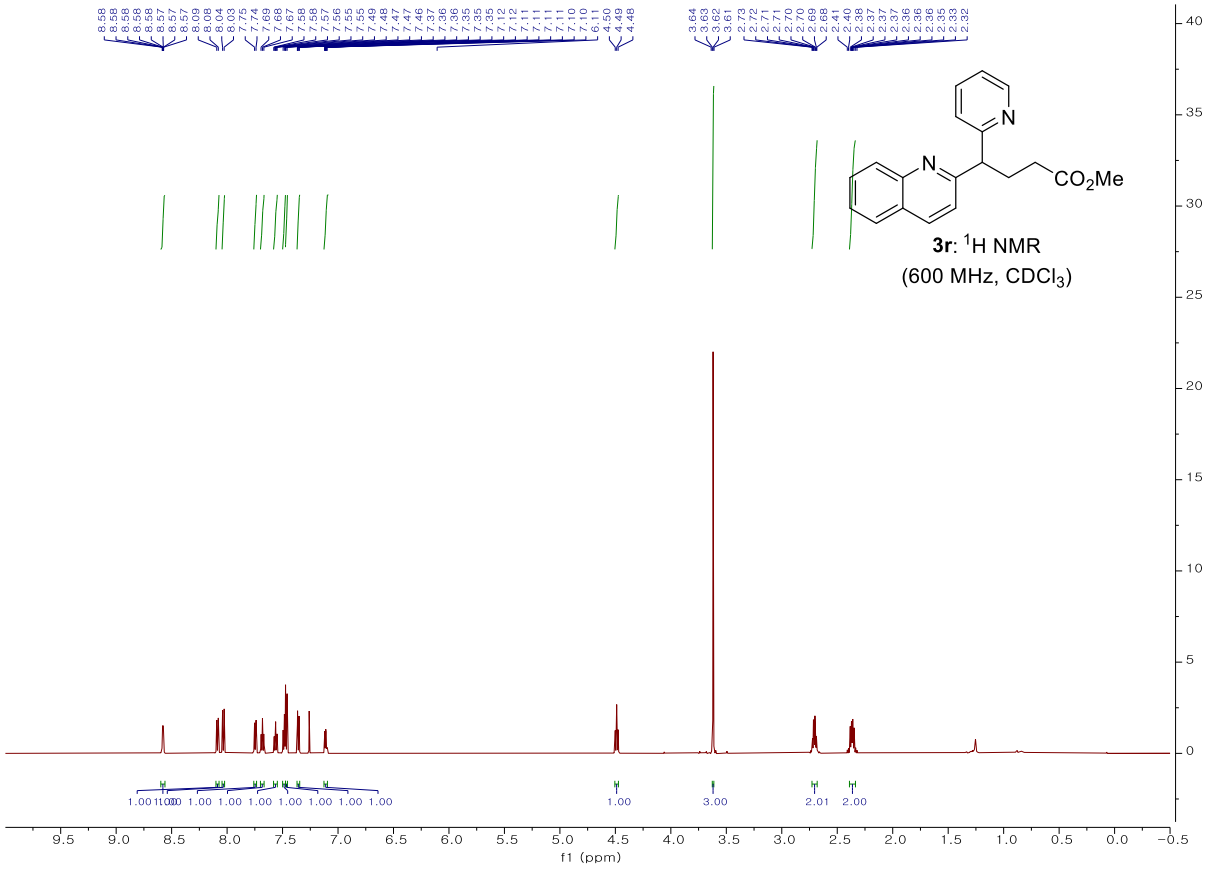

3r: ^{1}H NMR
(600 MHz, $CDCl_3$)

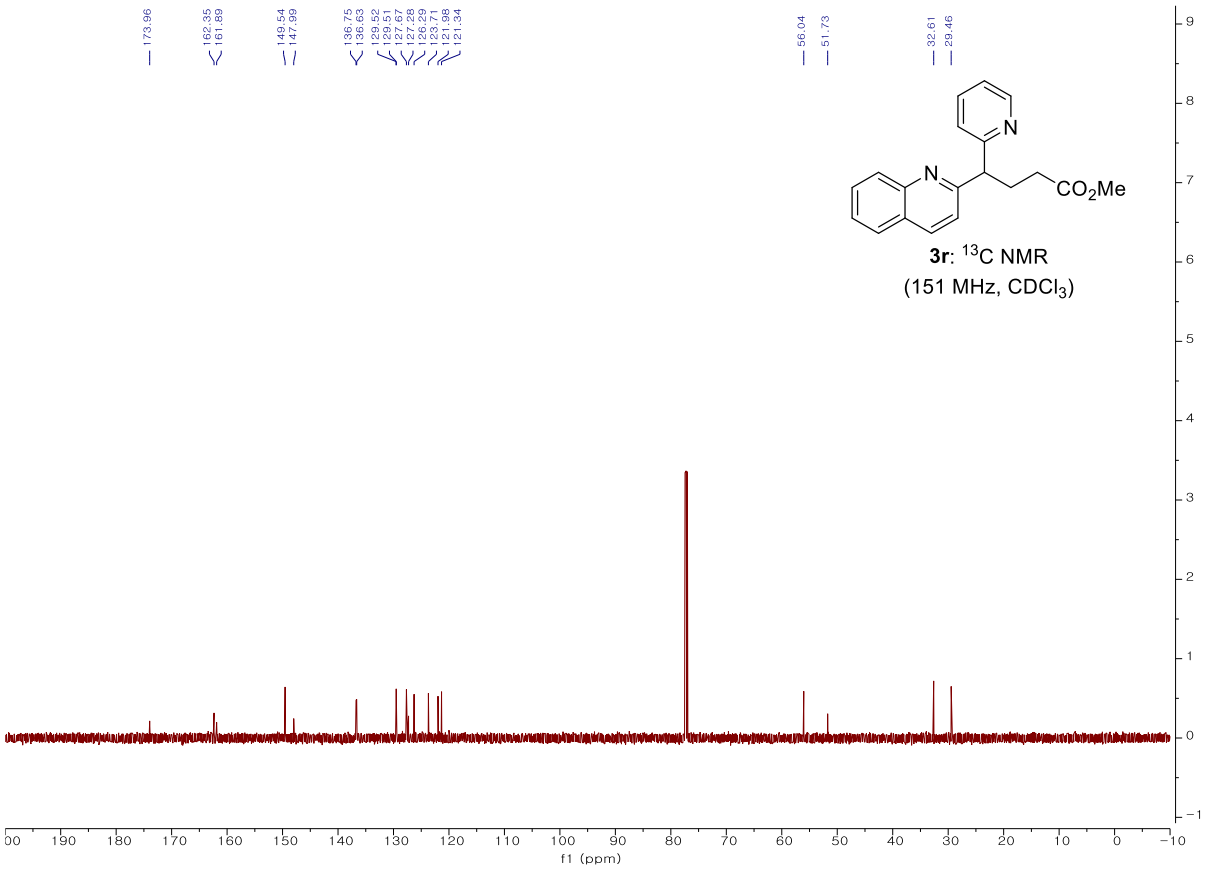

3r: ^{13}C NMR
(151 MHz, $CDCl_3$)

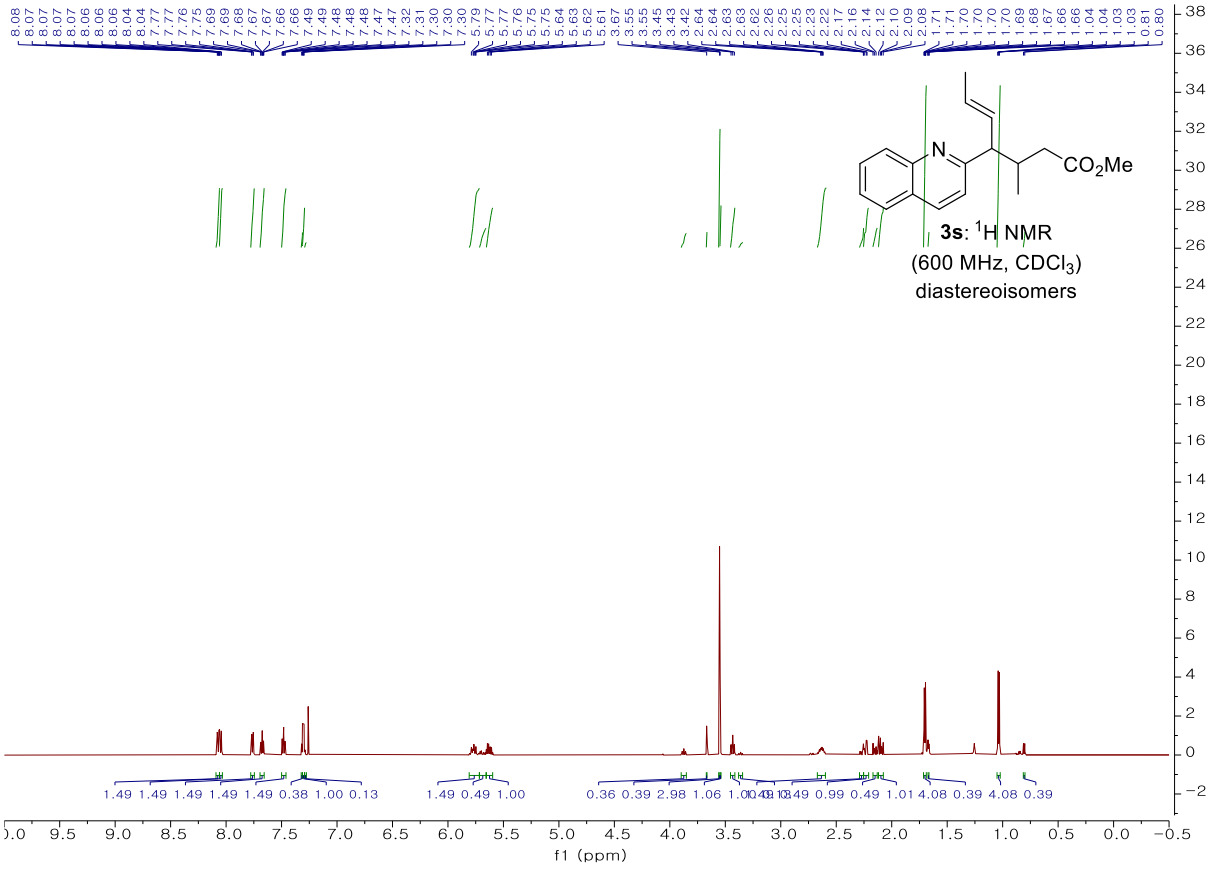
N
CO2Me
3s: 1H NMR
(600 MHz, CDCl3)
diastereoisomers
f1 (ppm)

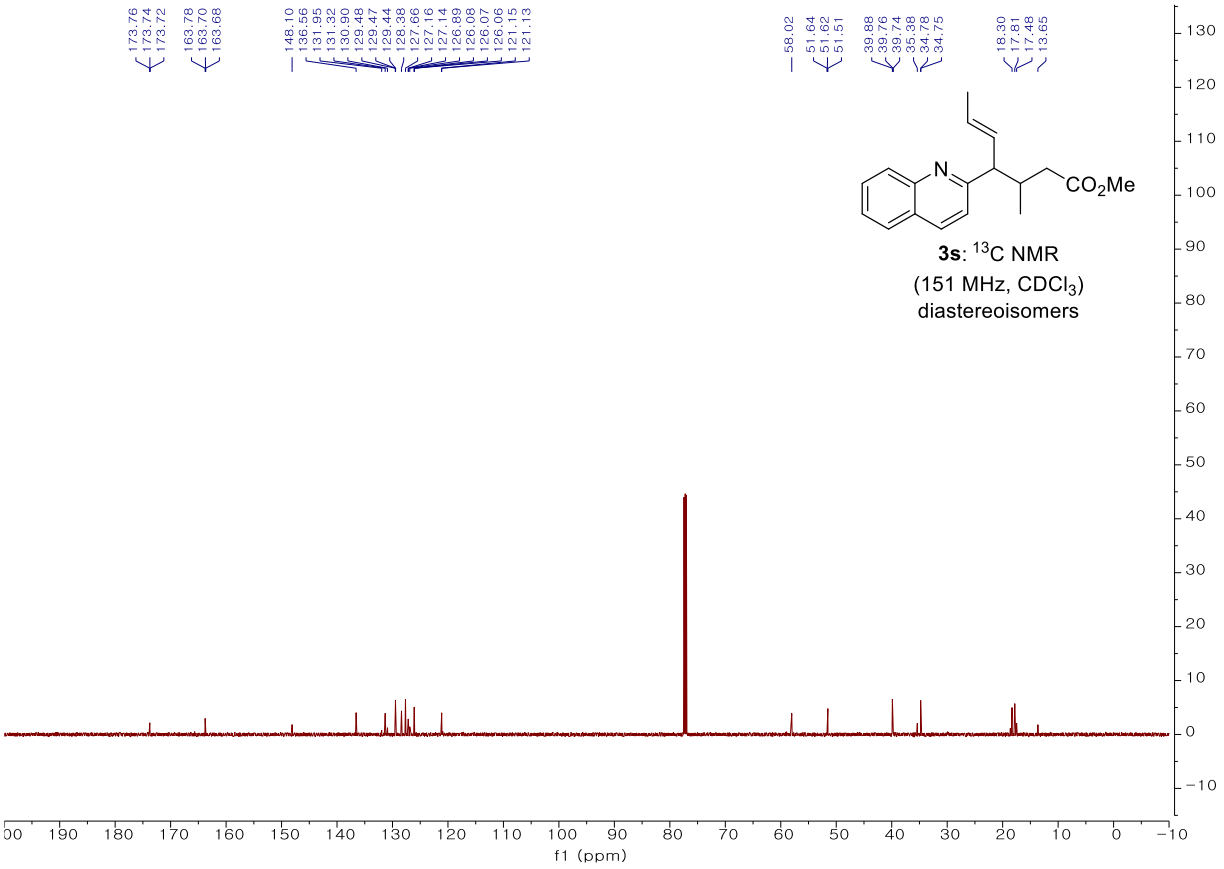
N
CO2Me
3s: 13C NMR
(151 MHz, CDCl3)
diastereoisomers
f1 (ppm)

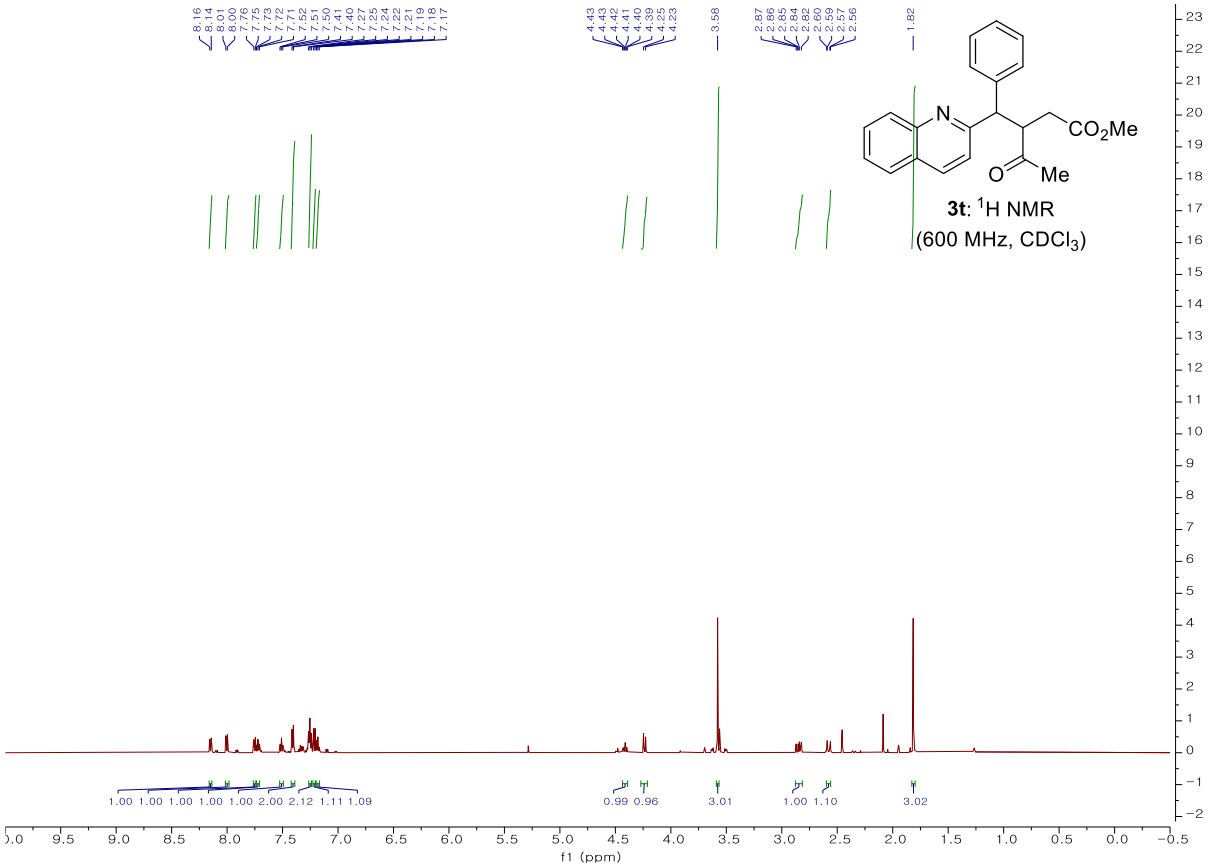
8.16
8.14
8.01
8.00
7.76
7.75
7.73
7.72
7.71
7.52
7.51
7.50
7.41
7.40
7.27
7.25
7.24
7.22
7.21
7.19
7.18
7.17
4.43
4.42
4.41
4.40
4.39
4.25
4.23
3.58
2.87
2.86
2.85
2.84
2.82
2.60
2.59
2.57
2.56
1.82
N
CO2Me
O
Me
3t: 1H NMR
(600 MHz, CDCl3)
1.00 1.00 1.00 1.00 1.00 2.00 2.12 1.11 1.09
0.99 0.96
3.01
1.00 1.10
3.02
f1 (ppm)

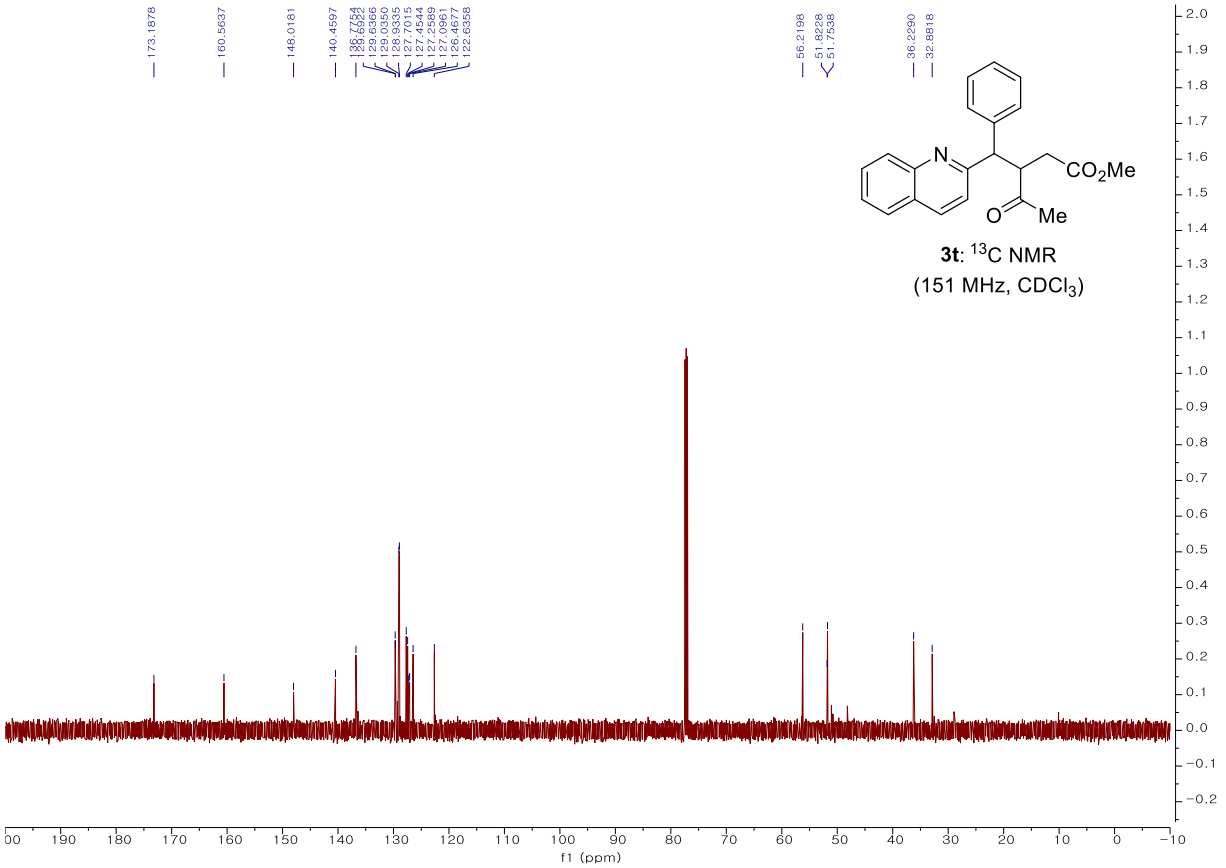
173.1878
160.5637
148.0181
140.4597
138.7754
138.6922
138.6586
129.0350
128.9335
127.7015
127.4544
127.2589
127.0961
126.4677
122.6358
56.2198
51.8228
51.7538
36.2290
32.8818
N
CO2Me
O
Me
3t: 13C NMR
(151 MHz, CDCl3)
f1 (ppm)